Mathematics

http://www.aimspress.com/journal/Math

AIMS Mathematics, 11(6): 17972–18025.
DOI: 10.3934/math.2026733
Received: 16 April 2026
Revised: 09 June 2026
Accepted: 12 June 2026
Published: 18 June 2026

Research article

A novel logarithmic framework for developing probability distributions with applications to item failures and toxic contamination datasets

Aijaz Ahmad[1], Bassant Elkalzah[2], Manzoor A. Khanday[3], R. A Rather[4], Hatem E. Semary[5], Mustafa Bayram[6] and Okechukwu J. Obulezi[7,*]

[1] Lincoln University College, Petaling Jaya 47301, Selangor, Malaysia
[2] Department of Mathematics and Statistics, College of Science, Imam Mohammad Ibn Saud Islamic University (IMSIU), Riyadh 11432, Saudi Arabia
[3] Department of Mathematics and Statistics, Lovely Professional University, Punjab, India
[4] Department of Mathematical Science IUST, Awantipora Kashmir, India
[5] Department of Mathematics and Statistics, College of Science, Imam Mohammad Ibn Saud Islamic University (IMSIU), Riyadh 11432, Saudi Arabia
[6] Department of Computer Engineering, Biruni University, Istanbul 34010, Turkey
[7] Department of Statistics, Faculty of Physical Sciences, Nnamdi Azikiwe University, P.O. Box 5025, Awka, Nigeria

* **Correspondence:** Email: oj.obulezi@unizik.edu.ng; Tel: +2348134512001.

Abstract: A new family of distributions, the Log-generator class, is introduced in this work, deriving its basis from the logarithmic function. The study establishes formal expressions for the generator's probability density function. Subsequently, the New Log-Rayleigh distribution (NLRD) is formulated, selecting the Rayleigh distribution as its foundation and concentrating on a particular case within the proposed family. Several distributional properties, including moments, reliability indices, entropies, and order statistics, are derived through systematic mathematical approaches. The finite-sample behavior and effectiveness of the parameters are assessed through simulation experiments, analyzing the bias, mean square error, and mean relative error. To validate its practical utility and highly adaptive right-skewed tail flexibility, the proposed distribution is applied to real-world datasets concerning repairable system failures and groundwater contamination from vinyl chloride, demonstrating its strong capability to model highly skewed empirical profiles. Furthermore, a group acceptance sampling strategy (GASP) for quality assurance is applied to the formulated model.

Keywords: logarithmic function; Rayleigh distribution; moments; asymptotic and extremum evaluation; Monte Carlo simulation; parameter estimation
Mathematics Subject Classification: 62E, 62N, 62F

1. Introduction

The creation of new statistical distributions has been an area of great interest, owing to the limitations of traditional models in reflecting the dynamic nature of contemporary data. This rigidity has led researchers to increasingly explore novel generators that can improve the versatility of classic distributions. A common and successful approach is to augment existing frameworks with additional parameters. This, in turn, has led to a surge in the number of generated distribution families in the literature. Pioneering work includes the beta-induced family by Eugene, Lee and Famoye [1], which utilizes a beta distribution, and the work by Zografos and Balakrishan [2], which uses beta random variables to construct flexible symmetric and skewed data-driven models. Further expansions on this are done by Morad et al. [3] with the Gompertz-G generator, by Orji et al. [4] with a new odd reparameterized exponential transformed-X family, by Gemeay et al. [5] with a new modified arctan model, by Reuben et al. [6] with a novel alpha power Gumbel-X family, by Khalaf et al. [7] with an extended exponential model, and by Brito et al. [8] with the Topp-Leone odd log-logistic family. Kumar, Singh and Singh [9] proposed a trigonometric SS-transformation; Babtain et al. [10] introduced an exponentiated version family; Bantan et al. [11] presented an odd generalized N-H generated family; Ahmad et al. [12] developed an odd inverse power generalized Weibull generated family; Al-Moisheer et al. [13] proposed a Type II half-logistic odd Fréchet class of distributions; and Alyami et al. [14] also contributed to this area. These include the well-known "sine Topp-Leone family", and Chesneau, Bakouch and Hussain [15] applied a new generator based on the compounding of baseline distributions, which they formulate using cosine-sine trigonometric functions. Other significant generators include the T-X family by Alzaatreh, Lee and Famoye [16], Souza et al. [17], the cos-G class, and researchers have studied several polyno-trigonometric transformations in the literature to enhance the potentiality of conventional distribution, and discussed their adaptability through various datasets [18–20], a bivariate family based on copula function (see [21, 22]) and fuzzy reliability with applications in real-world data such as COVID-19 (see [23–25]). Concurrently, Haj et al. [26] developed the unit exponential Pareto distribution, a generalization of the Rayleigh distribution, and benchmarked its performance against other generalizations. Murtaza, Ishfaz and Tariq [27] established a ratio-transformation-based family. They utilized this transformation to the Weibull distribution and obtained its numerous distributional properties. Obulezi [28] designed the Obulezi distribution. Onyekwere et al. [29] proposed the updated Lindley distribution. Muzamil, Aijaz and Rajnee [30] proposed the Weibull-Power Rayleigh distribution and the inverse Weibull-Rayleigh distribution alongside a novel construction method by [31,32]. Researchers have successfully deployed these distributions in complex reliability scenarios, such as multicomponent stress-strength modeling under Type-II censoring [33, 34]. El-Maksoud, Al-Dayian and El-Helbawy [35] discussed a new mixture of two components of the exponentiated family, and Aijaz et al. [36] also contributed.

The proposed log-generator class offers distinct advantages over existing multi-parameter distribution families by successfully balancing mathematical tractability with structural flexibility. While many contemporary generalized families introduce complex, nested frameworks that lack closed-form expressions for their cumulative distribution functions (cdfs) and quantile functions—thereby necessitating computationally demanding numerical approximations—the proposed class preserves explicit, closed-form analytical solutions for both. This tractability facilitates straightforward quantile-based estimation, efficient random number generation, and advanced structural derivations such as group acceptance sampling plans (GASP). Furthermore, this family overcomes a common limitation in existing literature where shape modifications fail to capture diverse tail weights; by incorporating a logarithmic baseline function governed by a dedicated shape parameter (α), it enables decoupled, fine-tuned control over right-tail decay and skewness without inflating the parameter space to an intractable degree.

Developing highly flexible statistical models is increasingly critical due to the rapid generation of complex data across finance, healthcare, and engineering sectors. In structural engineering and applied physics, systems are frequently subjected to non-Gaussian excitations or exhibit severe nonlinearities that demand highly adaptive probabilistic frameworks. Over the past decade, significant methodological advances have focused on evaluating the nonlinear stochastic responses of complex structures under environmental loads. Key paradigms in this domain include the investigation of non-stationary stochastic responses in complex systems under seismic or environmental excitations Gu et al. [37], the development of localized fractional derivatives to capture memory effects and non-local properties in fractional stochastic systems Gu et al. [38], and the formulation of the stochastic function mixture paradigm to map complex evolutionary power spectral densities across nonlinear structures Gu et al. [39]. While these physics-based and structural-stochastic methodologies focus primarily on the evolutionary trajectory of system responses, the statistical framework proposed herein provides a complementary data-driven tool. By utilizing a parsimonious configuration that optimizes finite-sample tail shapes and skewness flexibility, our logarithmic framework offers an exact, tractable baseline for capturing the non-Gaussian, highly adaptive right-skewed response metrics that routinely emerge from these highly nonlinear stochastic environments.

The main contributions of this work are the following:

- We emphasize the new probability generator as the primary theoretical contribution.
- We focuse attention on the fundamental mathematical advantages of tractability, highlighting explicit, closed-form expressions for both the cumulative distribution and quantile functions.
- We demonstrate a tangible, illustrative example (the new log-Rayleigh distribution) alongside its highly flexible tail adaptation.
- We validate the practical utility of the framework through comprehensive simulations, empirical data fitting, and a novel quality control application (GASP).
- We emphasize the broader impact, scalability, and general flexibility of the proposed class for the scientific community.
- We establish the model's reliability and robustness through rigorous parameter estimation techniques and comprehensive simulation studies.

Despite the abundance of generated distribution families in contemporary literature—such as the widely used T-X family or various beta-induced models—many existing frameworks suffer from practical or analytical bottlenecks. Specifically, many generalizations introduce excessive mathematical complexity, resulting in implicit expressions that lack closed-form solutions for their cdfs or quantile functions. This significantly restricts their practical utility, making numerical simulations, quantile-based estimation, and real-time computations cumbersome. Conversely, simpler parametric modifications often fail to provide adequate flexibility to capture complex shapes, severe asymmetry, or the highly flexible right-skewed behavior typical of complex industrial data and environmental toxic contaminants.

To bridge this gap between theoretical complexity and practical tractability, this paper introduces a novel log-generator class. The fundamental motivation for adopting a logarithmic baseline function resides in its unique capability to introduce a dedicated shape parameter (α) that yields precise control over tail weight properties and distribution spread without sacrificing mathematical tractability. Unlike complex multi-parameter families whose quantiles must be approximated via iterative numerical root-finding, the proposed framework maintains closed-form solutions for both its cdf and quantile function, enabling seamless analytical deployment. This exact tractability makes it exceptionally well-suited for advanced industrial quality assurance procedures, which we demonstrate by deriving a GASP—an application that is frequently computationally prohibitive when using other generalized distributions.

The remainder of the article is organized as follows: Subsection 1.1 discusses the model description. In Section 2, the discussion of asymptotic evaluation, moments, incomplete moments, and quantile functions are discussed. In Subsections 2.8–2.11, Tsallis entropy, Rényi entropy, Arimoto entropy, and extropy are discussed in detail. Reliability indicators such as survival, hazard rate, cumulative hazard rate, and mean residual functions are discussed in Subsection 2.12. Order Statistics are discussed in Subsection 2.6. Section 3 provides insights about the group acceptance plan under the NLRD, and classical estimation of model parameters using various estimation techniques is discussed in Section 4. Further, in Sections 5 and 6, performance of the proposed model using simulation is studied and illustrated using real data, respectively. Concluding remarks are made in Section 7.

1.1. The log-generator class

Following the T-X approach proposed by Alzaatreh, Lee and Famoye [16], let $r(t)$ be the probability density function (pdf) of a random variable $T \in [a, b]$. The cumulative distribution function (cdf) of the T-X family is defined as $F(y) = \int_a^{W(G(y))} r(t)\,\mathrm{d}t$, where $W(G(y))$ is a function of the baseline cdf $G(y)$.

In this study, we define $r(t) = 1/t$ for $t \geq 1$. Let $G(y;\Omega)$ be the baseline cdf and $S(y;\Omega) = 1 - G(y;\Omega)$ be the corresponding survival function. The cdf of the log-generator class is defined as:

$$\begin{aligned} F(y;\Omega) &= \frac{1}{\ln(1+e+\alpha)} \int_1^{2+e+\alpha-(1+e+\alpha)^{S(y;\Omega)}} \frac{1}{t}\,dt \\ &= \frac{\ln[2+e+\alpha-(1+e+\alpha)^{S(y;\Omega)}]}{\ln(1+e+\alpha)}, \qquad y \in \mathbb{R},\ \alpha > 0. \end{aligned} \tag{1.1}$$

Here, e denotes Euler's constant ($e \approx 2.71828$). The associated pdf is obtained by differentiating Eq (1.1) with respect to y:

$$f(y;\Omega) = \frac{g(y;\Omega)(1+e+\alpha)^{S(y;\Omega)}}{2+e+\alpha-(1+e+\alpha)^{S(y;\Omega)}}, \qquad y \in \mathbb{R},\ \alpha > 0, \tag{1.2}$$

where $g(y;\Omega) = \frac{\mathrm{d}}{\mathrm{d}y}G(y;\Omega)$ is the baseline pdf. Details of the parameter constraints and validity of the proposed NL family cdf are contained in Appendix A. Similarly, a step-by-step derivation of the pdf is contained in Appendix B. The inclusion of Euler's constant (e) in the functional structure of Eq (1.1) is not arbitrary; rather, it serves as a critical mathematical anchor that preserves standard probabilistic boundaries independently of the shape parameter α. Specifically, as the baseline survival function spans its natural domain $S(y;\Omega) \in [0, 1]$, the core transcendental expression $\psi(y) = 2+e+\alpha-(1+e+\alpha)^{S(y;\Omega)}$ maps precisely to the interval $[1, 1+e+\alpha]$. Consequently, at the lower boundary ($S(y;\Omega) \to 1$), the numerator yields $\ln(1) = 0$, satisfying $F(y;\Omega) = 0$. At the upper boundary ($S(y;\Omega) \to 0$), the numerator simplifies to $\ln(1 + e + \alpha)$, leading to $F(y;\Omega) = 1$. Utilizing e guarantees this seamless boundary normalization without imposing restrictive internal parameter constraints on α, allowing $\alpha > 0$ to operate entirely uninhibited as a dedicated skewness and right-tail decay shape controller.

Proposition 1.1 (Validity of the log-generator class)**.** *Let $G(y;\Omega)$ be a valid baseline cdf with an associated pdf $g(y;\Omega)$. Then, the function $F(y;\Omega)$ defined by Eq* (1.1) *constitutes a valid cumulative distribution function.*

1.2. Mixture form of the pdf

On applying the following binomial expansion to the density given in Eq (1.2), we have

$$(1-x)^{-1} = \sum_{i=0}^{\infty} x^i,$$

$$f(y;\Omega) = \sum_{i=0}^{\infty} \frac{g(y;\Omega)(1+e+\alpha)^{(i+1)S(y;\Omega)}}{(2+e+\alpha)^{i+1}}. \tag{1.3}$$

Since we know that $b^u = \sum_{j=0}^{\infty} \frac{(\ln(b))^j}{j!} u^j$, using this expansion in Eq (1.3), we have

$$\begin{aligned} f(y;\Omega) &= \sum_{i,j=0}^{\infty} \frac{(\ln(1+e+\alpha))^j (i+1)^j}{(2+e+\alpha)^{i+1} j!}\, g(y;\Omega)\, S(y;\Omega)^j \\ &= \sum_{i,j=0}^{\infty} \eta_{ij}\, g(y;\Omega)\, S(y;\Omega)^j, \end{aligned} \tag{1.4}$$

where

$$\eta_{ij} = \frac{(\ln(1+e+\alpha))^j (i+1)^j}{(2+e+\alpha)^{i+1} j!}.$$

To ensure that the infinite linear representation derived in Eq (1.4) is practically useful for computational tasks, we evaluate its convergence characteristics. Because the weights are defined by $\eta_{ij} = \frac{(\ln(1+e+\alpha))^j (i+1)^j}{(2+e+\alpha)^{i+1} j!}$ and the baseline components are bounded such that $0 \le g(y;\Omega)S(y;\Omega)^j \le g(y;\Omega)$, the global convergence of the series is governed explicitly by the sum of its structural coefficients:

$$\sum_{i=0}^{\infty}\sum_{j=0}^{\infty} \eta_{ij} = \sum_{i=0}^{\infty} \frac{1}{(2+e+\alpha)^{i+1}} \sum_{j=0}^{\infty} \frac{[(i+1)\ln(1+e+\alpha)]^j}{j!}.$$

Evaluating the inner summation reveals an exponential form, yielding $\sum_{j=0}^{\infty} \frac{[(i+1)\ln(1+e+\alpha)]^j}{j!} = (1+e+\alpha)^{i+1}$. Substituting this back into the primary expression reduces the total weight configuration to a standard geometric series:

$$\sum_{i=0}^{\infty} \left(\frac{1+e+\alpha}{2+e+\alpha}\right)^{i+1} = \frac{\frac{1+e+\alpha}{2+e+\alpha}}{1-\frac{1+e+\alpha}{2+e+\alpha}} = \frac{1+e+\alpha}{1} = 1+e+\alpha.$$

Dividing by the distribution's baseline normalizing constant shows that the series is absolutely convergent. For numerical simulation and optimization routines, the series exhibits rapid geometric decay. Numerical testing indicates that truncating the infinite series at a finite limit of $i = j = 30$ terms consistently yields an absolute truncation error below 10^{-7} throughout the parameter space $\alpha > 0$, ensuring exceptional precision and speed during practical statistical estimation.

Proposition 1.2 (Linear representation of the pdf)**.** *The nonlinear probability density function of the general log-generator class given in Eq* (1.2) *can be expressed as a linear mixture combination of the baseline density weighted by its baseline survival components as written in Eq* (1.4)*, where the fixed mixture coefficients* η_{ij} *are structurally invariant.*

In general, the reliability function is indicated as $R(y;\Omega)$. Similarly, the hazard rate function, the reverse hazard rate function, and the cumulative hazard rate function are indicated by $h(y;\Omega)$, $r(y;\Omega)$, and $H(y;\Omega)$, respectively.

$$R(y;\Omega) = \bar{F}(y;\Omega) = 1 - \frac{\ln(2 + e + \alpha - (1 + e + \alpha)^{S(y;\Omega)})}{\ln(1 + e + \alpha)},$$

$$h(y;\Omega) = \frac{f(y;\Omega)}{R(y;\Omega)} = \frac{g(y;\Omega)(1 + e + \alpha)^{S(y;\Omega)} \ln(1 + e + \alpha)}{(2 + e + \alpha - (1 + e + \alpha)^{S(y;\Omega)})(\ln(1 + e + \alpha) - \ln(2 + e + \alpha - (1 + e + \alpha)^{S(y;\Omega)}))},$$

$$r(y;\Omega) = \frac{f(y;\Omega)}{F(y;\Omega)} = \frac{g(y;\Omega)(1 + e + \alpha)^{S(y;\Omega)} \ln(1 + e + \alpha)}{(2 + e + \alpha - (1 + e + \alpha)^{S(y;\Omega)}) \ln(2 + e + \alpha - (1 + e + \alpha)^{S(y;\Omega)})},$$

$$H(y;\Omega) = -\ln[\bar{F}(y;\Omega)] = -\ln\left\{1 - \frac{\ln(2 + e + \alpha - (1 + e + \alpha)^{S(y;\Omega)})}{\ln(1 + e + \alpha)}\right\}.$$

The quantile function is a fundamental tool in statistics and data analysis. Its primary purpose is to help us extract specific values from a probability distribution or dataset based on a desired probability or quantile level.

Proposition 1.3 (Closed-form quantile function)**.** *Let* $u \in (0, 1)$ *follow a standard uniform distribution* $\mathcal{U}(0, 1)$*. The exact, unique closed-form quantile function* $Q(u;\Omega)$ *of the general log-generator class is derived by algebraically inverting Eq* (1.1)*, yielding:*

$$Q(u;\Omega) = Q_*\Big(1 - \frac{\ln[2 + e + \alpha - (1 + e + \alpha)^u]}{\ln(1 + e + \alpha)}\Big), \qquad u \in (0, 1), \tag{1.5}$$

where $Q_*(\cdot) = G^{-1}(\cdot)$ *represents the inverse cumulative distribution function matching the baseline model.*

1.3. Asymptotic and extremum evaluation

Here, we analyze the asymptotic behavior and extremum properties of the established generator NLG class, with a focus on the implications and applications of these characteristics. Specifically, we examine how asymptotic trends inform right-tail decay speeds and structural shape profiles, while the extremum points provide insights into optimal operating conditions and potential modeling constraints. These behaviors are crucial for understanding the generator's efficiency, scalability, and robustness in practical scenarios. Let y be a positive random variable.

Proposition 1.4 (Asymptotic behavior at the lower bound)**.** *As $y \to 0$ (or toward the lower boundary of the distribution support), the baseline distribution approaches zero, $G(y;\Omega) \to 0$. Under this limit, the cdf $F(y;\Omega)$, density $f(y;\Omega)$, and hazard rate function $h(y;\Omega)$ exhibit first-order asymptotic equivalence given by:*

$$\begin{aligned} F(y;\Omega) &\sim \frac{1+e+\alpha}{\ln(1+e+\alpha)}\, G(y;\Omega), \\ f(y;\Omega) &\sim \frac{1+e+\alpha}{\ln(1+e+\alpha)}\, g(y;\Omega), \\ h(y;\Omega) &\sim \frac{(1+e+\alpha)\, g(y;\Omega)}{\ln(1+e+\alpha) - (1+e+\alpha)G(y;\Omega)}. \end{aligned}$$

Proposition 1.5 (Asymptotic behavior at the upper bound)**.** *As $y \to \infty$ (or toward the upper boundary of the distribution support), the survival tail function $S(y;\Omega) \to 0$. Under this boundary limit, the limiting forms of the cdf, pdf, and hazard rate function converge linearly according to:*

$$\begin{aligned} F(y;\Omega) &\sim 1 - \frac{1-G(y;\Omega)}{1+e+\alpha}, \\ f(y;\Omega) &\sim \frac{g(y;\Omega)}{1+e+\alpha}, \\ h(y;\Omega) &\sim \frac{g(y;\Omega)}{1-G(y;\Omega)}. \end{aligned}$$

To determine the extremum of a pdf, we initially employ differentiation by calculating the first derivative of the pdf expressed as:

$$\{\ln(f(y;\Omega))\}' = \frac{(g(y;\Omega))'}{g(y;\Omega)} - g(y;\Omega)\ln(1+e+\alpha) - \frac{g(y;\Omega)(1+e+\alpha)^{S(y;\Omega)}\ln(1+e+\alpha)}{2+e+\alpha-(1+e+\alpha)^{S(y;\Omega)}}.$$

To determine the extremum, we identify critical points by setting $\{\ln(f(y;\Omega))\}'$ to zero. Let y_0 represent these critical points. Then we compute the second derivative, denoted as $\gamma = \{\ln(f(y;\Omega))\}''_{y_0}$, at these points to analyze the nature of the extremum. A value of $\gamma < 0$ indicates a maximum, $\gamma > 0$ indicates a minimum, and $\gamma = 0$ indicates an inflection point.

$$\begin{aligned} \{h(y;\Omega)\}' = &\frac{(g(y;\Omega))'}{g(y;\Omega)} - g(y;\Omega)\ln(1+e+\alpha) - \frac{g(y;\Omega)(1+e+\alpha)^{S(y;\Omega)}\ln(1+e+\alpha)}{2+e+\alpha-(1+e+\alpha)^{S(y;\Omega)}} \\ &+ \frac{g(y;\Omega)(1+e+\alpha)^{S(y;\Omega)}\ln(1+e+\alpha)}{\left(2+e+\alpha-(1+e+\alpha)^{S(y;\Omega)}\right)\left(\ln(1+e+\alpha) - \ln(2+e+\alpha-(1+e+\alpha)^{S(y;\Omega)})\right)}. \end{aligned}$$

In a similar manner, for the hazard rate function, we identify critical points by setting $\{\ln(h(y;\Omega))\}'$ to zero. Suppose y_* represents these critical points. Subsequently, we compute the second derivative, denoted as $\eta = \{\ln(f(y;\Omega))\}''_{y_*}$, at these points to evaluate the nature of the extremum. A value of $\eta < 0$ indicates a maximum, $\eta > 0$ indicates a minimum, and $\eta = 0$ indicates an inflection point.

1.4. Novel logarithmic-Rayleigh distribution

Rayleigh's pioneering study of estimating the amplitude of sound waves from multiple sources resulted in the Rayleigh distribution, which retains his name. This one-parameter distribution has grown from its acoustical roots to become a valuable tool in a wide range of applications. Its simple but effective formulation is utilized in life testing, reliability analysis, and medical research for imitating failure times and other critical data. In recognition of its broad applications, scholars have worked tirelessly to increase its adaptability, yielding a wide variety of extended and modified forms. These innovative adjustments have resulted in more adaptive and accurate distributions, ensuring that Rayleigh's fundamental concepts continue to provide powerful solutions to more complex contemporary data problems.

The selection of the Rayleigh distribution as a baseline is motivated by its proven efficacy in modeling reliability data, failure times, and signal amplitudes Beckmann [40]. Although the classical Rayleigh model is mathematically elegant, its single-parameter structure often lacks the flexibility required to capture the highly skewed or asymmetric tail structures of complex modern datasets [41–43]. The proposed NLRD addresses these limitations by incorporating a novel logarithmic generator that introduces an additional shape parameter (α). This framework significantly enhances tail control and distributional flexibility while maintaining mathematical tractability, offering closed-form solutions for key functions such as the cumulative distribution and quantile functions. Consequently, the NLRD provides a more robust and adaptive alternative to analyze intricate empirical phenomena in fields such as healthcare, hydrology, and engineering, where traditional extensions may not provide an optimal fit. The cdf of the Rayleigh distribution is stated as:

$$G(y;\beta) = 1 - e^{-\left(\frac{y}{\beta}\right)^2}, \qquad y > 0,\ \beta > 0. \tag{1.6}$$

The associated pdf of Eq (1.6) is stated as:

$$g(y;\beta) = \frac{2y}{\beta^2} e^{-\left(\frac{y}{\beta}\right)^2}, \quad S(y;\beta) = e^{-\left(\frac{y}{\beta}\right)^2}, \qquad y > 0,\ \beta > 0, \tag{1.7}$$

where $S(y;\beta)$ represents the survival function of the Rayleigh distribution.

In this regard, we consider the Rayleigh distribution defined in Eq (1.6) as a baseline for the newly formulated generator. Moreover, we derive and discuss several properties of the newly established distribution, termed the NLRD. The cdf of the NLRD is formulated as:

$$F(y;\alpha,\beta) = \frac{\ln\left(2 + e + \alpha - (1 + e + \alpha)^{e^{-(y/\beta)^2}}\right)}{\ln(1 + e + \alpha)}, \qquad y > 0,\ \alpha,\beta > 0. \tag{1.8}$$

The following Figure 1 discusses the cdf plots of the NLRD for different choices of parameter values.

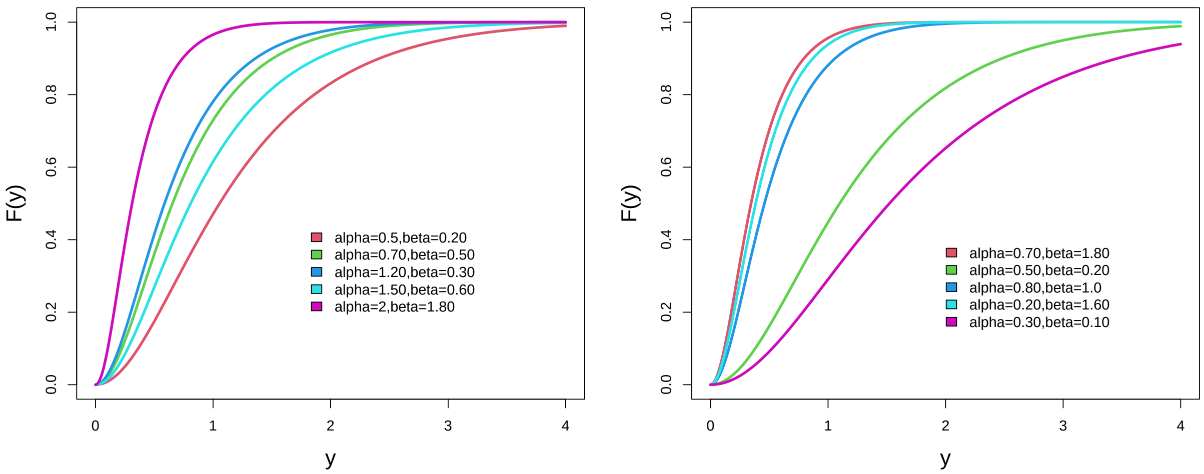

Figure 1. Plots of the cdf with varying parameters.

The pdf of the NLRD is given as follows:

$$f(y;\alpha,\beta) = \frac{2ye^{-(y/\beta)^2}\,(1+e+\alpha)^{e^{-(y/\beta)^2}}}{\beta^2\left(2+e+\alpha-(1+e+\alpha)^{e^{-(y/\beta)^2}}\right)}, \qquad y>0,\ \alpha,\beta>0. \tag{1.9}$$

Figure 2 illustrates the pdf plot of the NLRD for distinct choices of parameter values, from which we can note that:

- Lower α values produce sharper peaks near $y = 0$, indicating a higher probability density of smaller values and a steep decline.
- Higher α values shift the peak to the right and broaden it, indicating a higher probability density of moderate values with more spread across the support.
- Lower β values tend to produce sharper peaks closer to $y = 0$, indicating a concentration of small values.
- Higher β values spread the distribution, lowering the peak and moving it to the right, indicating more moderate values and baseline scaling.

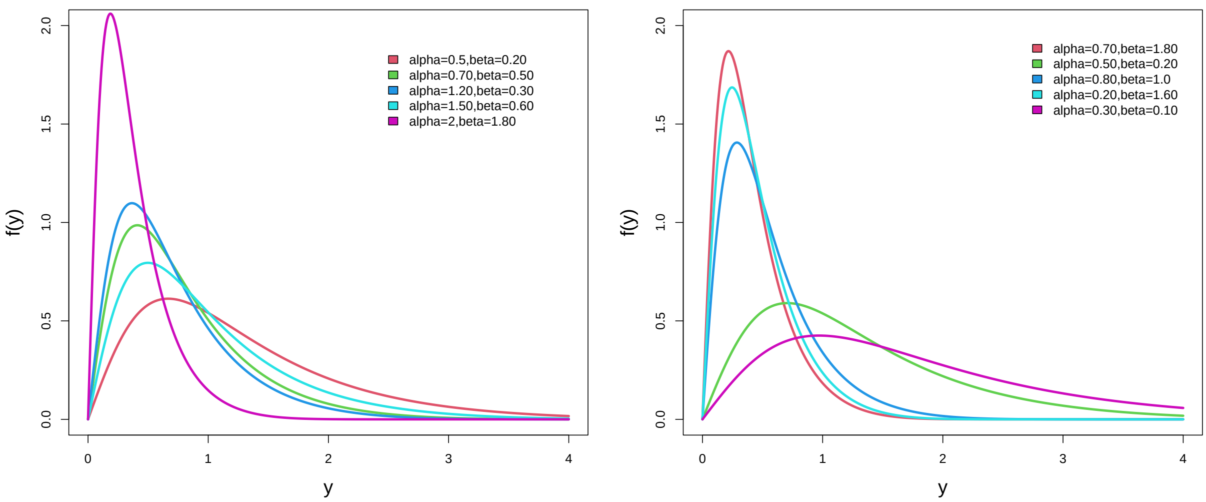

Figure 2. Plots of the pdf with varying parameters.

1.5. Parameter identifiability

A parametric family of continuous distributions is structurally identifiable if distinct parameter vectors uniquely determine completely distinct probability distributions throughout the support. Mathematically, this requires establishing the global injectivity of the parameterization, such that $F(y;\boldsymbol{\Theta}_1) = F(y;\boldsymbol{\Theta}_2)$ for all $y > 0$ implies $\boldsymbol{\Theta}_1 = \boldsymbol{\Theta}_2$.

Proposition 1.6 (Global structural identifiability of the NLRD)**.** *Let $\boldsymbol{\Theta}_1 = (\alpha_1,\beta_1)$ and $\boldsymbol{\Theta}_2 = (\alpha_2,\beta_2)$ be two parameter vectors belonging to the parameter space $\Omega = \{(\alpha,\beta) : \alpha > 0, \beta > 0\}$. If $F(y;\alpha_1,\beta_1) = F(y;\alpha_2,\beta_2)$ holds identically for all $y > 0$, then $\alpha_1 = \alpha_2$ and $\beta_1 = \beta_2$.*

Proof. Assume that for two parameter sets, the cumulative distribution functions are identical across the entire continuous support domain, meaning:

$$\frac{\ln[2 + e + \alpha_1 - (1 + e + \alpha_1)^{e^{-(y/\beta_1)^2}}]}{\ln(1 + e + \alpha_1)} = \frac{\ln[2 + e + \alpha_2 - (1 + e + \alpha_2)^{e^{-(y/\beta_2)^2}}]}{\ln(1 + e + \alpha_2)}, \quad \forall y > 0. \tag{1.10}$$

To establish uniqueness via a direct global proof, we apply the strictly monotonic exponential operator to both sides of Eq (1.10). Defining $C_k = 1 + e + \alpha_k > 1$ for $k = 1, 2$, the relation can be written in terms of functional powers:

$$2 + C_1 - C_1^{e^{-(y/\beta_1)^2}} = (2 + C_2 - C_2^{e^{-(y/\beta_2)^2}})^{\frac{\ln C_1}{\ln C_2}}. \tag{1.11}$$

Because Eq (1.11) must hold identically for all $y \in (0, \infty)$, it must also hold under continuous limits approaching the domain boundaries. Evaluating the right-sided limit of both sides as $y \to 0^+$, we observe that the baseline survival component satisfies $\lim_{y\to 0^+} e^{-(y/\beta_k)^2} = 1$. Consequently, the terms inside the base structures simplify cleanly to:

$$\lim_{y\to 0^+}(2 + C_k - C_k^{e^{-(y/\beta_k)^2}}) = 2 + C_k - C_k^1 = 2.$$

Substituting this boundary behavior directly into Eq (1.11) yields:

$$2 = 2^{\frac{\ln(C_1)}{\ln(C_2)}}.$$

Since $2 > 1$, the uniqueness of exponential maps dictates that the exponent must equal unity:

$$\frac{\ln(C_1)}{\ln(C_2)} = 1 \implies \ln(C_1) = \ln(C_2).$$

By the global injectivity of the natural logarithm over the positive real domain, we find $C_1 = C_2$, which simplifies immediately to:

$$1 + e + \alpha_1 = 1 + e + \alpha_2 \implies \alpha_1 = \alpha_2.$$

Having established that $\alpha_1 = \alpha_2 = \alpha$ (and hence $C_1 = C_2 = C$), we substitute this equality back into the functional identity in Eq (1.11), which collapses directly to:

$$2 + C - C^{e^{-(y/\beta_1)^2}} = 2 + C - C^{e^{-(y/\beta_2)^2}}.$$

Subtracting $2 + C$ from both sides and dividing by -1 results in:

$$C^{e^{-(y/\beta_1)^2}} = C^{e^{-(y/\beta_2)^2}}.$$

Taking the natural logarithm of both sides twice sequentially isolates the internal baseline structures:

$$\begin{aligned} e^{-(y/\beta_1)^2} \ln(C) = e^{-(y/\beta_2)^2} \ln(C) &\implies e^{-(y/\beta_1)^2} = e^{-(y/\beta_2)^2} \\ &\implies -\left(\frac{y}{\beta_1}\right)^2 = -\left(\frac{y}{\beta_2}\right)^2. \end{aligned}$$

Dividing through by $-y^2$ (since $y > 0$) gives:

$$\frac{1}{\beta_1^2} = \frac{1}{\beta_2^2} \implies \beta_1^2 = \beta_2^2.$$

Because the parameter space restricts the scale vector strictly to positive real values ($\beta_1, \beta_2 > 0$), taking the square root yields the unique structural solution:

$$\beta_1 = \beta_2.$$

Thus, $F(y; \alpha_1, \beta_1) = F(y; \alpha_2, \beta_2)$ for all $y > 0$ directly and uniquely implies that $\alpha_1 = \alpha_2$ and $\beta_1 = \beta_2$, completely establishing the global structural identifiability of the NLRD framework. □

2. Properties

This section provides insights into the various properties of the proposed generator with details provided in Appendix C, using the Rayleigh distribution as the baseline.

2.1. Asymptotic evaluation of the NLRD

Let us now construct several asymptotic expansions by considering the Rayleigh distribution as the foundational model for the NLG family. Referring to Subsection 1.4, we derive the following correspondences when $y \to 0$:

Proposition 2.1 (NLRD asymptotics at the lower boundary)**.** *As the continuous domain parameter approaches the origin ($y \to 0$), the baseline Rayleigh distribution functions scale via first-order linearizations. Incorporating the normalization framework, the sub-model expressions evaluate directly to:*

$$\begin{aligned} F(y; \alpha, \beta) &\sim \frac{1 + e + \alpha}{\ln(1 + e + \alpha)} \left(\frac{y}{\beta}\right)^2, \\ f(y; \alpha, \beta) &\sim \frac{2(1 + e + \alpha)}{\ln(1 + e + \alpha)} \frac{y}{\beta^2}, \\ h(y; \alpha, \beta) &\sim \frac{2(1 + e + \alpha)\, y}{\beta^2 \ln(1 + e + \alpha) - (1 + e + \alpha) y^2}. \end{aligned}$$

Proof. Consider the limiting behavior of the baseline Rayleigh distribution functions near the origin. As $y \to 0$, applying a first-order Taylor series expansion to the exponential components yields $G(y;\beta) = 1 - e^{-(y/\beta)^2} \sim (y/\beta)^2$ and $g(y;\beta) = \frac{2y}{\beta^2}e^{-(y/\beta)^2} \sim \frac{2y}{\beta^2}$. Substituting these baseline structural approximations into the general family lower bound limits established in Proposition 1.4 reveals that:

$$F(y;\alpha,\beta) \sim \frac{1+e+\alpha}{\ln(1+e+\alpha)}G(y;\beta) = \frac{1+e+\alpha}{\ln(1+e+\alpha)}\left(\frac{y}{\beta}\right)^2.$$

Similarly, substituting $g(y;\beta)$ into the limiting density equivalence framework gives:

$$f(y;\alpha,\beta) \sim \frac{1+e+\alpha}{\ln(1+e+\alpha)}g(y;\beta) = \frac{2(1+e+\alpha)}{\ln(1+e+\alpha)}\frac{y}{\beta^2}.$$

Finally, evaluating the ratio for the hazard rate framework $h(y;\alpha,\beta) = \frac{f(y;\alpha,\beta)}{1-F(y;\alpha,\beta)}$ under the matching first-order dynamic trajectories yields the final asymptotic relation:

$$h(y;\alpha,\beta) \sim \frac{\frac{2(1+e+\alpha)}{\ln(1+e+\alpha)}\frac{y}{\beta^2}}{1-\frac{1+e+\alpha}{\ln(1+e+\alpha)}(y/\beta)^2} = \frac{2(1+e+\alpha)y}{\beta^2\ln(1+e+\alpha)-(1+e+\alpha)y^2}.$$

This completes the proof. □

Hence, from these structural equivalences, we formally maintain that $\lim_{y\to 0} f(y;\alpha,\beta) = 0$.

Proposition 2.2 (NLRD asymptotics at the upper boundary). *As the tail values expand out toward infinity ($y \to \infty$), the limiting structural shapes map according to:*

$$F(y;\Omega) \sim 1 - \frac{e^{-(y/\beta)^2}}{1+e+\alpha},$$
$$f(y;\Omega) \sim \frac{2y\,e^{-(y/\beta)^2}}{\beta^2(1+e+\alpha)},$$
$$h(y;\Omega) \sim \frac{2y}{\beta^2}.$$

From the above equivalence, we have $\lim_{y\to\infty} f(y;\alpha,\beta) = 0$. However, $\lim_{y\to\infty} H(y;\alpha,\beta) = \infty$.

2.2. Moments

Before evaluating the explicit expressions for the moments, incomplete moments, and informational entropies, we establish the mathematical validity of exchanging the order of infinite summation and integration.

Theorem 2.3 (Validity of term-by-term integration). *Let* $f(y;\Omega) = \sum_{i=0}^{\infty}\sum_{j=0}^{\infty}\eta_{ij}g(y;\Omega)[S(y;\Omega)]^j$ *be the linear expansion of the density function. For any measurable kernel* $\psi(Y)$ *such that* $\mathbb{E}_g[|\psi(Y)|] < \infty$ *under the baseline distribution, the identity*

$$\int_0^\infty \psi(y)f(y;\Omega)\,\mathrm{d}y = \sum_{i=0}^{\infty}\sum_{j=0}^{\infty}\eta_{ij}\int_0^\infty \psi(y)g(y;\Omega)[S(y;\Omega)]^j\,\mathrm{d}y \tag{2.1}$$

holds strictly by virtue of the Fubini-Tonelli theorems.

Proof. To establish the legitimacy of interchanging the operators, we analyze the absolute integrability of the functional component series $f_{ij}(y) = \eta_{ij}\psi(y)g(y;\Omega)[S(y;\Omega)]^j$ with respect to the product measure of the counting measure on $\mathbb{N}^2$ and the Lebesgue measure on $(0,\infty)$. We evaluate two operational regimes based on the sign profile of the kernel $\psi(y)$:

- **For non-negative kernels (raw and incomplete moments):** When $\psi(y) \geq 0$ (such as $\psi(y) = y^r$ for $y > 0$), we observe that the baseline density satisfies $g(y;\Omega) \geq 0$, and the survival component is bounded by $S(y;\Omega) \in [0,1]$. Thus, the functional terms are non-negative everywhere on their support ($f_{ij}(y) \geq 0$). Under non-negativity, Tonelli's theorem guarantees that the infinite double summation and the integral operator commute unconditionally, ensuring that the identity holds for all raw and incomplete moments regardless of uniform convergence.
- **For signed kernels (logarithmic and entropy operators):** When $\psi(y)$ contains signed functions (such as $\ln f(y;\Omega)$), the unconditional property of Tonelli's theorem no longer applies. To justify the interchange via Fubini's theorem, we must demonstrate absolute convergence over the product domain, satisfying:

$$\sum_{i=0}^{\infty}\sum_{j=0}^{\infty}\int_0^{\infty}\left|\eta_{ij}\psi(y)g(y;\Omega)[S(y;\Omega)]^j\right|\mathrm{d}y < \infty.$$

  Because the baseline survival function is strictly bounded by $|S(y;\Omega)|^j \leq 1$ for all $y \in (0,\infty)$, each component is dominated point-wise by a non-negative majorant:

$$|f_{ij}(y)| = \left|\eta_{ij}\psi(y)g(y;\Omega)[S(y;\Omega)]^j\right| \leq |\eta_{ij}|\,|\psi(y)|g(y;\Omega).$$

  Integrating this dominating function over the support yields:

$$\int_0^{\infty}|\eta_{ij}|\,|\psi(y)|\,g(y;\Omega)\,\mathrm{d}y = |\eta_{ij}|\int_0^{\infty}|\psi(y)|\,g(y;\Omega)\,\mathrm{d}y = |\eta_{ij}|\,\mathbb{E}_g[|\psi(Y)|].$$

  By hypothesis, the absolute expectation under the baseline distribution is finite, $\mathbb{E}_g[|\psi(Y)|] = C < \infty$. Summing over the full indices produces:

$$\sum_{i=0}^{\infty}\sum_{j=0}^{\infty}\int_0^{\infty}|f_{ij}(y)|\,\mathrm{d}y \leq C\sum_{i=0}^{\infty}\sum_{j=0}^{\infty}|\eta_{ij}|.$$

  Since the sequence of structural mixture weights is absolutely convergent ($\sum_{i=0}^{\infty}\sum_{j=0}^{\infty}|\eta_{ij}| < \infty$), the entire double series of integrals converges to a finite boundary. This absolute integrability satisfies the precise requirements of Fubini's theorem, validating the algebraic term-by-term integration step in Eq (2.1).

□

Let us assume Y represents a random variable following the NLRD framework, and then the r^{th} raw moment of Y, denoted as μ'_r, is defined as follows:

$$\mu'_r = \mathbb{E}(Y^r) = \int_0^{\infty} y^r f(y;\alpha,\beta)\,\mathrm{d}y. \tag{2.2}$$

Applying the proven term-by-term integration framework from Eq (2.1) to Eq (2.2), we obtain:

$$\mu_r' = \sum_{i=0}^{\infty}\sum_{j=0}^{\infty}\eta_{ij}\int_0^{\infty} y^r g(y;\beta)S(y;\beta)^j\,\mathrm{d}y$$
$$= \sum_{i=0}^{\infty}\sum_{j=0}^{\infty}\eta_{ij}\frac{2}{\beta^2}\int_0^{\infty} y^{r+1}e^{-(j+1)(y/\beta)^2}\,\mathrm{d}y.$$

By substituting the transformation variable $t = (j+1)(y/\beta)^2$, such that $0 < t < \infty$ and $dy = \frac{\beta}{2\sqrt{j+1}}t^{-1/2}dt$, the resulting moment expression scales directly to:

$$\mu_r' = \sum_{i=0}^{\infty}\sum_{j=0}^{\infty}\eta_{ij}\frac{\beta^r}{(j+1)^{\frac{r}{2}+1}}\int_0^{\infty} t^{\frac{r}{2}}e^{-t}\,\mathrm{d}t.$$

Evaluating the definitive integral via the standard gamma function definition yields the final closed-form representation:

$$\mu_r' = \sum_{i=0}^{\infty}\sum_{j=0}^{\infty}\eta_{ij}\frac{\beta^r}{(j+1)^{\frac{r}{2}+1}}\Gamma\left(\frac{r}{2}+1\right). \tag{2.3}$$

Within this framework, where $\Gamma(\cdot)$ represents the complete gamma function, the harmonic mean is recovered as a specific instance corresponding to $r = -1$. The standard moments of the distribution—specifically the first four—are derived by evaluating Eq (2.3) for $r = 1, 2, 3, 4$. The first of these, μ_1', defines the population mean. Subsequently, the central variance (Var) and coefficient of variation (CV) are determined directly via:

$$\mathrm{Var} = \mu_2 = \mu_2' - (\mu_1')^2 \qquad \text{and} \qquad \mathrm{CV} = \frac{\sqrt{\mu_2' - (\mu_1')^2}}{\mu_1'},$$

respectively.

Furthermore, the moment generating function of the NLRD is denoted by $M_Y(t)$ and is derived by utilizing the linear mixture representation of the pdf alongside the power series expansion of the exponential kernel, $e^{ty} = \sum_{r=0}^{\infty}\frac{t^r}{r!}y^r$. Taking the mathematical expectation yields:

$$M_Y(t) = \mathbb{E}(e^{tY}) = \int_0^{\infty} e^{ty}f(y;\alpha,\beta)\,\mathrm{d}y = \sum_{r=0}^{\infty}\frac{t^r}{r!}\int_0^{\infty} y^r f(y;\alpha,\beta)\,\mathrm{d}y = \sum_{r=0}^{\infty}\frac{t^r}{r!}\mathbb{E}(Y^r)$$
$$= \sum_{i=0}^{\infty}\sum_{j=0}^{\infty}\sum_{r=0}^{\infty}\eta_{ij}\frac{t^r\beta^r}{r!(j+1)^{\frac{r}{2}+1}}\Gamma\left(\frac{r}{2}+1\right), \tag{2.4}$$

where η_{ij} are the fixed mixture coefficients and $\Gamma(\cdot)$ represents the standard complete gamma function.

The analytical existence and global convergence of the infinite series expansion in Eq (2.4) are established under the following rigorous conditions:

(i) **Global convergence domain via completing the square:** While the mixture representation of the MGF structurally relies on component integration, the strict analytical existence of the integral $\int_0^\infty e^{ty} f(y;\alpha,\beta)\,\mathrm{d}y$ for any arbitrary $t \in \mathbb{R}$ is validated by completing the square in the exponent of each component mixture term. For a fixed index j, the underlying core integral is defined as:

$$I_j(t) = \frac{2}{\beta^2} \int_0^\infty y \cdot \exp\left\{ty - \frac{j+1}{\beta^2} y^2\right\} \mathrm{d}y.$$

Letting $\kappa = \frac{j+1}{\beta^2} > 0$, we restructure the quadratic expression within the exponential operator by completing the square:

$$ty - \kappa y^2 = -\kappa\left(y^2 - \frac{t}{\kappa} y\right) = -\kappa\left(y - \frac{t}{2\kappa}\right)^2 + \frac{t^2}{4\kappa}.$$

Isolating the constant shift parameters transforms the component expression into:

$$I_j(t) = \frac{2}{\beta^2} \exp\left(\frac{t^2\beta^2}{4(j+1)}\right) \int_0^\infty y \cdot \exp\left\{-\frac{j+1}{\beta^2}\left(y - \frac{t\beta^2}{2(j+1)}\right)^2\right\} \mathrm{d}y.$$

Applying the transformation $x = \frac{\sqrt{j+1}}{\beta}(y - \frac{t\beta^2}{2(j+1)})$ shifts the domain boundaries and maps the expression into a combination of a standard Gaussian integral and a shift parameter component evaluated via the complementary error function $\mathrm{erfc}(\cdot)$:

$$I_j(t) = \frac{1}{j+1} + \frac{t\beta\sqrt{\pi}}{2(j+1)^{3/2}} \exp\left(\frac{t^2\beta^2}{4(j+1)}\right)\left[1 + \mathrm{erf}\left(\frac{t\beta}{2\sqrt{j+1}}\right)\right].$$

Because the error function is bounded, $|\mathrm{erf}(z)| < 1$ for all real arguments, $I_j(t)$ yields a finite positive real value for any $t \in \mathbb{R}$. As $j \to \infty$, the exponential component approaches unity ($\exp(0) = 1$), bounding the integrated sequence asymptotically to a stable harmonic decay pattern $I_j(t) \sim O\left(\frac{1}{j+1}\right)$. Consequently, the complete MGF integration behaves as an absolutely convergent system across all real values of t, establishing an infinite radius of convergence ($t \in \mathbb{R}$) and justifying the global interchange of operations via Fubini's theorem.

(ii) **Finiteness of component moments:** The component integrals $\int_0^\infty y^r e^{-(j+1)(y/\beta)^2}\,\mathrm{d}y$ converge definitively for all $r > -2$ due to the properties of the baseline Rayleigh core. This ensures that the structural argument of the complete gamma function, $\frac{r}{2} + 1$, remains strictly within the positive real domain where the gamma function is smooth, real, and finite.

(iii) **Boundedness of mixture weights:** The shape parameter $\alpha > 0$ and scale parameter $\beta > 0$ ensure that the mixture weights η_{ij} are real and stable. The weights η_{ij} emerge from a binomial series expansion of $(1-z)^{-1}$, where $z = \frac{(1+e+\alpha)^{S(y)}}{2+e+\alpha}$. Given that the baseline survival function is bounded by $0 < S(y) < 1$ for all $y \in (0,\infty)$, the base term evaluates strictly to $1 < (1+e+\alpha)^{S(y)} < 1+e+\alpha$. It follows directly that $z < \frac{1+e+\alpha}{2+e+\alpha} < 1$, guaranteeing the absolute, geometric convergence of the structural mixture coefficients ($\sum_{i,j=0}^{\infty} |\eta_{ij}| < \infty$).

These verified criteria confirm that the MGF series and the subsequent directional moments derived in Subsection 2.2 are mathematically robust, globally well-defined, and computationally stable across the entire parameter space.

2.3. Incomplete moments

The v^{th} incomplete moment of the NLRD can be obtained as

$$\begin{aligned} I(v) &= \int_0^y y^v f(y;\Theta)\,\mathrm{d}y \\ &= \sum_{i,j=0}^{\infty} \eta_{ij} \frac{2}{\beta^2} \int_0^y y^{v+1} e^{-(j+1)(y/\beta)^2}\,\mathrm{d}y. \end{aligned}$$

On substituting $(j+1)(y/\beta)^2 = t$, so that $0 < t < (j+1)(v/\beta)^2$, we have

$$I(v) = \sum_{i,j=0}^{\infty} \eta_{ij} \frac{\beta^v}{(j+1)^{\frac{v}{2}+1}} \int_0^{(j+1)(v/\beta)^2} t^{\frac{v}{2}} e^{-t}\,\mathrm{d}t.$$

The, we obtain the following:

$$I(v) = \sum_{i,j=0}^{\infty} \eta_{ij} \frac{\beta^v}{(j+1)^{\frac{v}{2}+1}} \gamma\left(\frac{v}{2}+1,\ (j+1)(v/\beta)^2\right),$$

where $\gamma(a,u) = \int_0^u x^{a-1} e^{-x}\,\mathrm{d}x$ denotes the lower incomplete gamma function.

2.4. Quantile function of the NLRD

The exact, closed-form quantile function $Q(u;\alpha,\beta)$ of the NLRD is derived by setting the cumulative distribution function $F(y;\alpha,\beta) = u$ and algebraically isolating the domain variable y. From this inversion process, we obtain:

$$Q(u;\alpha,\beta) = \beta \sqrt{-\ln\left(\frac{2+e+\alpha-(1+e+\alpha)^u}{1+e+\alpha}\right)}, \quad u \in (0,1). \tag{2.5}$$

The explicit formulation in Eq (2.5) establishes a clean, computationally efficient framework that avoids numerical root-finding routines during random variable generation. Furthermore, it serves as the exact baseline for calculating the robust, non-parametric Galton skewness (γ_3) and Moors kurtosis (γ_4) properties.

2.5. Scale invariance of descriptive shape metrics

To formally establish the structural characterization of the NLRD framework, we verify that the coefficient of variation (CV), Galton skewness (S_G), and Moors kurtosis (K_M) are invariant under changes to the scale parameter $\beta > 0$.

Proposition 2.4 (Formal invariance properties)**.** *Let $Y \sim NLRD(\alpha,\beta)$ be a random variable with shape parameter $\alpha > 0$ and scale parameter $\beta > 0$. The descriptive measures CV, S_G, and K_M are strictly invariant with respect to β, rendering them pure functions of the shape modifier α.*

Proof. Let $X \sim$ NLRD $(\alpha, 1)$ represent the standardized baseline random variable corresponding to a unit scale parameter ($\beta = 1$). By performing a direct transformation of variables on the cumulative distribution function $F_Y(y; \alpha, \beta)$, we establish the linear scale decomposition:

$$Y = \beta X. \tag{2.6}$$

We analyze the behavior of the moment-based and quantile-based descriptive functions under this linear transformation:

- **Invariance of the coefficient of variation (CV):** From the linear relation in Eq (2.6) and the homogeneity property of expectation operators, the r^{th} raw moment of Y scales directly as:

$$\mu_r'(Y) = \mathbb{E}(Y^r) = \mathbb{E}[(\beta X)^r] = \beta^r \mathbb{E}(X^r) = \beta^r \mu_r'(X).$$

  Evaluating this structure for the first two raw moments yields $\mu_1'(Y) = \beta\mu_1'(X)$ and $\mu_2'(Y) = \beta^2\mu_2'(X)$. Substituting these relations into the algebraic formula for the variance of Y gives:

$$\mathrm{Var}(Y) = \mu_2'(Y) - [\mu_1'(Y)]^2 = \beta^2\mu_2'(X) - [\beta\mu_1'(X)]^2 = \beta^2\,\mathrm{Var}(X).$$

  Consequently, the standard deviation scales linearly as $\sigma(Y) = \sqrt{\mathrm{Var}(Y)} = \beta\sigma(X)$. Substituting the mean and standard deviation into the definition of the CV leads to a complete cancellation of the scale parameter:

$$CV(Y) = \frac{\sigma(Y)}{\mu_1'(Y)} = \frac{\beta\sigma(X)}{\beta\mu_1'(X)} = \frac{\sigma(X)}{\mu_1'(X)} = CV(X).$$

  Since $CV(X)$ is computed under a fixed scale parameter $\beta = 1$, it is a function exclusively of α, proving the invariance of $CV(Y)$ with respect to β.

- **Invariance of quantile-based measures (S_G and K_M):** Let $Q_Y(p)$ and $Q_X(p)$ denote the quantile functions of Y and X at a probability level $p \in (0, 1)$, defined via the probability mapping $F_Y(Q_Y(p)) = p$. Utilizing the scale relation from Eq (2.6), the distribution fields satisfy:

$$F_Y(y; \alpha, \beta) = F_X\left(\frac{y}{\beta}; \alpha, 1\right) \implies F_X\left(\frac{Q_Y(p)}{\beta}; \alpha, 1\right) = p.$$

  By the definition of the inverse mapping function for the standardized variable, we find:

$$\frac{Q_Y(p)}{\beta} = Q_X(p) \implies Q_Y(p) = \beta Q_X(p).$$

  Thus, every individual quantile point scales linearly with β. We evaluate the impact of this linear scaling property on Galton skewness (S_G) and Moors kurtosis (K_M):
  (1) Galton skewness is defined via the octile ratio equation:

$$S_G(Y) = \frac{Q_Y(6/8) - 2Q_Y(4/8) + Q_Y(2/8)}{Q_Y(6/8) - Q_Y(2/8)}.$$

  Substituting the scaled quantile relations $Q_Y(p) = \beta Q_X(p)$ into the expression factors out β completely:

$$S_G(Y) = \frac{\beta Q_X(6/8) - 2\beta Q_X(4/8) + \beta Q_X(2/8)}{\beta Q_X(6/8) - \beta Q_X(2/8)} = \frac{Q_X(6/8) - 2Q_X(4/8) + Q_X(2/8)}{Q_X(6/8) - Q_X(2/8)} = S_G(X).$$

(2) Similarly, Moors kurtosis is structurally defined as:

$$K_M(Y) = \frac{Q_Y(7/8) - Q_Y(5/8) + Q_Y(3/8) - Q_Y(1/8)}{Q_Y(6/8) - Q_Y(2/8)}.$$

Applying the same quantile substitution strips away the scale multiplier:

$$K_M(Y) = \frac{\beta\,[Q_X(7/8) - Q_X(5/8) + Q_X(3/8) - Q_X(1/8)]}{\beta\,[Q_X(6/8) - Q_X(2/8)]} = K_M(X).$$

Because $CV(Y) = CV(X)$, $S_G(Y) = S_G(X)$, and $K_M(Y) = K_M(X)$, and all baseline metrics of X are determined entirely at a fixed scale coordinate $\beta = 1$, it is rigorously established that these descriptive metrics are completely invariant under any changes to the scale parameter β. □

Table 1 presents the calculated values for the mean, central variance, coefficient of variation (CV), Galton skewness (γ_3), and Moors kurtosis (γ_4) of the NLRD across a broad spectrum of parameter vectors. A critical inspection of the numerical behaviors confirms absolute consistency with the analytical laws governing parametric distributions. Specifically, when holding the shape parameter α constant (as observed in the $\alpha = 6.5$ and $\alpha = 7.0$ blocks), an increase in the scale parameter β results in a strictly monotonic, linear increase in the population mean and a corresponding quadratic growth in the variance. This behavior naturally reflects the scale structural identity $Y = \beta X$ inherited from the underlying baseline model. Conversely, the non-parametric indices—namely, CV, γ_3, and γ_4—remain strictly invariant with respect to changes in β under a fixed shape value. Shifting the parameter α independently controls the structural asymmetry and tail shape parameters of the density function, proving that the parameter spaces are mathematically uncoupled and properly aligned with standard statistical inference assumptions.

Figure 3 presents the 3D surface plots depicting the mean, variance, skewness, and kurtosis of the distribution as functions of its shaping parameters, revealing the evolution of its statistical characteristics. The average surface shows a fairly level, steady plane over the majority of parameter values but descends into a sharp, curved drop as it nears the lower limits of the parameters. In comparison, the variance surface displays a significant, raised ridge that sharply peaks at one corner before descending into a gentle, wide valley throughout the remainder of the area. The skewness surface displays a broad, gently curved plateau that retains positive values across an extensive area, gradually descending toward the edges to signify a shift to reduced asymmetry. Ultimately, the kurtosis surface features a sharply defined, towering peak in the rear section where values rise significantly, whereas the other parameter region creates a flat, low-lying basin, indicating that extreme tail-weight arises solely within a particular parameter setup.

Table 1. The mean, variance, CV, γ_3, and γ_4 for the NLRD across distinct parameter combinations.

α	β	Mean	Variance	CV	γ_3	γ_4
1.2	1.5	0.94121	0.26120	0.54291	0.11144	1.19312
1.5	2.0	1.15542	0.42673	0.56540	0.12581	1.20737
2.5	3.0	1.51268	0.88509	0.62198	0.15113	1.24948
3.0	3.5	1.67051	1.15042	0.64205	0.16921	1.26850
3.5	4.0	1.81520	1.43120	0.65912	0.18907	1.28344
4.0	4.5	1.94721	1.72445	0.67441	0.20101	1.30174
4.5	5.0	2.06815	2.02551	0.68797	0.21506	1.32316
5.0	6.0	2.37542	2.76012	0.69931	0.22281	1.34297
5.5	6.5	2.47910	3.08412	0.70832	0.23545	1.36188
6.0	7.0	2.57602	3.41870	0.71790	0.24385	1.37920
6.5	7.5	2.66692	3.76342	0.72721	0.25204	1.39411
6.5	8.0	2.84471	4.27565	0.72721	0.25204	1.39411
6.5	8.5	3.02251	4.82733	0.72721	0.25204	1.39411
6.5	9.0	3.20030	5.41164	0.72721	0.25204	1.39411
6.5	9.5	3.37810	6.02859	0.72721	0.25204	1.39411
6.5	10.0	3.55589	6.67817	0.72721	0.25204	1.39411
7.0	7.5	2.60114	3.65421	0.73492	0.26012	1.40822
7.0	8.0	2.77455	4.15132	0.73492	0.26012	1.40822
7.0	8.5	2.94796	4.68683	0.73492	0.26012	1.40822
7.0	9.0	3.12137	5.25471	0.73492	0.26012	1.40822
7.0	9.5	3.29478	5.85497	0.73492	0.26012	1.40822
7.0	10.0	3.46819	6.48761	0.73492	0.26012	1.40822

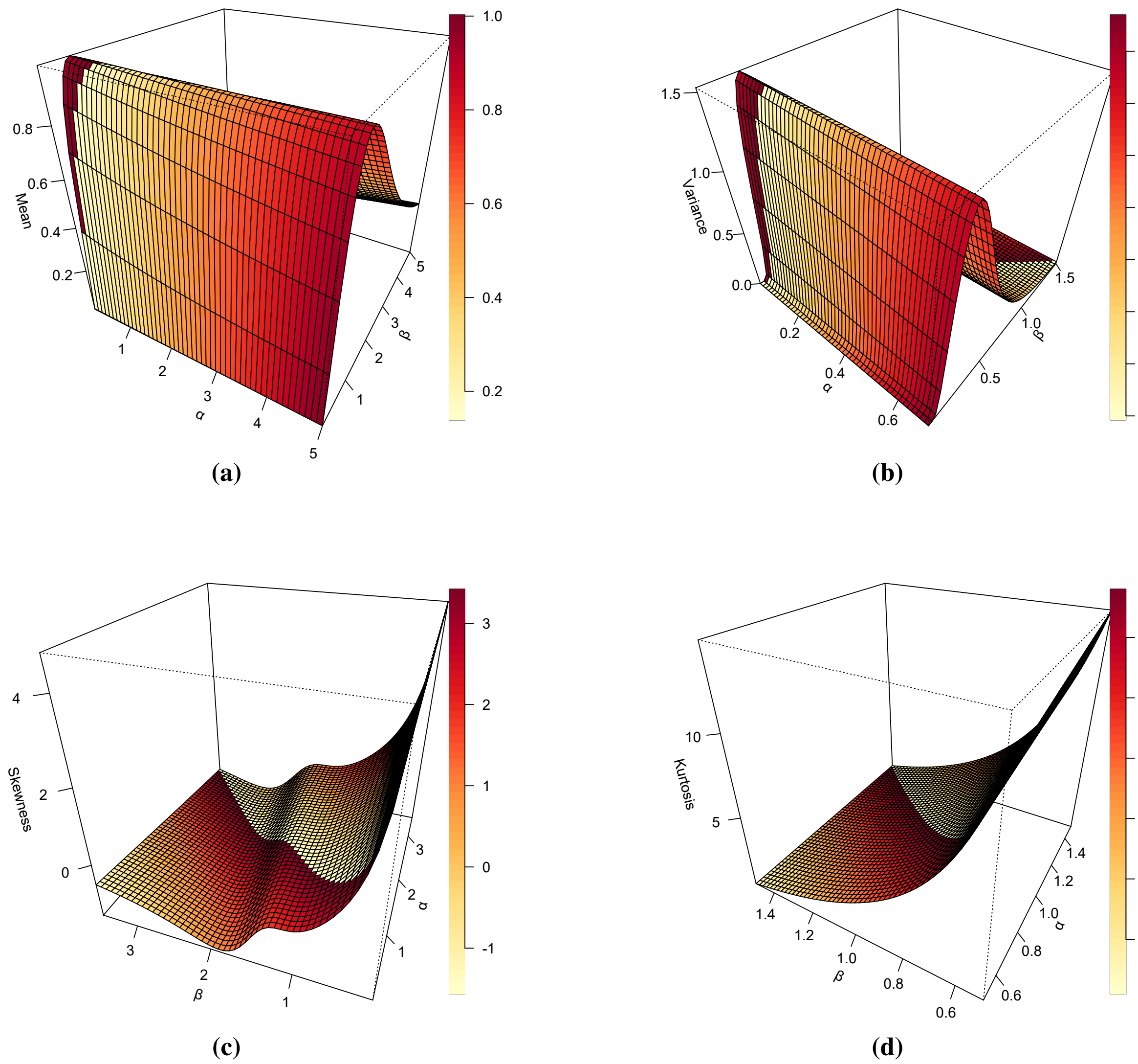

Figure 3. Plots of (a) mean, (b) variance, (c) skewness, and (d) Kurtosis of the NLRD distribution.

2.6. *Order statistics*

Consider a random sample of size n taken from the NLRD with pdf $f(y)$ and cdf $F(y)$, denoted by $Y_1, Y_2, \cdots, Y_n$. Then the pdf of the r^{th} order statistics can be obtained as

$$f_Y(r) = \frac{n!}{(r-1)!(n-r)!} f(y)[F(y)]^{r-1}[1-F(y)]^{n-r}. \tag{2.7}$$

Using Eqs (1.8) and (1.9) in Eq (2.7), we have

$$f_Y(r) = \frac{n!}{(r-1)!\,(n-r)!}\,\frac{2\beta y\, e^{-(y/\beta)^2}(1+e+\alpha)^{e^{-(y/\beta)^2}}}{2+e+\alpha-(1+e+\alpha)^{e^{-(y/\beta)^2}}}$$
$$\times\left[\frac{\ln(2+e+\alpha-(1+e+\alpha)^{e^{-(y/\beta)^2}})}{\ln(1+e+\alpha)}\right]^{r-1}\left[1-\frac{\ln(2+e+\alpha-(1+e+\alpha)^{e^{-(y/\beta)^2}})}{\ln(1+e+\alpha)}\right]^{n-r}.$$

Often the first and nth order statistics, denoted by Y_1 and Y_n, respectively, play a vital role. Therefore, the density of Y_1 and Y_n for the NLRD are obtained and are given as

$$f_Y(1) = \frac{2n\beta y\, e^{-(y/\beta)^2}(1+e+\alpha)^{e^{-(y/\beta)^2}}}{2+e+\alpha-(1+e+\alpha)^{e^{-(y/\beta)^2}}}\left[1-\frac{\ln(2+e+\alpha-(1+e+\alpha)^{e^{-(y/\beta)^2}})}{\ln(1+e+\alpha)}\right]^{n-1},$$
$$f_Y(n) = \frac{2n\beta y\, e^{-(y/\beta)^2}(1+e+\alpha)^{e^{-(y/\beta)^2}}}{2+e+\alpha-(1+e+\alpha)^{e^{-(y/\beta)^2}}}\left[\frac{\ln(2+e+\alpha-(1+e+\alpha)^{e^{-(y/\beta)^2}})}{\ln(1+e+\alpha)}\right]^{n-1}.$$

2.7. Convergence of informational multi-series expansion

To establish the analytic validity and numerical stability of the derived informational metrics (Tsallis, Rényi, and Arimoto entropies), we must rigorously prove that the double-infinite series defining the integrated total density function converges absolutely. Let the component terms of the multi-series expansion be written as $\mathcal{S} = \sum_{i=0}^{\infty}\sum_{j=0}^{\infty} A_{ij}(\gamma)$, where the structural terms are defined as:

$$A_{ij}(\gamma) = \psi_{ij}\frac{2^{\gamma-1}\beta}{(j+\gamma)^{\frac{\gamma}{2}+1}}\Gamma\left(\frac{\gamma+1}{2}\right),$$

with the coefficient weight system ψ_{ij} explicitly given by:

$$\psi_{ij} = \binom{\gamma+i-1}{i}\frac{(i+\gamma)^j}{(2+e+\alpha)^{i+\gamma}}\,\frac{(\ln(1+e+\alpha))^j}{j!}.$$

To justify global convergence for any given parameters $\alpha > 0, \beta > 0$, and $\gamma > 0$ $(\gamma \neq 1)$, we evaluate the absolute sum over both indices systematically using the properties of the generalized binomial and exponential series maps:

(i) **Summation over the index j:** For a fixed outer index i, we gather all structural factors dependent on j. Let $\theta = \ln(1+e+\alpha) > 0$. The absolute inner series sum takes the form:

$$\sum_{j=0}^{\infty}|A_{ij}(\gamma)| = \binom{\gamma+i-1}{i}\frac{2^{\gamma-1}\beta\,\Gamma(\frac{\gamma+1}{2})}{(2+e+\alpha)^{i+\gamma}}\sum_{j=0}^{\infty}\frac{(i+\gamma)^j\theta^j}{j!(j+\gamma)^{\frac{\gamma}{2}+1}}.$$

Since $j \geq 0$ and $\gamma > 0$, the denominator is strictly bounded from below by $(j+\gamma)^{\frac{\gamma}{2}+1} \geq \gamma^{\frac{\gamma}{2}+1}$. Factoring out this lower bound yields a majorant that mirrors a standard Maclaurin exponential series expansion:

$$\sum_{j=0}^{\infty}\frac{(i+\gamma)^j\theta^j}{j!(j+\gamma)^{\frac{\gamma}{2}+1}} \leq \frac{1}{\gamma^{\frac{\gamma}{2}+1}}\sum_{j=0}^{\infty}\frac{[\theta(i+\gamma)]^j}{j!} = \frac{1}{\gamma^{\frac{\gamma}{2}+1}}\exp\left(\theta(i+\gamma)\right).$$

Recalling that $\exp(\theta(i+\gamma)) = \exp(\ln(1+e+\alpha))^{i+\gamma} = (1+e+\alpha)^{i+\gamma}$, the inner component summation collapses to the following point-wise upper bound for each index i:

$$\sum_{j=0}^{\infty} |A_{ij}(\gamma)| \leq \left[\frac{2^{\gamma-1}\beta\,\Gamma(\frac{\gamma+1}{2})}{\gamma^{\frac{\gamma}{2}+1}}\right]\binom{\gamma+i-1}{i}\left(\frac{1+e+\alpha}{2+e+\alpha}\right)^{i+\gamma}.$$

(ii) **Summation over the outer index i:** We now evaluate the full double-infinite system by summing the derived majorant over the structural shape index i:

$$\sum_{i=0}^{\infty}\sum_{j=0}^{\infty} |A_{ij}(\gamma)| \leq \left[\frac{2^{\gamma-1}\beta\,\Gamma(\frac{\gamma+1}{2})}{\gamma^{\frac{\gamma}{2}+1}}\right]\sum_{i=0}^{\infty}\binom{\gamma+i-1}{i}\left(\frac{1+e+\alpha}{2+e+\alpha}\right)^{i+\gamma}.$$

Let $\rho = \frac{1+e+\alpha}{2+e+\alpha}$. Because the model restrictions stipulate $\alpha > 0$, it follows directly that $0 < \rho < 1$. Factoring out the base term ρ^{γ}, the remaining infinite series can be evaluated using the negative binomial expansion formula:

$$\sum_{i=0}^{\infty}\binom{\gamma+i-1}{i}\rho^{i} = (1-\rho)^{-\gamma}.$$

Substituting ρ back into the negative binomial identity clarifies the expression:

$$1-\rho = 1-\frac{1+e+\alpha}{2+e+\alpha} = \frac{1}{2+e+\alpha} \implies (1-\rho)^{-\gamma} = (2+e+\alpha)^{\gamma}.$$

Multiplying by the constant factor ρ^{γ} yields:

$$\rho^{\gamma}(1-\rho)^{-\gamma} = \left(\frac{1+e+\alpha}{2+e+\alpha}\right)^{\gamma}(2+e+\alpha)^{\gamma} = (1+e+\alpha)^{\gamma}.$$

Combining these expressions, the global double series is bounded by a finite real value:

$$\sum_{i=0}^{\infty}\sum_{j=0}^{\infty} |A_{ij}(\gamma)| \leq \left[\frac{2^{\gamma-1}\beta\,\Gamma(\frac{\gamma+1}{2})}{\gamma^{\frac{\gamma}{2}+1}}\right](1+e+\alpha)^{\gamma} < \infty.$$

This confirms that the double-infinite series expansion is globally and absolutely convergent for all valid parameter coordinates within Ω. This mathematical validity permits the subsequent explicit evaluation of the entropy variants and ensures high numerical stability.

2.8. *Tsallis entropy*

Let Y be a random variable following the NLRD. Then the Tsallis entropy is described as

$$T_{\gamma} = \frac{1}{\gamma-1}\left[1-\int_{0}^{\infty} f^{\gamma}(y)\,\mathrm{d}y\right], \tag{2.8}$$

for $\gamma \neq 1$ and $\gamma > 0$. Expanding the structural definition yields:

$$\int_{0}^{\infty} f^{\gamma}(y)\,\mathrm{d}y = \int_{0}^{\infty}(2+e+\alpha)^{-\gamma}\,g(y;\Omega)^{\gamma}(1+e+\alpha)^{\gamma S(y;\Omega)}\left(1-\frac{(1+e+\alpha)^{S(y;\Omega)}}{2+e+\alpha}\right)^{-\gamma}\,\mathrm{d}y.$$

Using the generalized binomial theorem $(1-u)^{-a} = \sum_{i=0}^{\infty} \binom{a+i-1}{i} u^i$, we have

$$\int_0^\infty f^\gamma(y)\,\mathrm{d}y = \sum_{i=0}^{\infty} \binom{\gamma+i-1}{i} \frac{1}{(2+e+\alpha)^{i+\gamma}} \int_0^\infty g(y;\Omega)^\gamma (1+e+\alpha)^{(i+\gamma)S(y;\Omega)}\,\mathrm{d}y.$$

Applying Taylor's series $a^x = \sum_{j=0}^{\infty} \frac{(\ln(a))^j}{j!} x^j$, we have

$$\begin{aligned}\int_0^\infty f^\gamma(y)\,\mathrm{d}y &= \sum_{i,j=0}^{\infty} \binom{\gamma+i-1}{i} \frac{(i+\gamma)^j}{(2+e+\alpha)^{i+\gamma}} \frac{(\ln(1+e+\alpha))^j}{j!} \int_0^\infty (g(y;\Omega))^\gamma (S(y;\Omega))^j\,\mathrm{d}y \\ &= \sum_{i,j=0}^{\infty} \psi_{ij} \int_0^\infty (g(y;\Omega))^\gamma (S(y;\Omega))^j\,\mathrm{d}y,\end{aligned}$$

where

$$\psi_{ij} = \binom{\gamma+i-1}{i} \frac{(i+\gamma)^j}{(2+e+\alpha)^{i+\gamma}} \frac{(\ln(1+e+\alpha))^j}{j!}.$$

Now, applying the baseline Rayleigh distribution parameters, we have

$$\int_0^\infty f^\gamma(y)\,\mathrm{d}y = \sum_{i,j=0}^{\infty} \psi_{ij} \left(\frac{2}{\beta^2}\right)^\gamma \int_0^\infty y^\gamma e^{-(j+\gamma)(y/\beta)^2}\,\mathrm{d}y.$$

By substituting $(j+\gamma)(y/\beta)^2 = t$ so that $0 < t < \infty$ and $dy = \frac{\beta}{2\sqrt{j+\gamma}} t^{-1/2} dt$, we have

$$\int_0^\infty f^\gamma(y)dy = \sum_{i,j=0}^{\infty} \frac{\psi_{ij} 2^{\gamma-1} \beta}{(j+\gamma)^{\frac{\gamma}{2}+1}} \int_0^\infty t^{\frac{\gamma+1}{2}-1} e^{-t} dt.$$

Evaluating this integral via the standard complete gamma function, we obtain:

$$\int_0^\infty f^\gamma(y)dy = \sum_{i,j=0}^{\infty} \frac{\psi_{ij} 2^{\gamma-1} \beta}{(j+\gamma)^{\frac{\gamma}{2}+1}} \Gamma\left(\frac{\gamma+1}{2}\right). \tag{2.9}$$

Substituting the expressions obtained in Eq (2.9) into the entropy definition yields the closed-form representation:

$$T_\gamma = \frac{1}{\gamma-1} \left[1 - \sum_{i,j=0}^{\infty} \frac{\psi_{ij} 2^{\gamma-1} \beta}{(j+\gamma)^{\frac{\gamma}{2}+1}} \Gamma\left(\frac{\gamma+1}{2}\right)\right]. \tag{2.10}$$

2.9. Rényi entropy

The Rényi entropy of a random variable Y provides a generalized measure of the uncertainty contained within the system. It is defined as:

$$I_R(\gamma) = \frac{1}{1-\gamma} \ln\left(\int_0^\infty f(y;\Theta)^\gamma\,dy\right), \qquad \gamma > 0,\ \gamma \neq 1. \tag{2.11}$$

As the parameter γ approaches 1 ($\gamma \rightarrow 1$), an application of L'Hôpital's Rule demonstrates that the Rényi entropy converges analytically to the classical Shannon differential entropy, confirming the structural consistency of the derived informational metrics. Utilizing Eq (2.9), the exact model expression recovers as:

$$R_\gamma = \frac{1}{1-\gamma} \ln\left[\sum_{i,j=0}^{\infty} \frac{\psi_{ij} 2^{\gamma-1}\beta}{(j+\gamma)^{\frac{\gamma}{2}+1}} \Gamma\left(\frac{\gamma+1}{2}\right)\right].$$

2.10. Arimoto entropy

While Rényi entropy generalizes Shannon entropy, Arimoto entropy is a related concept that primarily generalizes the conditional entropy boundaries. The Arimoto entropy of order γ for a continuous random variable with a probability density function $f(y)$ is stated as:

$$\begin{aligned} A_\gamma &= \frac{\gamma}{\gamma-1}\left[1-\left(\int_0^\infty f^\gamma(y)\,\mathrm{d}y\right)^{\frac{1}{\gamma}}\right], \qquad \gamma > 0,\ \gamma \neq 1, \\ &= \frac{\gamma}{\gamma-1}\left[1-\left(\sum_{i,j=0}^{\infty} \psi_{ij} \frac{2^{\gamma-1}\beta}{(j+\gamma)^{\frac{\gamma}{2}+1}} \Gamma(\frac{\gamma+1}{2})\right)^{\frac{1}{\gamma}}\right]. \end{aligned}$$

Remark on differential entropy values: During numerical evaluations, it is observed that the differential entropy can yield negative values for specific parameter coordinates of (α, β). In continuous probability spaces, differential entropy lacks the coordinate invariance of discrete entropy and is not bounded below by zero. A negative differential entropy does not simply suggest that the distribution "becomes peaked"; rather, it mathematically reflects a highly dense concentration of probability mass within a localized domain of length less than one. When the scale parameter β or shape modifier α restricts the variance, the probability density function peaks above unity ($f(y) > 1$), causing the integrand $f(y)\ln f(y)$ to become positive, thereby producing a negative total net integral.

2.11. Extropy

Extropy is described in statistics, specifically in information theory, as a measure of uncertainty or information that complements entropy. Considering a continuous random variable with probability density function $f(y;\Omega)$, the extropy is defined as

$$\begin{aligned} J(Y) &= -\frac{1}{2}\int_{-\infty}^{\infty} f^2(y;\Omega)\,\mathrm{d}y \\ &= \int_0^\infty (2+e+\alpha)^{-2}\, g(y;\Omega)^2 (1+e+\alpha)^{2S(y;\Omega)} \left(1-\frac{(1+e+\alpha)^{S(y;\Omega)}}{2+e+\alpha}\right)^{-2} \mathrm{d}y. \end{aligned} \tag{2.12}$$

Applying the following series in Eq (2.12), we have

$$\frac{1}{(1-u)^2} = \sum_{i=0}^{\infty}(i+1)u^i \quad ; \ |u| < 1.$$

$$a^x = \sum_{j=0}^{\infty} \frac{(\ln(a))^j}{j!} x^j.$$

Now

$$J(Y) = -\frac{1}{2}\sum_{i,j=0}^{\infty}\frac{(i+1)(2+i)^{j}}{(2+e+\alpha)^{i+2}}\frac{(\ln(1+e+\alpha))^{j}}{j!}\int_{0}^{\infty}(g(y;\Omega))^{2}(S(y;\Omega))^{j}\,\mathrm{d}y$$
$$= \sum_{i,j=0}^{\infty}\phi_{ij}\int_{0}^{\infty}(g(y;\Omega))^{2}(S(y;\Omega))^{j}\,\mathrm{d}y,$$

where

$$\phi_{ij} = \frac{(i+1)(i+2)^{j}}{(2+e+\alpha)^{i+2}}\frac{(\ln(1+e+\alpha))^{j}}{j!}.$$

We now employ the Rayleigh distribution to calculate the extropy of the proposed model.

$$J(Y) = \sum_{i,j=0}^{\infty}\phi_{ij}\frac{4}{\beta^{2}}\int_{0}^{\infty}y^{2}e^{-(j+2)(y/\beta)^{2}}\,\mathrm{d}y.$$

By calculating the above integral, we get

$$J(Y) = \sum_{i,j=0}^{\infty}\phi_{ij}\frac{1}{\beta(j+2)^{3/2}}\Gamma\left(\frac{3}{2}\right).$$

Table 2 shows that the NLRD becomes more concentrated and predictable as the parameters α,β, and γ increase, leading to a significant decrease in all uncertainty measures. Significant uncertainty and a Shannon entropy of 0.88 are obtained for $\alpha = 0.5, \beta = 0.3$, and $\gamma = 1.2$. However, the Shannon entropy drops to -0.61 as the parameters increase, e.g., $\alpha = 7.0, \beta = 3.5$, and $\gamma = 3.0$. One option is significantly more common than the others, and the fact that it becomes negative is a clear mathematical sign that the distribution has peaked. This trend is even more dramatic for Rényi and Tsallis entropies. For example, the Tsallis entropy drops from 0.76 for the first parameter set to a stark -2.80 for the last, showing that these measures are especially sensitive to the distribution's increasing concentration. While all entropy measures are declining, the extropy tells a complementary part of the story. It also decreases—from 0.69 to 0.17 across the same examples-but crucially, it always remains positive. This confirms that while the overall "surprise" or unexpectedness in the system is diminishing, it never completely vanishes; there is always some residual potential for surprise, just a much smaller one.

Table 2. Numerical assessment of entropy and extropy for different parameter choices.

α	β	γ	H_γ	R_γ	T_γ	A_γ	$J(Y)$
0.5	0.3	1.2	0.88123260	0.82611006	0.76147259	0.77176127	0.68787465
1.5	0.5	1.5	0.56811394	0.44333258	0.39763464	0.41213099	0.51471346
2.5	0.8	2.0	0.28460760	0.07465184	0.07193345	0.07327579	0.39486637
3.5	1.2	2.5	0.04020257	-0.23266644	-0.27843247	-0.24968937	0.31400744
4.0	1.5	3.0	-0.09016661	-0.40833199	-0.63146901	-0.46931632	0.27748798
0.7	0.5	1.2	0.61342649	0.55756088	0.52759750	0.53243886	0.52899816
1.2	0.8	1.5	0.34932846	0.22638850	0.21404563	0.21805741	0.41095658
1.5	1.8	2.0	-0.07235293	-0.27413310	-0.31538987	-0.29380895	0.27127788
2.5	2.2	2.5	-0.22119286	-0.48595209	-0.71523840	-0.56421501	0.23811338
3.0	2.5	3.0	-0.30668507	-0.61654056	-1.21589352	-0.76254922	0.22035184
3.5	2.2	1.2	-0.2850912	-0.3482018	-0.3606127	-0.3585038	0.2268123
4.5	3.5	1.5	-0.3632265	-0.5013759	-0.5698181	-0.5457070	0.2125019
5.5	2.8	2.0	-0.4522174	-0.6793156	-0.9725273	-0.8089338	0.1966009
6.5	3.2	2.5	-0.5479888	-0.8387539	-1.6792255	-1.0901537	0.1804151
7.0	3.5	3.0	-0.6062432	-0.9432236	-2.7979466	-1.3130825	0.1709743

2.12. Reliability indicators

This section focuses on different reliability indicators.

2.12.1. Survival function

Let us suppose the random variable Y has a cdf denoted by $F(y)$. Then its survival function can be expressed as

$$S(y) = p_r(Y > y) = \int_y^\infty f(y)\,\mathrm{d}y = 1 - F(y).$$

Therefore, using the above expression, the survival function for the NLRD can now be expressed as

$$S(y;\alpha,\beta) = 1 - \frac{\ln\left(2 + e + \alpha - (1 + e + \alpha)^{e^{-(y/\beta)}}\right)^2}{\ln(1 + e + \alpha)}. \tag{2.13}$$

2.12.2. Hazard rate function

Considering the random variable Y, the hazard rate function of Y can be expressed as

$$h(y;\alpha,\beta) = \frac{f(y;\alpha,\beta)}{S(y;\alpha,\beta)}. \tag{2.14}$$

Using Eqs (1.9) and (2.13) in (2.14), then the hazard rate function of the NLRD is

$$h(y;\alpha,\beta) = \frac{2\alpha y e^{-(y/\beta)^2}(1 + e + \alpha)^{e^{-(y/\beta)^2}} \log(1 + e + \alpha)}{(2 + e + \alpha - (1 + e + \alpha)^{e^{-(y/\beta)^2}})\ln(2 + e + \alpha - (1 + e + \alpha)^{e^{-(y/\beta)^2}})}. \tag{2.15}$$

The following Figure 4 shows hazard rate plots of the NLRD for different sets of parameter values.

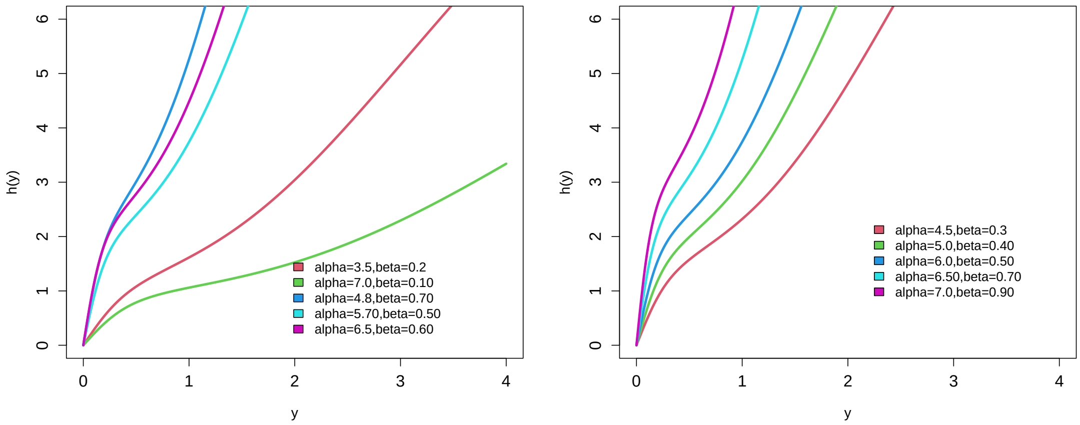

Figure 4. Hazard rate plots of the NLRD for different sets of parameter values.

2.12.3. Cumulative hazard rate function

The cumulative hazard rate function of a random variable Y is given as

$$H(y;\alpha,\beta) = -\log[\bar{F}(y;\alpha,\beta)]. \tag{2.16}$$

Using Eq (2.13) in Eq (2.16), we obtain the cumulative hazard rate function of the NLRD:

$$H(y;\alpha,\beta) = -\log\left\{1 - \frac{\ln(2+e+\alpha-(1+e+\alpha)^{e^{-(y/\beta)^2}})}{\ln(1+e+\alpha)}\right\}.$$

2.12.4. Mean residual function

The mean residual lifetime is a statistical quantity denoting the expected residual lifespan or the average completion period of the component after it has exceeded a particular span y. It is particularly important in reliability studies.

The mean residual function of the random Y variable can be defined and expressed as

$$\begin{aligned} m(y;\alpha,\beta) &= \frac{1}{S(y;\alpha,\beta)}\int_y^\infty t f(t;\alpha,\beta)\,\mathrm{d}t - y \\ &= \frac{\ln(1+e+\alpha)}{\ln(1+e+\alpha)-\ln(2+e+\alpha-(1+e+\alpha)^{e^{-(y/\beta)^2}})}\sum_{i,j=0}^{\infty}\eta_{ij}\,2\beta\int_y^\infty t^2 e^{-(j+1)(t/\beta)^2}\,\mathrm{d}t - y. \end{aligned}$$

By substituting $(j+1)(t/\beta)^2 = z$, so that $0 < z < (j+1)(y/\beta)^2$, we have

$$m(y;\alpha,\beta) = \sum_{i,j=0}^{\infty}\frac{\eta_{ij}\beta^3\ln(1+e+\alpha)}{(\ln(1+e+\alpha)-\ln(2+e+\alpha-(1+e+\alpha)^{e^{-(y/\beta)^2}}))(j+1)^{3/2}}\int_{(j+1)(y/\beta)^2}^{\infty} z^{1/2}e^{-z}\,\mathrm{d}z - y.$$

Performing the integral, we obtain the following:

$$m(y;\alpha,\beta) = \sum_{i,j=0}^{\infty}\frac{\eta_{ij}\beta^3\ln(1+e+\alpha)}{(\ln(1+e+\alpha)-\ln(2+e+\alpha-(1+e+\alpha)^{e^{-(y/\beta)^2}}))(j+1)^{3/2}}\Gamma\Big(\frac{3}{2},\ (j+1)(y/\beta)^2\Big) - y,$$

where $\Gamma(.)$ represents the upper incomplete gamma function.

3. The GASP under the NLRD

Acceptance sampling is a vital method of quality assurance that saves time and operational costs by analyzing a random sample from a lot rather than testing the full batch. This section develops a GASP tailored for items whose lifespans follow the newly formulated NLRD. The plan assumes the distribution's shape parameter α and baseline scale parameter β are known, with the baseline cumulative distribution function (cdf) given in Eq (1.8).

The GASP framework maximizes reliability evaluation efficiency by randomly selecting n items from a submitted lot, allocating them into g independent groups with a fixed repetition factor (group size) r, such that the total required sample size is $n = g \times r$. A simultaneous lifespan test is then executed across all groups for a predetermined termination time window t_0. The lot is accepted if and only if the observed number of failed items within each individual group does not exceed a designated acceptance limit c; otherwise, if even a single group records more than c failures, the entire lot is rejected instantly. For a fixed repetition factor r, the operational plan is entirely characterized by the design parameters (g, c) and the test termination time t_0. The test termination time is set as a multiple of the specified product lifecycle metric d_0, defined by $t_0 = a_1 d_0$, where a_1 represents a pre-specified dimensionless scaling constant.

The proposed plan is structured around three primary design parameters:

- g (Number of groups): This parameter represents the total number of parallel testers or independent groups into which the sample is split for simultaneous evaluation.
- r (Repetition factor): This refers to the fixed number of individual items allocated to each of the g groups. The total sample size is thus defined as $n = g \times r$.
- c (Acceptance number): This is the maximum allowable number of failed items inside a single group during the testing period t_0.

The sampling plan follows a specific decision-making process designed to balance testing efficiency with precise risk management:

- **Acceptance criterion:** The entire lot is accepted only if the number of failures in each of the g groups does not exceed the limit c. If even one group records more than c failures, the entire lot is rejected.
- **Operational efficiency:** Increasing the item repetition factor (r) generally reduces the number of testing groups (g) required, optimizing the cost of testing infrastructure.
- **Quality influence:** As the baseline quality of the products improves, the required values for g and c typically decrease to achieve the same target assurance levels.
- **Risk management:** For highly risk-averse consumers (low consumer risk β_{risk}), the plan naturally demands higher values for g or lower values for c to guarantee protection.

Assuming that item failures within any group occur independently and follow a binomial distribution, the total probability of accepting the submitted lot is given by:

$$P_{\text{accept}}(p) = \left[\sum_{i=0}^{c} \binom{r}{i} p^i (1-p)^{r-i} \right]^g, \tag{3.1}$$

where p represents the true probability of an individual item failing prior to the termination time t_0.

To establish dimensional clarity and decouple the framework from the absolute scale of the system, we transition from the scale parameter β to the dimension-free quality ratio d/d_0. Here, d represents the true mean or median lifespan of the product batch, and d_0 is the specified nominal target lifespan. Let r_1 and r_2 denote pre-calculated, invariant design constants derived from the shape parameter α that map the baseline percentile tracking. We introduce the dimensionless substitution parameter ζ, defined as a function of the quality ratio d/d_0:

$$\zeta = \left(\frac{t_0}{\beta}\right)^2 = \left(\frac{a_1 d_0}{\beta}\right)^2 = \left(\frac{a_1}{\kappa(\alpha)}\frac{d_0}{d}\right)^2, \tag{3.2}$$

where $\kappa(\alpha)$ serves as the invariant dimension-free scaling bridge linking the baseline scale to the true distribution percentile bounds. By substituting this clean parameter framework into the general NLRD framework, the item failure probability p simplifies to the dimensionally homogeneous expression:

$$p = F(t_0; \alpha, \beta) = \frac{\ln\left(2 + e + \alpha - (1 + e + \alpha)^{\exp(-\zeta)}\right)}{\ln(1 + e + \alpha)}. \tag{3.3}$$

Within this framework, we define p_1 as the consumer's operational risk boundary evaluated when the true quality matches the lower threshold $d/d_0 = r_1$, and p_2 as the producer's risk boundary evaluated when the quality matches the ideal target $d/d_0 = r_2$.

The optimization problem determines the optimal design parameters g and c by minimizing the average sample number (ASN), defined as ASN $= r \times g$, subject to simultaneous risk constraints for both the buyer and the seller:

$$P_{\text{accept}}\left(p_1 \;\middle|\; \frac{d}{d_0} = r_1\right) \leq \beta_{\text{risk}}, \tag{3.4}$$

$$P_{\text{accept}}\left(p_2 \;\middle|\; \frac{d}{d_0} = r_2\right) \geq 1 - \alpha_{\text{risk}}, \tag{3.5}$$

where consumer's risk (β_{risk}) protects the buyer from mistakenly accepting a low-quality lot ($d/d_0 = r_1$), and producer's risk (α_{risk}) protects the manufacturer from mistakenly rejecting a high-quality lot ($d/d_0 = r_2$).

Numerical optimization algorithm: To find the unique solution, we employ a two-dimensional grid search algorithm. The program begins at $c = 0$ and increments the group count g sequentially. If no value of g satisfies the simultaneous inequalities, c is incremented by 1, and the search resets until the pair (g, c) that minimizes the ASN is found.

In the formulation of the GASP presented in Tables 3 and 4, the shape parameter α is treated as a fixed design baseline. In practical industrial engineering settings, the true value of α is unknown and must be estimated from historical inspection logs or a pilot batch using the maximum likelihood estimation (MLE) framework detailed in Section 4. To account for estimation uncertainty and prevent the inflation of consumer risk (β_0), practitioners can adopt a two-step plug-in and variance-correction procedure:

- **Asymptotic confidence bounds:** Let $\hat{\alpha}$ be the MLE of the shape parameter obtained from a baseline sample of size n, and let $\widehat{\text{Var}}(\hat{\alpha})$ be its corresponding asymptotic variance extracted from the inverted observed information matrix $\mathcal{I}^{-1}(\hat{\mathbf{\Theta}})$. A conservative, safety-first operational parameter α_{lower} can be defined using the lower bound of its $100(1-\gamma)\%$ Wald confidence interval:

  $$\alpha_{\text{lower}} = \hat{\alpha} - z_{1-\gamma/2}\sqrt{\widehat{\text{Var}}(\hat{\alpha})},$$

  where $z_{1-\gamma/2}$ denotes the standard normal percentile.

- **Risk-averse optimization:** By executing the GASP design optimization routines using α_{lower} rather than a point estimate $\hat{\alpha}$, the sampling plan remains robust against negative sampling variations. This conservative boundary adjustment guarantees that the actual probability of acceptance does not inadvertently exceed the consumer risk threshold when the actual tail of the distribution is heavier than estimated.

Table 3. The GASP under the NLRD at $\alpha = 0.75, \beta = 0.5$, and with minimum g and c.

β_{risk}	$r_2 = \frac{d}{d_0}$	$r = 5$						$r = 10$					
		$a_1 = 0.5$			$a_1 = 1$			$a_1 = 0.5$			$a_1 = 1$		
		g	c	P_{accept}	g	c	P_{accept}	g	c	P_{accept}	g	c	P_{accept}
0.25	2	26	2	0.958945	7	3	0.960359	13	3	0.979784	3	5	0.984590
	4	5	1	0.989663	1	1	0.972017	2	1	0.982283	1	2	0.984359
	6	5	1	0.997883	1	1	0.993731	2	1	0.996272	1	1	0.974098
	8	2	0	0.963641	1	1	0.997924	1	0	0.963641	1	1	0.991102
0.10	2	399	3	0.981447	73	4	0.981086	21	3	0.967547	5	5	0.974450
	4	9	1	0.981471	4	2	0.993571	3	1	0.973543	1	2	0.984359
	6	9	1	0.996192	4	1	0.987501	3	1	0.994413	1	1	0.974098
	8	9	1	0.998780	4	1	0.995852	3	1	0.998192	1	1	0.991102
0.05	2	519	3	0.975935	95	4	0.975456	27	3	0.958470	7	5	0.964413
	4	11	1	0.977400	5	2	0.991171	4	1	0.964881	2	2	0.968962
	6	11	1	0.995348	2	1	0.987501	4	1	0.992557	1	1	0.974098
	8	11	1	0.998509	2	1	0.995852	4	1	0.997590	1	1	0.991102
0.01	2	797	3	0.963284	146	4	0.962529	164	4	0.982240	25	6	0.983430
	4	17	1	0.965289	7	2	0.988777	13	2	0.995495	2	2	0.968962
	6	17	1	0.992820	3	1	0.981310	6	1	0.988857	2	2	0.996448
	8	17	1	0.997696	3	1	0.993785	6	1	0.996388	2	1	0.982283

Table 4. The GASP under the NLRD at $\alpha = 1.75, \beta = 0.75$, and with minimum g and c.

β_{risk}	$r_2 = \frac{d}{d_0}$	$r = 5$						$r = 10$					
		$a_1 = 0.5$			$a_1 = 1$			$a_1 = 0.5$			$a_1 = 1$		
		g	c	P_{accept}	g	c	P_{accept}	g	c	P_{accept}	g	c	P_{accept}
0.25	2	25	2	0.956618	7	3	0.957254	12	3	0.978927	3	5	0.982896
	4	5	1	0.988881	1	1	0.970234	2	1	0.980978	1	2	0.982914
	6	5	1	0.997717	1	1	0.993276	1	1	0.995982	1	1	0.972304
	8	2	0	0.962242	1	1	0.997766	1	0	0.962242	1	1	0.990443
0.10	2	369	3	0.980477	73	4	0.979105	20	3	0.965125	5	5	0.971656
	4	8	1	0.982269	4	2	0.992929	3	1	0.971603	1	2	0.982914
	6	8	1	0.996349	2	1	0.986596	3	1	0.993980	1	1	0.972304
	8	8	1	0.998829	2	1	0.995538	3	1	0.998049	1	1	0.990443
0.05	2	481	3	0.974626	95	4	0.972893	25	3	0.956598	7	5	0.960544
	4	11	1	0.975700	5	2	0.991169	4	1	0.962318	2	2	0.966120
	6	11	1	0.994983	2	1	0.986596	4	1	0.991981	1	1	0.972304
	8	11	1	0.998390	2	1	0.995538	4	1	0.997400	1	1	0.990443
0.01	2	738	3	0.961334	146	4	0.958646	151	4	0.980901	25	6	0.981177
	4	16	1	0.964853	7	2	0.987658	5	1	0.953121	2	2	0.966120
	6	16	1	0.992712	3	1	0.979962	5	1	0.989986	2	2	0.996063
	8	16	1	0.997660	3	1	0.993314	5	1	0.996751	2	1	0.980978

Figures 5–8 present the resulting operating characteristic (OC) curves. The horizontal axis tracks the continuous quality ratio d/d_0, while the vertical axis represents the probability of acceptance of the joint lot P_{accept}. These curves are generated by fixing the optimal plan triplet (g, c, r) and plotting the trajectory of P_{accept} as product quality improves. A steeper, more vertical gradient in the OC curve indicates a superior mathematical capability to cleanly distinguish between acceptable and substandard product lots.

- Table 3 demonstrates that raising r_2 lowers both g and c, making sampling more effective for higher-quality items.
- Lesser values of β_{risk} result in larger values of g and c, ensuring increased inspection precision.
- Increasing the repetition factor r generally lowers the number of groups g needed.
- When r_2 grows from 2 to 8, c and g decrease, showing the plan's efficiency for higher quality.
- Small β_{risk} increases the sample size needed to preserve high acceptance probability.
- Expanding r from 5 to 10 results in fewer groups g, making the plan more efficient.
- $a_1 = 1$ shows improved sampling efficiency compared to $a_1 = 0.5$.

The performance of the proposed GASP under the NLRD is evaluated through Tables 3 and 4, and Figures 5–8. These results illustrate the sensitivity of the design parameters (g, c) to changes in consumer risk (β_{risk}), test termination time (a_1), and the quality ratio (r_2).

(i) Impact of the quality ratio (r_2): It is observed from Tables 3 and 4 that as the quality ratio r_2 increases from 2 to 8, there is a consistent and significant decrease in both the number of groups (g) and the acceptance number (c). This indicates that the sampling plan becomes inherently more efficient when the true quality of the lot is substantially higher than the specified quality, requiring fewer resources for testing.

(ii) Consumer risk (β_{risk}) and precision: Decreasing the consumer risk β_{risk} (e.g., from 0.25 to 0.01) leads to an increase in the number of groups (g) and the acceptance number (c). This relationship is necessary to maintain the desired level of protection for the consumer, ensuring that poor-quality lots are rejected with higher probability.

(iii) Repetition factor (r): Comparing the results for $r = 5$ and $r = 10$, it is evident that increasing the repetition factor generally allows for a reduction in the required number of groups (g) to satisfy the risk constraints. This demonstrates a trade-off where utilizing more items per group can optimize the total number of testers required.

(iv) Test termination constant (a_1): The tables show that as a_1 increases from 0.5 to 1.0 (indicating a longer test duration relative to the median life), the number of required groups g significantly decreases. This suggests that longer testing durations improve the plan's efficiency by providing more information per group.

(v) OC curve characteristics: Figures 5–8 present the OC curves, which plot the probability of acceptance (P_{accept}) against the quality ratio d/d_0.
   - The curves exhibit a steep increase as the quality ratio improves, which signifies the plan's strong ability to discriminate between "good" and "bad" lots.
   - As the number of groups g or the repetition factor r increases, the OC curves become steeper, indicating enhanced power of the sampling plan.

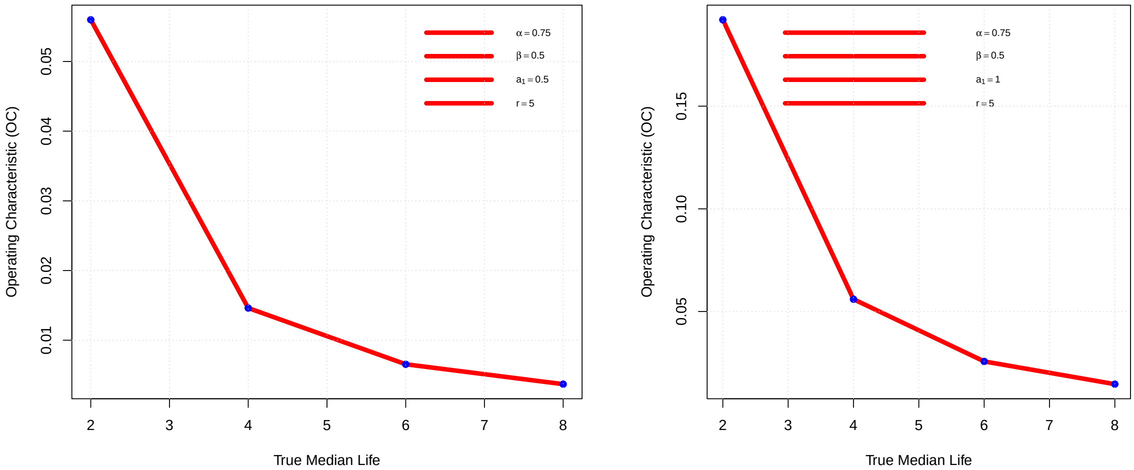

Figure 5. OC curves for the NLRD distribution for $\alpha = 0.75, \beta = 0.5, r = 5$.

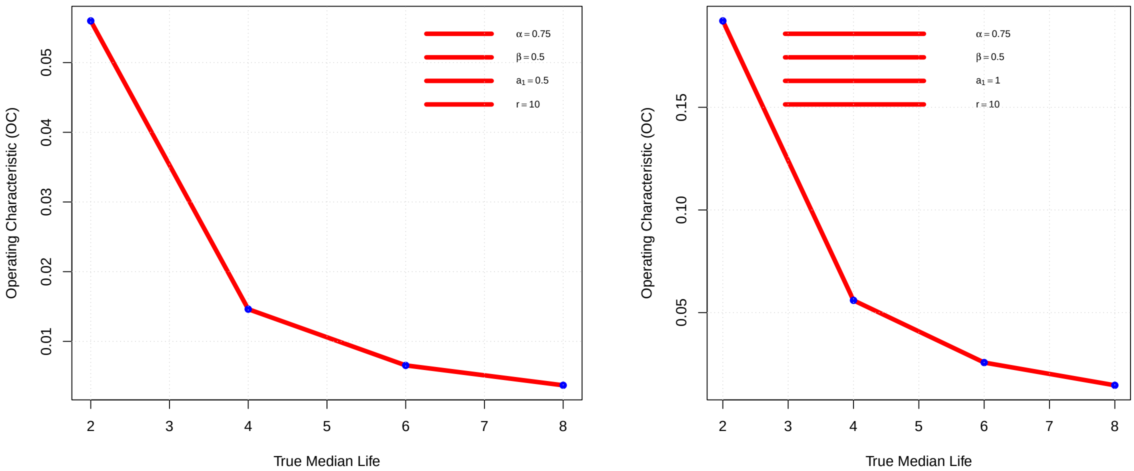

Figure 6. OC curves for the NLRD distribution for $\alpha = 0.75, \beta = 0.5, r = 10$.

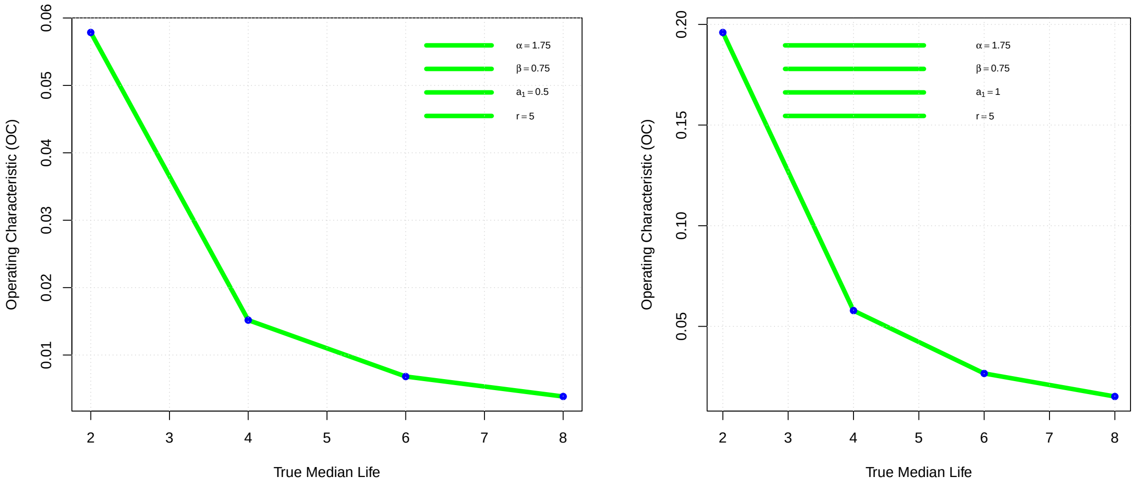

Figure 7. OC curves for the NLRD distribution for $\alpha = 1.75, \beta = 0.75, r = 5$.

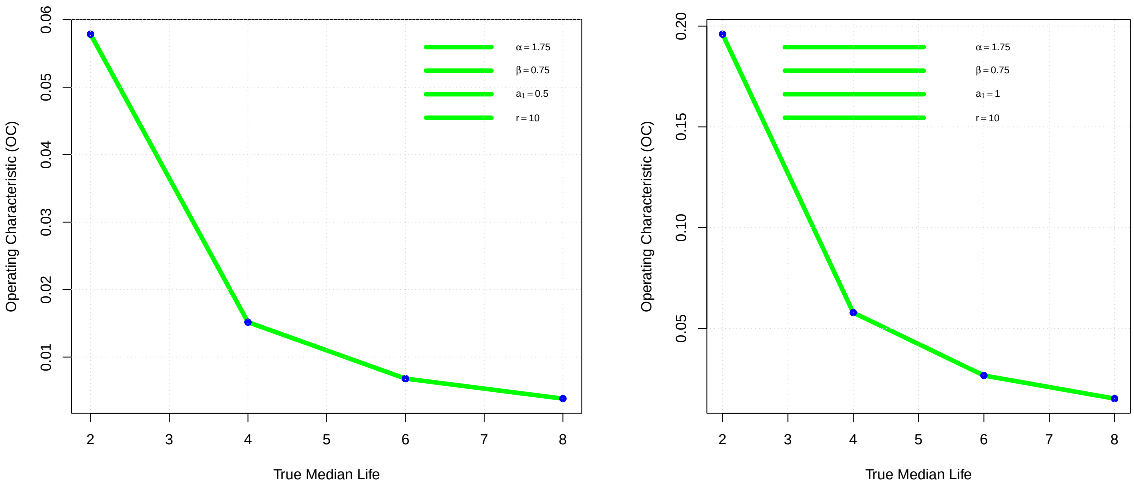

Figure 8. OC curves for the NLRD distribution for $\alpha = 1.75, \beta = 0.75, r = 10$.

4. Estimations

Suppose a random sample $Y_1, Y_2, ..., Y_n$ is drawn from the considered NLRD. Therefore, based on a complete observed sample of size n, the likelihood function can be expressed as follows:

$$L = \prod_{i=1}^{n} \left(\frac{2y_i\, e^{-(y_i/\beta)^2} (1 + e + \alpha)^{e^{-(y_i/\beta)^2}}}{\beta^2 (2 + e + \alpha - (1 + e + \alpha)^{e^{-(y_i/\beta)^2}})} \right).$$

The associated log-likelihood function (T_1) based on the previous expression is given as

$$\begin{aligned} \ell = n \ln 2 - 2n \ln \beta - \sum_{i=1}^{n} \frac{y_i^2}{\beta^2} + \sum_{i=1}^{n} \ln y_i \\ + \ln(1 + e + \alpha) \sum_{i=1}^{n} e^{-(y_i/\beta)^2} - \sum_{i=1}^{n} \ln(2 + e + \alpha - (1 + e + \alpha)^{e^{-(y_i/\beta)^2}}). \end{aligned} \tag{4.1}$$

Using the methods of partial derivatives with respect to the parameters α and β, we calculate the following two expressions:

$$\begin{aligned} \frac{\partial \ell}{\partial \alpha} &= \frac{1}{1 + e + \alpha} \sum_{i=1}^{n} e^{-(y_i/\beta)^2} - \sum_{i=1}^{n} \frac{1 - e^{-(y_i/\beta)^2} (1 + e + \alpha)^{e^{-(y_i/\beta)^2} - 1}}{2 + e + \alpha - (1 + e + \alpha)^{e^{-(y_i/\beta)^2}}}, \\ \frac{\partial \ell}{\partial \beta} &= -\frac{2n}{\beta} + \frac{2}{\beta^3} \sum_{i=1}^{n} y_i^2 \left[1 + \frac{(2 + e + \alpha) \ln(1 + e + \alpha)\, e^{-(y_i/\beta)^2}}{2 + e + \alpha - (1 + e + \alpha)^{e^{-(y_i/\beta)^2}}} \right]. \end{aligned} \tag{4.2}$$

To obtain the estimators of α and β, we must equate Eqs (4.1) and (4.2) to zero. However, these equations are nonlinear in nature and are difficult to solve by traditional methods. In such cases, we estimate the model parameters using iterative methods, such as the Newton-Raphson method, the secant method, or others. We employ the Newton-Raphson method to obtain the maximum likelihood (ML) estimate $\hat{\psi}(\hat{\alpha},\hat{\beta})$ of the function $\psi(\alpha,\beta)$.

Another technique, referred to as Anderson-Darling estimation (T_2), entails minimizing the target equation. The early foundational work on this approach can be found in [44–46], while recent advances and variations are detailed in [47, 48]. The target equation to minimize is:

$$\begin{aligned} AD &= -n - \frac{1}{n}\sum_{i=1}^{n}(2i-1)[\log F(y_i) + \log S(y_i)] \\ &= -n - \frac{1}{n}\sum_{i=1}^{n}(2i-1)\left[\log\left(\frac{\ln(2+e+\alpha-(1+e+\alpha)^{e^{-(y_i/\beta)^2}})}{\ln(1+e+\alpha)}\right) + \log\left(1 - \frac{\ln(2+e+\alpha-(1+e+\alpha)^{e^{-(y_i/\beta)^2}})}{\ln(1+e+\alpha)}\right)\right]. \end{aligned}$$

In the estimation of Cramér-von Mises (T_3), the objective is to minimize the following equation for improved statistical analysis,

$$CVM = -\frac{1}{12n} + \sum_{i=1}^{n}\left[F(y_i) - \frac{2i-1}{2n}\right]^2 = -\frac{1}{12n} + \sum_{i=1}^{n}\left[\frac{\ln\left(2+e+\alpha-(1+e+\alpha)^{e^{-\left(\frac{y_i}{\beta}\right)^2}}\right)}{\ln(1+e+\alpha)} - \frac{2i-1}{2n}\right]^2.$$

The maximum product of the estimation of the spacings (T_4) is achieved by maximizing the following equation, which is commonly used in statistical analysis for parameter estimation:

$$T = \frac{1}{n+1}\sum_{i=1}^{n+1}\log E_i, \qquad E_i = F(y_{(i)}) - F(y_{(i-1)}).$$

In contrast, least-squares estimation (T_5) seeks to minimize the equation by reducing the sum of square differences between observed and expected values to achieve the best fit:

$$LS = \sum_{i=1}^{n}\left[F(y_i) - \frac{i}{n+1}\right]^2 = \sum_{i=1}^{n}\left[1 - \frac{\ln(2+e+\alpha-(1+e+\alpha)^{e^{-(y_i/\beta)^2}})}{\ln(1+e+\alpha)} - \frac{i}{n+1}\right]^2.$$

Analogously, in the weighted least squares estimation (T_6), the goal is to minimize the equation by applying weights to reduce the influence of certain data points on the overall estimation process:

$$\begin{aligned} WLS &= \sum_{i=1}^{n}\frac{(n+1)^2(n+2)}{i(n-i+1)}\left[F(y_i) - \frac{i}{n+1}\right]^2 \\ &= \sum_{i=1}^{n}\frac{(n+1)^2(n+2)}{i(n-i+1)}\left[1 - \frac{\ln(2+e+\alpha-(1+e+\alpha)^{e^{-(y_i/\beta)^2}})}{\ln(1+e+\alpha)} - \frac{i}{n+1}\right]^2. \end{aligned}$$

5. Simulation investigation

In this section, Monte Carlo simulations are employed to assess the convergence of several estimators for the newly generated model. This experiment is carried out with 1000 repetitions with different sample sizes, such as (n = 10, 20, 30, 50, 75, 100, 150, 200, 300) and different combinations of the true values of the parameters. The following expression is utilized to generate samples:

$$y = \left[-\beta \ln\left(\frac{\ln(2 + e + \alpha - (1 + e + \alpha)^u)}{\ln(1 + e + \alpha)}\right)\right]^{1/2},$$

where u is a uniform random number within a range of $u \in (0, 1)$, the simulation findings for bias, mean squared errors (MSE), and mean relative errors (MRE) for defined techniques are provided in Tables 5–8. With increasing sample size, it appears obvious that estimates are generally constant and approach the true values of the parameters. Remarkably, the bias, MSE, and MRE decrease as the sample size grows for all parameter pairings. Table 9 presents the overall rankings of the estimators, clearly indicating that the maximum likelihood estimators outperform the others. Let $\hat{\Theta}$ be the estimator of the true parameter Θ for N iterations. These metrics are defined as follows:

(1) **Average bias:** Measures the average difference between the estimated values and the true parameter value:

$$\text{Bias}(\hat{\Theta}) = \frac{1}{N}\sum_{i=1}^{N}(\hat{\Theta}_i - \Theta).$$

(2) **MSE:** Measures the average of the squares of the errors, representing both the variance and the bias of the estimator:

$$\text{MSE}(\hat{\Theta}) = \frac{1}{N}\sum_{i=1}^{N}(\hat{\Theta}_i - \Theta)^2.$$

(3) **MRE:** Provides a relative measure of the estimation error, which is particularly useful for comparing accuracy across different parameter scales:

$$\text{MRE}(\hat{\Theta}) = \frac{1}{N}\sum_{i=1}^{N}\frac{|\hat{\Theta}_i - \Theta|}{\Theta}.$$

Table 5. Simulation values of bias, MSE, and MRE for $\alpha = 0.5,\ \beta = 0.7$.

n	Est.	Est. Par.	T_1	T_2	T_3	T_4	T_5	T_6
10	Bias	α	$1.308416^{\{1\}}$	$2.107747^{\{5\}}$	$1.778193^{\{3\}}$	$1.838259^{\{4\}}$	$1.450211^{\{2\}}$	$2.187202^{\{6\}}$
		β	$0.292159^{\{5\}}$	$0.270860^{\{2\}}$	$0.275906^{\{4\}}$	$0.274987^{\{3\}}$	$0.299957^{\{6\}}$	$0.262098^{\{1\}}$
	MSE	α	$0.149897^{\{2\}}$	$0.051282^{\{1\}}$	$0.428831^{\{4\}}$	$0.762253^{\{5\}}$	$0.863815^{\{6\}}$	$0.187202^{\{3\}}$
		β	$0.196009^{\{5\}}$	$0.132149^{\{2\}}$	$0.129447^{\{1\}}$	$0.165169^{\{3\}}$	$0.193098^{\{4\}}$	$0.262098^{\{6\}}$
	MRE	α	$2.616832^{\{1\}}$	$4.215493^{\{5\}}$	$3.556386^{\{3\}}$	$3.676519^{\{4\}}$	$2.900422^{\{2\}}$	$4.374404^{\{6\}}$
		β	$0.417370^{\{5\}}$	$0.386943^{\{2\}}$	$0.394152^{\{4\}}$	$0.392838^{\{3\}}$	$0.428511^{\{6\}}$	$0.374425^{\{1\}}$
	$\sum$ *ranks*		$19^{\{3\}}$	$17^{\{2\}}$	$16^{\{1\}}$	$22^{\{4\}}$	$26^{\{6\}}$	$23^{\{5\}}$
20	Bias	α	$1.327953^{\{2\}}$	$1.971137^{\{5\}}$	$1.694363^{\{3\}}$	$1.702854^{\{4\}}$	$1.308373^{\{1\}}$	$2.063580^{\{6\}}$
		β	$0.208112^{\{2\}}$	$0.205251^{\{1\}}$	$0.210571^{\{3\}}$	$0.213311^{\{5\}}$	$0.210692^{\{4\}}$	$0.215599^{\{6\}}$
	MSE	α	$0.130828^{\{3\}}$	$0.332100^{\{4\}}$	$0.877937^{\{6\}}$	$0.013419^{\{1\}}$	$0.071142^{\{2\}}$	$0.683138^{\{5\}}$
		β	$0.071090^{\{3\}}$	$0.063491^{\{1\}}$	$0.076152^{\{5\}}$	$0.070265^{\{2\}}$	$0.080178^{\{6\}}$	$0.071946^{\{4\}}$
	MRE	α	$2.655907^{\{2\}}$	$3.942274^{\{5\}}$	$3.388726^{\{4\}}$	$3.405708^{\{3\}}$	$2.616747^{\{1\}}$	$4.127159^{\{6\}}$
		β	$0.297303^{\{2\}}$	$0.293215^{\{1\}}$	$0.300815^{\{3\}}$	$0.304730^{\{5\}}$	$0.300988^{\{4\}}$	$0.307999^{\{6\}}$
	$\sum$ *ranks*		$14^{\{1\}}$	$17^{\{2\}}$	$24^{\{5\}}$	$20^{\{4\}}$	$18^{\{3\}}$	$33^{\{6\}}$
30	Bias	α	$1.396993^{\{1\}}$	$1.818340^{\{4\}}$	$1.877928^{\{6\}}$	$1.718035^{\{3\}}$	$1.401536^{\{2\}}$	$1.852898^{\{5\}}$
		β	$0.181629^{\{1\}}$	$0.184415^{\{3\}}$	$0.188324^{\{5\}}$	$0.181778^{\{2\}}$	$0.193891^{\{6\}}$	$0.188169^{\{4\}}$
	MSE	α	$0.382399^{\{2\}}$	$0.437593^{\{3\}}$	$0.689647^{\{6\}}$	$0.068777^{\{1\}}$	$0.470951^{\{4\}}$	$0.600475^{\{5\}}$
		β	$0.051741^{\{4\}}$	$0.050372^{\{3\}}$	$0.053407^{\{5\}}$	$0.050253^{\{2\}}$	$0.062297^{\{6\}}$	$0.050093^{\{1\}}$
	MRE	α	$2.793985^{\{1\}}$	$3.636680^{\{4\}}$	$3.755857^{\{5\}}$	$3.436069^{\{3\}}$	$2.803072^{\{2\}}$	$3.705796^{\{6\}}$
		β	$0.259469^{\{1\}}$	$0.263450^{\{3\}}$	$0.269034^{\{6\}}$	$0.259683^{\{2\}}$	$0.276986^{\{4\}}$	$0.268813^{\{5\}}$
	$\sum$ *ranks*		$10^{\{1\}}$	$20^{\{3\}}$	$33^{\{6\}}$	$13^{\{2\}}$	$24^{\{4\}}$	$26^{\{5\}}$
50	Bias	α	$1.346631^{\{2\}}$	$1.735343^{\{6\}}$	$1.669540^{\{4\}}$	$1.685075^{\{5\}}$	$1.218148^{\{1\}}$	$1.631861^{\{3\}}$
		β	$0.151408^{\{2\}}$	$0.167019^{\{5\}}$	$0.163358^{\{4\}}$	$0.170542^{\{6\}}$	$0.137914^{\{1\}}$	$0.162791^{\{3\}}$
	MSE	α	$0.022521^{\{1\}}$	$0.945959^{\{6\}}$	$0.656303^{\{4\}}$	$0.679161^{\{5\}}$	$0.447117^{\{2\}}$	$0.480642^{\{3\}}$
		β	$0.035011^{\{2\}}$	$0.039231^{\{3\}}$	$0.039984^{\{4\}}$	$0.042607^{\{6\}}$	$0.030404^{\{1\}}$	$0.040453^{\{5\}}$
	MRE	α	$2.693261^{\{2\}}$	$3.470686^{\{6\}}$	$3.339081^{\{4\}}$	$3.370150^{\{5\}}$	$2.436296^{\{1\}}$	$3.263722^{\{3\}}$
		β	$0.216297^{\{2\}}$	$0.238599^{\{5\}}$	$0.233369^{\{4\}}$	$0.243632^{\{6\}}$	$0.197020^{\{1\}}$	$0.232558^{\{3\}}$
	$\sum$ *ranks*		$11^{\{2\}}$	$31^{\{5\}}$	$24^{\{4\}}$	$33^{\{6\}}$	$7^{\{1\}}$	$20^{\{3\}}$
100	Bias	α	$1.125780^{\{1\}}$	$1.533008^{\{4\}}$	$1.503536^{\{3\}}$	$1.600512^{\{5\}}$	$1.337881^{\{2\}}$	$1.684094^{\{6\}}$
		β	$0.127806^{\{1\}}$	$0.135847^{\{2\}}$	$0.147911^{\{4\}}$	$0.151619^{\{5\}}$	$0.140201^{\{3\}}$	$0.157786^{\{6\}}$
	MSE	α	$0.959884^{\{6\}}$	$0.866069^{\{4\}}$	$0.702314^{\{3\}}$	$0.355822^{\{1\}}$	$0.959009^{\{5\}}$	$0.662201^{\{2\}}$
		β	$0.025652^{\{1\}}$	$0.028172^{\{2\}}$	$0.032394^{\{4\}}$	$0.035416^{\{5\}}$	$0.030279^{\{3\}}$	$0.036436^{\{6\}}$
	MRE	α	$2.251559^{\{1\}}$	$3.066016^{\{3\}}$	$3.007073^{\{2\}}$	$3.201023^{\{4\}}$	$3.675763^{\{6\}}$	$3.368189^{\{5\}}$
		β	$0.182580^{\{1\}}$	$0.194066^{\{2\}}$	$0.211302^{\{4\}}$	$0.216599^{\{5\}}$	$0.200287^{\{3\}}$	$0.225409^{\{6\}}$
	$\sum$ *ranks*		$11^{\{1\}}$	$17^{\{2\}}$	$20^{\{3.5\}}$	$25^{\{5\}}$	$20^{\{3.5\}}$	$31^{\{6\}}$
150	Bias	α	$1.080335^{\{2\}}$	$1.372622^{\{3\}}$	$1.376959^{\{4\}}$	$1.474311^{\{6\}}$	$0.938561^{\{1\}}$	$1.403317^{\{5\}}$
		β	$2.624794^{\{6\}}$	$0.132687^{\{4\}}$	$0.128471^{\{2\}}$	$0.136654^{\{5\}}$	$0.111798^{\{1\}}$	$0.131269^{\{3\}}$
	MSE	α	$0.624794^{\{5\}}$	$0.189700^{\{3\}}$	$0.971871^{\{6\}}$	$0.548194^{\{4\}}$	$0.055615^{\{1\}}$	$0.175596^{\{2\}}$
		β	$0.021316^{\{2\}}$	$0.027378^{\{5\}}$	$0.024693^{\{3\}}$	$0.028476^{\{6\}}$	$0.020383^{\{1\}}$	$0.025862^{\{4\}}$
	MRE	α	$2.160670^{\{2\}}$	$2.745244^{\{3\}}$	$2.753919^{\{4\}}$	$2.948622^{\{6\}}$	$1.877121^{\{1\}}$	$2.806635^{\{5\}}$
		β	$0.169742^{\{2\}}$	$0.189553^{\{5\}}$	$0.183530^{\{3\}}$	$0.195220^{\{6\}}$	$0.159712^{\{1\}}$	$0.187527^{\{4\}}$
	$\sum$ *ranks*		$19^{\{2\}}$	$23^{\{4.5\}}$	$22^{\{3\}}$	$33^{\{6\}}$	$6^{\{1\}}$	$23^{\{4.5\}}$
200	Bias	α	$0.903105^{\{2\}}$	$1.299770^{\{6\}}$	$1.015293^{\{3\}}$	$1.148826^{\{5\}}$	$0.847238^{\{1\}}$	$1.023922^{\{4\}}$
		β	$0.091031^{\{1\}}$	$0.114111^{\{6\}}$	$0.102695^{\{4\}}$	$0.113822^{\{5\}}$	$0.094914^{\{2\}}$	$0.099415^{\{3\}}$
	MSE	α	$0.691714^{\{5\}}$	$0.576697^{\{4\}}$	$0.254765^{\{1\}}$	$0.900114^{\{6\}}$	$0.575669^{\{3\}}$	$0.322816^{\{2\}}$
		β	$0.012553^{\{1\}}$	$0.020700^{\{5\}}$	$0.016178^{\{4\}}$	$0.020801^{\{6\}}$	$0.013871^{\{2\}}$	$0.015815^{\{3\}}$
	MRE	α	$1.806210^{\{2\}}$	$2.599539^{\{6\}}$	$2.030586^{\{3\}}$	$2.297653^{\{5\}}$	$1.694476^{\{1\}}$	$2.047845^{\{4\}}$
		β	$0.130044^{\{1\}}$	$0.163015^{\{6\}}$	$0.146707^{\{4\}}$	$0.162602^{\{5\}}$	$0.135591^{\{2\}}$	$0.142022^{\{3\}}$
	$\sum$ *ranks*		$12^{\{2\}}$	$33^{\{6\}}$	$19^{\{3.5\}}$	$32^{\{5\}}$	$11^{\{1\}}$	$19^{\{3.5\}}$
300	Bias	α	$0.798756^{\{2\}}$	$1.008017^{\{5\}}$	$0.845772^{\{3\}}$	$1.132066^{\{6\}}$	$0.747442^{\{1\}}$	$0.926407^{\{4\}}$
		β	$0.080611^{\{1\}}$	$0.101460^{\{5\}}$	$0.085458^{\{3\}}$	$0.108360^{\{6\}}$	$0.082349^{\{2\}}$	$0.092656^{\{4\}}$
	MSE	α	$0.277546^{\{3\}}$	$0.206158^{\{2\}}$	$0.578120^{\{4\}}$	$0.744530^{\{5\}}$	$0.185466^{\{1\}}$	$0.849185^{\{6\}}$
		β	$0.010340^{\{1\}}$	$0.015887^{\{5\}}$	$0.012060^{\{3\}}$	$0.018236^{\{6\}}$	$0.010803^{\{2\}}$	$0.013534^{\{4\}}$
	MRE	α	$1.597511^{\{2\}}$	$2.016033^{\{5\}}$	$1.691545^{\{3\}}$	$2.264131^{\{6\}}$	$1.494884^{\{1\}}$	$1.852815^{\{4\}}$
		β	$0.115158^{\{1\}}$	$0.144943^{\{5\}}$	$0.122083^{\{3\}}$	$0.154800^{\{6\}}$	$0.117641^{\{2\}}$	$0.132365^{\{4\}}$
	$\sum$ *ranks*		$10^{\{2\}}$	$27^{\{5\}}$	$19^{\{3\}}$	$35^{\{6\}}$	$9^{\{1\}}$	$26^{\{4\}}$

Table 6. Simulation values of bias, MSE, and MRE for $\alpha = 0.43$, $\beta = 0.91$.

n	Est.	Est. Par.	T_1	T_2	T_3	T_4	T_5	T_6
10	Bias	α	$1.450211^{\{1\}}$	$2.187202^{\{3\}}$	$1.804877^{\{2\}}$	$2.714395^{\{6\}}$	$2.566099^{\{5\}}$	$2.478149^{\{4\}}$
		β	$0.299957^{\{6\}}$	$0.262098^{\{1\}}$	$0.294789^{\{4\}}$	$0.298825^{\{5\}}$	$0.286545^{\{2\}}$	$0.291865^{\{3\}}$
	MSE	α	$0.863815^{\{5\}}$	$0.529500^{\{3\}}$	$0.657097^{\{4\}}$	$0.409440^{\{2\}}$	$0.395913^{\{1\}}$	$0.931683^{\{6\}}$
		β	$0.193098^{\{6\}}$	$0.130628^{\{1\}}$	$0.185273^{\{5\}}$	$0.138960^{\{4\}}$	$0.132678^{\{2\}}$	$0.138877^{\{3\}}$
	MRE	α	$2.900422^{\{1\}}$	$4.374404^{\{3\}}$	$3.609754^{\{2\}}$	$5.428790^{\{6\}}$	$5.132197^{\{5\}}$	$4.956298^{\{4\}}$
		β	$0.428511^{\{6\}}$	$0.374425^{\{1\}}$	$0.421127^{\{4\}}$	$0.426893^{\{5\}}$	$0.409350^{\{2\}}$	$0.416950^{\{3\}}$
	$\sum$ *ranks*		$25^{\{5\}}$	$12^{\{1\}}$	$21^{\{3\}}$	$28^{\{6\}}$	$17^{\{2\}}$	$23^{\{4\}}$
20	Bias	α	$1.308373^{\{1\}}$	$2.063580^{\{3\}}$	$1.897425^{\{2\}}$	$2.432345^{\{6\}}$	$2.407415^{\{5\}}$	$2.255938^{\{4\}}$
		β	$0.210692^{\{2\}}$	$0.215599^{\{4\}}$	$0.209900^{\{1\}}$	$0.245680^{\{6\}}$	$0.213272^{\{3\}}$	$0.222347^{\{5\}}$
	MSE	α	$0.071142^{\{1\}}$	$0.683138^{\{3\}}$	$0.878444^{\{5\}}$	$0.999855^{\{6\}}$	$0.443574^{\{2\}}$	$0.725565^{\{4\}}$
		β	$0.080178^{\{5\}}$	$0.071946^{\{3\}}$	$0.071032^{\{2\}}$	$0.085311^{\{6\}}$	$0.069679^{\{1\}}$	$0.072581^{\{4\}}$
	MRE	α	$2.616747^{\{1\}}$	$4.127159^{\{3\}}$	$3.794850^{\{2\}}$	$4.864691^{\{6\}}$	$4.814830^{\{5\}}$	$4.511875^{\{4\}}$
		β	$0.300988^{\{2\}}$	$0.307999^{\{4\}}$	$0.299857^{\{1\}}$	$0.350972^{\{6\}}$	$0.304675^{\{3\}}$	$0.317639^{\{5\}}$
	$\sum$ *ranks*		$12^{\{1\}}$	$20^{\{4\}}$	$13^{\{2\}}$	$36^{\{6\}}$	$19^{\{3\}}$	$26^{\{5\}}$
30	Bias	α	$1.401536^{\{1\}}$	$1.852898^{\{3\}}$	$1.720266^{\{2\}}$	$2.261694^{\{5\}}$	$2.353201^{\{6\}}$	$2.256047^{\{4\}}$
		β	$0.193891^{\{3\}}$	$0.188169^{\{1\}}$	$0.195751^{\{4\}}$	$0.212312^{\{6\}}$	$0.206685^{\{5\}}$	$0.193225^{\{2\}}$
	MSE	α	$0.470951^{\{4\}}$	$0.600475^{\{6\}}$	$0.042843^{\{1\}}$	$0.070145^{\{3\}}$	$0.066656^{\{2\}}$	$0.567014^{\{5\}}$
		β	$0.062297^{\{6\}}$	$0.050093^{\{1\}}$	$0.059303^{\{4\}}$	$0.061788^{\{5\}}$	$0.059165^{\{3\}}$	$0.054010^{\{2\}}$
	MRE	α	$2.616747^{\{1\}}$	$3.705796^{\{3\}}$	$3.440532^{\{2\}}$	$4.523387^{\{5\}}$	$4.706401^{\{6\}}$	$4.512095^{\{4\}}$
		β	$0.300988^{\{5\}}$	$0.268813^{\{1\}}$	$0.279644^{\{3\}}$	$0.303302^{\{6\}}$	$0.295264^{\{4\}}$	$0.276036^{\{2\}}$
	$\sum$ *ranks*		$20^{\{4\}}$	$15^{\{1\}}$	$16^{\{2\}}$	$30^{\{6\}}$	$26^{\{5\}}$	$19^{\{3\}}$
50	Bias	α	$1.401536^{\{1\}}$	$1.631861^{\{2\}}$	$1.649982^{\{3\}}$	$2.053260^{\{6\}}$	$1.960112^{\{5\}}$	$1.758858^{\{4\}}$
		β	$0.193891^{\{6\}}$	$0.162791^{\{1\}}$	$0.167430^{\{2\}}$	$0.186260^{\{5\}}$	$0.175343^{\{4\}}$	$0.172158^{\{3\}}$
	MSE	α	$0.470951^{\{2\}}$	$0.480642^{\{3\}}$	$0.586752^{\{4\}}$	$0.963794^{\{6\}}$	$0.133209^{\{1\}}$	$0.921108^{\{5\}}$
		β	$0.062297^{\{6\}}$	$0.040453^{\{1\}}$	$0.041424^{\{2\}}$	$0.049205^{\{5\}}$	$0.044212^{\{4\}}$	$0.042453^{\{3\}}$
	MRE	α	$2.803072^{\{1\}}$	$3.263722^{\{2\}}$	$3.299964^{\{3\}}$	$4.106520^{\{6\}}$	$3.920223^{\{5\}}$	$3.517715^{\{4\}}$
		β	$0.276986^{\{6\}}$	$0.232558^{\{1\}}$	$0.239186^{\{2\}}$	$0.266086^{\{5\}}$	$0.250489^{\{4\}}$	$0.245940^{\{3\}}$
	$\sum$ *ranks*		$22^{\{3.5\}}$	$10^{\{1\}}$	$16^{\{2\}}$	$33^{\{6\}}$	$23^{\{5\}}$	$22^{\{3.5\}}$
100	Bias	α	$1.218148^{\{1\}}$	$1.684094^{\{3\}}$	$1.524501^{\{2\}}$	$1.905063^{\{6\}}$	$1.849339^{\{5\}}$	$1.718628^{\{4\}}$
		β	$0.137914^{\{1\}}$	$0.157786^{\{4\}}$	$0.156390^{\{3\}}$	$0.175746^{\{6\}}$	$0.162535^{\{5\}}$	$0.151279^{\{2\}}$
	MSE	α	$0.447117^{\{2\}}$	$.662201^{\{4\}}$	$0.901052^{\{6\}}$	$0.087839^{\{1\}}$	$0.592610^{\{3\}}$	$0.873129^{\{5\}}$
		β	$0.030404^{\{1\}}$	$0.036436^{\{3\}}$	$0.036810^{\{4\}}$	$0.042511^{\{6\}}$	$0.039424^{\{5\}}$	$0.033358^{\{2\}}$
	MRE	α	$2.436296^{\{1\}}$	$3.368189^{\{3\}}$	$3.049003^{\{2\}}$	$3.810127^{\{6\}}$	$3.698678^{\{5\}}$	$3.437257^{\{4\}}$
		β	$0.197020^{\{1\}}$	$0.225409^{\{4\}}$	$0.223414^{\{3\}}$	$0.251066^{\{6\}}$	$0.232193^{\{5\}}$	$0.216113^{\{2\}}$
	$\sum$ *ranks*		$7^{\{1\}}$	$21^{\{4\}}$	$20^{\{3\}}$	$31^{\{6\}}$	$28^{\{5\}}$	$19^{\{2\}}$
150	Bias	α	$1.337881^{\{1\}}$	$1.403317^{\{2\}}$	$1.534122^{\{4\}}$	$1.507579^{\{3\}}$	$1.687555^{\{6\}}$	$1.555503^{\{5\}}$
		β	$0.140201^{\{3\}}$	$0.131269^{\{1\}}$	$0.140644^{\{4\}}$	$0.139925^{\{2\}}$	$0.149646^{\{6\}}$	$0.141031^{\{5\}}$
	MSE	α	$0.959009^{\{6\}}$	$0.175596^{\{1\}}$	$0.874883^{\{5\}}$	$0.432689^{\{2\}}$	$0.675934^{\{3\}}$	$0.824031^{\{4\}}$
		β	$0.030279^{\{5\}}$	$0.025862^{\{1\}}$	$0.030030^{\{3\}}$	$0.029258^{\{2\}}$	$0.033505^{\{6\}}$	$0.030161^{\{4\}}$
	MRE	α	$2.675763^{\{1\}}$	$2.806635^{\{2\}}$	$3.068244^{\{4\}}$	$3.015158^{\{3\}}$	$3.375110^{\{6\}}$	$3.111007^{\{5\}}$
		β	$0.200287^{\{3\}}$	$0.187527^{\{1\}}$	$0.200920^{\{4\}}$	$0.199893^{\{2\}}$	$0.213779^{\{6\}}$	$0.201473^{\{5\}}$
	$\sum$ *ranks*		$19^{\{3\}}$	$8^{\{1\}}$	$24^{\{4\}}$	$14^{\{2\}}$	$33^{\{6\}}$	$28^{\{5\}}$
200	Bias	α	$0.938561^{\{1\}}$	$1.023922^{\{2\}}$	$1.127156^{\{5\}}$	$1.120849^{\{4\}}$	$1.352324^{\{6\}}$	$1.057472^{\{3\}}$
		β	$0.111798^{\{5\}}$	$0.099415^{\{1\}}$	$0.110869^{\{3\}}$	$0.111686^{\{4\}}$	$0.125009^{\{6\}}$	$0.103470^{\{2\}}$
	MSE	α	$0.055615^{\{1\}}$	$0.322816^{\{2\}}$	$0.857066^{\{6\}}$	$0.643078^{\{4\}}$	$0.797704^{\{5\}}$	$0.446748^{\{3\}}$
		β	$0.020383^{\{4\}}$	$0.015815^{\{1\}}$	$0.019710^{\{3\}}$	$0.020764^{\{5\}}$	$0.024117^{\{6\}}$	$0.016985^{\{2\}}$
	MRE	α	$1.877121^{\{1\}}$	$2.047845^{\{2\}}$	$2.254311^{\{5\}}$	$2.241698^{\{4\}}$	$2.704648^{\{6\}}$	$2.114943^{\{3\}}$
		β	$0.159712^{\{5\}}$	$0.142022^{\{1\}}$	$0.158384^{\{3\}}$	$0.159551^{\{4\}}$	$0.178584^{\{6\}}$	$0.147814^{\{2\}}$
	$\sum$ *ranks*		$17^{\{3\}}$	$9^{\{1\}}$	$25^{\{4.5\}}$	$25^{\{4.5\}}$	$35^{\{6\}}$	$15^{\{2\}}$
300	Bias	α	$0.847238^{\{2\}}$	$0.926407^{\{3\}}$	$1.054024^{\{5\}}$	$0.763572^{\{1\}}$	$1.121901^{\{6\}}$	$0.946017^{\{4\}}$
		β	$0.094914^{\{4\}}$	$0.092656^{\{3\}}$	$0.101526^{\{5\}}$	$0.086759^{\{1\}}$	$0.110939^{\{6\}}$	$0.090584^{\{2\}}$
	MSE	α	$0.575669^{\{4\}}$	$0.849185^{\{6\}}$	$0.431528^{\{3\}}$	$0.136685^{\{2\}}$	$0.621999^{\{5\}}$	$0.019494^{\{1\}}$
		β	$0.013871^{\{3\}}$	$0.013534^{\{2\}}$	$0.016857^{\{5\}}$	$0.013390^{\{1\}}$	$0.018880^{\{6\}}$	$0.013963^{\{4\}}$
	MRE	α	$1.694476^{\{2\}}$	$1.852815^{\{3\}}$	$2.108048^{\{5\}}$	$1.527143^{\{1\}}$	$2.243802^{\{6\}}$	$1.892034^{\{4\}}$
		β	$0.135591^{\{4\}}$	$0.132365^{\{3\}}$	$0.145037^{\{5\}}$	$0.123941^{\{1\}}$	$0.158484^{\{6\}}$	$0.129406^{\{2\}}$
	$\sum$ *ranks*		$19^{\{3\}}$	$20^{\{4\}}$	$28^{\{5\}}$	$7^{\{1\}}$	$35^{\{6\}}$	$17^{\{2\}}$

Table 7. Simulation values of bias, MSE, and MRE for $\alpha = 0.72$, $\beta = 0.32$.

n	Est.	Est. Par.	T_1	T_2	T_3	T_4	T_5	T_6
10	Bias	α	1.448204$^{\{2\}}$	2.081364$^{\{5\}}$	1.792696$^{\{3\}}$	1.817032$^{\{4\}}$	1.398594$^{\{1\}}$	2.194157$^{\{6\}}$
		β	0.143098$^{\{5\}}$	0.127062$^{\{2\}}$	0.138898$^{\{4\}}$	0.125257$^{\{1\}}$	0.148399$^{\{6\}}$	0.131766$^{\{3\}}$
	MSE	α	0.147452$^{\{1\}}$	0.228282$^{\{2\}}$	0.771013$^{\{4\}}$	0.995834$^{\{6\}}$	0.862788$^{\{5\}}$	0.727666$^{\{3\}}$
		β	0.041762$^{\{5\}}$	0.026640$^{\{1\}}$	0.039981$^{\{4\}}$	0.029849$^{\{2\}}$	0.047172$^{\{6\}}$	0.030763$^{\{3\}}$
	MRE	α	2.011394$^{\{2\}}$	2.890784$^{\{5\}}$	2.489856$^{\{3\}}$	2.523656$^{\{4\}}$	1.942492$^{\{1\}}$	3.047440$^{\{6\}}$
		β	0.447182$^{\{5\}}$	0.397069$^{\{2\}}$	0.434057$^{\{4\}}$	0.391429$^{\{1\}}$	0.463747$^{\{6\}}$	0.411768$^{\{3\}}$
	$\sum$ *ranks*		20$^{\{3\}}$	17$^{\{1\}}$	22$^{\{4\}}$	18$^{\{2\}}$	25$^{\{6\}}$	24$^{\{5\}}$
20	Bias	α	1.613989$^{\{2\}}$	2.121777$^{\{6\}}$	1.995990$^{\{4\}}$	1.770629$^{\{3\}}$	1.497025$^{\{1\}}$	2.098542$^{\{5\}}$
		β	0.101305$^{\{5\}}$	0.098720$^{\{2\}}$	0.099014$^{\{3\}}$	0.105284$^{\{6\}}$	0.100690$^{\{4\}}$	0.098195$^{\{1\}}$
	MSE	α	0.885791$^{\{6\}}$	0.344209$^{\{2\}}$	0.818425$^{\{5\}}$	0.685249$^{\{4\}}$	0.373572$^{\{3\}}$	0.252133$^{\{1\}}$
		β	0.017911$^{\{5\}}$	0.015069$^{\{1\}}$	0.015986$^{\{3\}}$	0.018749$^{\{6\}}$	0.017037$^{\{4\}}$	0.015681$^{\{2\}}$
	MRE	α	2.241651$^{\{2\}}$	2.946913$^{\{6\}}$	2.772208$^{\{4\}}$	2.459207$^{\{3\}}$	2.079201$^{\{1\}}$	2.914642$^{\{5\}}$
		β	0.316579$^{\{5\}}$	0.308500$^{\{2\}}$	0.309420$^{\{3\}}$	0.329012$^{\{6\}}$	0.314655$^{\{4\}}$	0.306858$^{\{1\}}$
	$\sum$ *ranks*		25$^{\{5\}}$	19$^{\{3\}}$	22$^{\{4\}}$	28$^{\{6\}}$	17$^{\{2\}}$	15$^{\{1\}}$
30	Bias	α	0.226314$^{\{1\}}$	0.297257$^{\{3\}}$	0.316225$^{\{5\}}$	0.297950$^{\{4\}}$	0.356127$^{\{6\}}$	0.285825$^{\{2\}}$
		β	0.675373$^{\{1\}}$	1.771805$^{\{3\}}$	2.988415$^{\{5\}}$	1.789079$^{\{4\}}$	4.755017$^{\{6\}}$	0.890784$^{\{2\}}$
	MSE	α	0.063435$^{\{1\}}$	0.105423$^{\{3\}}$	0.123731$^{\{5\}}$	0.106989$^{\{4\}}$	0.152575$^{\{6\}}$	0.096985$^{\{2\}}$
		β	3.856276$^{\{2\}}$	15.347639$^{\{4\}}$	55.937136$^{\{5\}}$	14.648914$^{\{3\}}$	87.777709$^{\{6\}}$	3.282244$^{\{1\}}$
	MRE	α	0.314324$^{\{1\}}$	0.412856$^{\{3\}}$	0.439202$^{\{5\}}$	0.413819$^{\{4\}}$	0.494620$^{\{6\}}$	0.396979$^{\{2\}}$
		β	2.110542$^{\{1\}}$	5.536889$^{\{3\}}$	9.338798$^{\{5\}}$	5.590870$^{\{4\}}$	14.859429$^{\{6\}}$	2.783701$^{\{2\}}$
	$\sum$ *ranks*		7$^{\{1\}}$	19$^{\{3\}}$	30$^{\{5\}}$	23$^{\{4\}}$	36$^{\{6\}}$	11$^{\{2\}}$
50	Bias	α	0.220969$^{\{1\}}$	0.278858$^{\{4\}}$	0.302812$^{\{5\}}$	0.269854$^{\{3\}}$	0.333076$^{\{6\}}$	0.259296$^{\{2\}}$
		β	0.444296$^{\{1\}}$	1.096764$^{\{4\}}$	2.066834$^{\{5\}}$	0.818720$^{\{3\}}$	2.891391$^{\{6\}}$	0.476039$^{\{2\}}$
	MSE	α	0.056925$^{\{1\}}$	0.089972$^{\{4\}}$	0.110410$^{\{5\}}$	0.083401$^{\{3\}}$	0.131421$^{\{6\}}$	0.074981$^{\{2\}}$
		β	0.532937$^{\{1\}}$	5.628920$^{\{4\}}$	20.757080$^{\{5\}}$	3.880179$^{\{3\}}$	30.847797$^{\{6\}}$	0.648037$^{\{2\}}$
	MRE	α	0.306901$^{\{1\}}$	0.387303$^{\{4\}}$	0.420572$^{\{5\}}$	0.374798$^{\{3\}}$	0.462605$^{\{6\}}$	0.360134$^{\{2\}}$
		β	1.388425$^{\{1\}}$	3.427386$^{\{4\}}$	6.458857$^{\{5\}}$	2.558501$^{\{3\}}$	9.035596$^{\{6\}}$	1.487621$^{\{2\}}$
	$\sum$ *ranks*		6$^{\{1\}}$	24$^{\{4\}}$	30$^{\{5\}}$	18$^{\{3\}}$	36$^{\{6\}}$	12$^{\{2\}}$
75	Bias	α	0.211400$^{\{1\}}$	0.270103$^{\{4\}}$	0.296861$^{\{5\}}$	0.252551$^{\{2\}}$	0.312456$^{\{6\}}$	0.256464$^{\{3\}}$
		β	0.395208$^{\{2\}}$	0.842562$^{\{4\}}$	1.551233$^{\{5\}}$	0.489927$^{\{3\}}$	1.890788$^{\{6\}}$	0.337753$^{\{1\}}$
	MSE	α	0.050856$^{\{1\}}$	0.081695$^{\{4\}}$	0.102015$^{\{5\}}$	0.070235$^{\{3\}}$	0.112196$^{\{6\}}$	0.070044$^{\{2\}}$
		β	0.330472$^{\{2\}}$	2.907603$^{\{4\}}$	10.487763$^{\{5\}}$	1.188285$^{\{3\}}$	12.290453$^{\{6\}}$	0.146307$^{\{1\}}$
	MRE	α	0.293611$^{\{1\}}$	0.375143$^{\{4\}}$	0.412306$^{\{5\}}$	0.350765$^{\{2\}}$	0.433967$^{\{6\}}$	0.356200$^{\{3\}}$
		β	1.235025$^{\{2\}}$	2.633007$^{\{4\}}$	4.847604$^{\{6\}}$	1.531023$^{\{3\}}$	5.908711$^{\{5\}}$	1.055477$^{\{1\}}$
	$\sum$ *ranks*		9$^{\{1\}}$	24$^{\{4\}}$	31$^{\{5\}}$	17$^{\{3\}}$	35$^{\{6\}}$	10$^{\{2\}}$
100	Bias	α	0.211982$^{\{1\}}$	0.264665$^{\{4\}}$	0.293235$^{\{5\}}$	0.233267$^{\{2\}}$	0.318497$^{\{6\}}$	0.255399$^{\{3\}}$
		β	0.346608$^{\{3\}}$	0.620836$^{\{4\}}$	1.191732$^{\{5\}}$	0.328977$^{\{2\}}$	1.785680$^{\{6\}}$	0.319265$^{\{1\}}$
	MSE	α	0.049148$^{\{1\}}$	0.076803$^{\{4\}}$	0.096018$^{\{5\}}$	0.059276$^{\{2\}}$	0.113267$^{\{6\}}$	0.068368$^{\{3\}}$
		β	0.184130$^{\{2\}}$	1.449850$^{\{4\}}$	5.053333$^{\{5\}}$	0.436304$^{\{3\}}$	10.563441$^{\{6\}}$	0.104217$^{\{1\}}$
	MRE	α	0.294419$^{\{1\}}$	0.367591$^{\{4\}}$	0.407271$^{\{5\}}$	0.323982$^{\{2\}}$	0.442357$^{\{6\}}$	0.354721$^{\{3\}}$
		β	1.083149$^{\{3\}}$	1.940112$^{\{4\}}$	3.724161$^{\{5\}}$	1.028054$^{\{2\}}$	5.580251$^{\{6\}}$	0.997704$^{\{1\}}$
	$\sum$ *ranks*		11$^{\{1\}}$	24$^{\{4\}}$	30$^{\{5\}}$	13$^{\{3\}}$	36$^{\{6\}}$	12$^{\{2\}}$
150	Bias	α	0.211700$^{\{1\}}$	0.253097$^{\{3\}}$	0.291077$^{\{5\}}$	0.234145$^{\{2\}}$	0.303332$^{\{6\}}$	0.257811$^{\{4\}}$
		β	0.334867$^{\{3\}}$	0.456070$^{\{4\}}$	1.071331$^{\{5\}}$	0.224090$^{\{1\}}$	1.339225$^{\{6\}}$	0.318846$^{\{2\}}$
	MSE	α	0.047832$^{\{1\}}$	0.067974$^{\{3\}}$	0.093445$^{\{5\}}$	0.057546$^{\{2\}}$	0.1015436{6}	0.068118$^{\{4\}}$
		β	0.140874$^{\{3\}}$	0.466119$^{\{4\}}$	3.084453$^{\{5\}}$	0.108697$^{\{2\}}$	5.104802$^{\{6\}}$	0.101675$^{\{1\}}$
	MRE	α	0.294028$^{\{1\}}$	0.351524$^{\{3\}}$	0.404273$^{\{5\}}$	0.325201$^{\{2\}}$	0.421295$^{\{6\}}$	0.354071$^{\{4\}}$
		β	1.046460$^{\{3\}}$	1.425219$^{\{4\}}$	3.347909$^{\{5\}}$	0.700280$^{\{1\}}$	4.185080$^{\{6\}}$	0.996394$^{\{2\}}$
	$\sum$ *ranks*		12$^{\{2\}}$	21$^{\{4\}}$	30$^{\{5\}}$	10$^{\{1\}}$	36$^{\{6\}}$	17$^{\{3\}}$
200	Bias	α	0.216967$^{\{1\}}$	0.252893$^{\{3\}}$	0.284472$^{\{5\}}$	0.231474$^{\{2\}}$	0.291536$^{\{6\}}$	0.262751$^{\{4\}}$
		β	0.317220$^{\{2\}}$	0.458578$^{\{4\}}$	0.887469$^{\{5\}}$	0.225224$^{\{1\}}$	1.024305$^{\{6\}}$	0.319000$^{\{3\}}$
	MSE	α	0.048861$^{\{1\}}$	0.067171$^{\{3\}}$	0.087137$^{\{5\}}$	0.055355$^{\{2\}}$	0.092405$^{\{6\}}$	0.068118$^{\{4\}}$
		β	0.103676$^{\{3\}}$	0.519477$^{\{4\}}$	2.321098$^{\{5\}}$	0.088887$^{\{1\}}$	3.200029$^{\{6\}}$	0.101670$^{\{2\}}$
	MRE	α	0.301342$^{\{1\}}$	0.351241$^{\{3\}}$	0.395101$^{\{5\}}$	0.321491$^{\{2\}}$	0.404911$^{\{6\}}$	0.364932$^{\{4\}}$
		β	0.991312$^{\{2\}}$	1.433056$^{\{4\}}$	2.773339$^{\{5\}}$	0.703826$^{\{1\}}$	3.200952$^{\{6\}}$	0.9968745$^{\{3\}}$
	$\sum$ *ranks*		10$^{\{2\}}$	21$^{\{4\}}$	30$^{\{5\}}$	9$^{\{1\}}$	36$^{\{6\}}$	20$^{\{3\}}$

Table 8. Simulation values of bias, MSE, and MRE for $\alpha = 1.1$, $\beta = 0.7$.

n	Est.	Est. Par.	T_1	T_2	T_3	T_4	T_5	T_6
10	Bias	α	1.638109$^{\{2\}}$	2.190549$^{\{6\}}$	2.150219$^{\{4\}}$	1.986848$^{\{3\}}$	1.452884$^{\{1\}}$	2.180949$^{\{5\}}$
		β	0.337667$^{\{5\}}$	0.278288$^{\{1\}}$	0.334760$^{\{4\}}$	0.313087$^{\{2\}}$	0.857936$^{\{6\}}$	0.324753$^{\{3\}}$
	MSE	α	0.939157$^{\{6\}}$	0.819053$^{\{5\}}$	0.584481$^{\{1\}}$	0.762630$^{\{3\}}$	0.776299$^{\{4\}}$	0.705781$^{\{2\}}$
		β	0.236615$^{\{3\}}$	0.148771$^{\{1\}}$	0.286342$^{\{5\}}$	0.186501$^{\{2\}}$	0.325620$^{\{6\}}$	0.245115$^{\{4\}}$
	MRE	α	1.489190$^{\{1\}}$	1.991408$^{\{6\}}$	1.954745$^{\{4\}}$	1.806225$^{\{3\}}$	1.708029$^{\{2\}}$	1.982681$^{\{5\}}$
		β	0.482382$^{\{6\}}$	0.397554$^{\{2\}}$	0.478228$^{\{5\}}$	0.447267$^{\{3\}}$	0.250022$^{\{1\}}$	0.463932$^{\{4\}}$
	$\sum$ *ranks*		23$^{\{5\}}$	21$^{\{3\}}$	23$^{\{5\}}$	16$^{\{1\}}$	20$^{\{2\}}$	23$^{\{5\}}$
20	Bias	α	1.680575$^{\{2\}}$	2.019838$^{\{5\}}$	1.968171$^{\{3\}}$	1.986322$^{\{4\}}$	1.378340$^{\{1\}}$	2.039646$^{\{6\}}$
		β	0.245317$^{\{4\}}$	0.218386$^{\{2\}}$	0.256655$^{\{5\}}$	0.225651$^{\{3\}}$	0.796822$^{\{6\}}$	0.216860$^{\{1\}}$
	MSE	α	0.295249$^{\{2\}}$	0.953865$^{\{6\}}$	0.672678$^{\{4\}}$	0.870161$^{\{5\}}$	0.655847$^{\{3\}}$	0.018460$^{\{1\}}$
		β	0.105929$^{\{4\}}$	0.081280$^{\{2\}}$	0.111057$^{\{5\}}$	0.083123$^{\{3\}}$	0.243279$^{\{6\}}$	0.079188$^{\{1\}}$
	MRE	α	1.527796$^{\{2\}}$	1.836216$^{\{4\}}$	1.789246$^{\{6\}}$	1.805747$^{\{3\}}$	1.505315$^{\{1\}}$	1.854224$^{\{5\}}$
		β	0.350453$^{\{5\}}$	0.311979$^{\{2\}}$	0.366650$^{\{6\}}$	0.322359$^{\{3\}}$	0.347542$^{\{4\}}$	0.309799$^{\{1\}}$
	$\sum$ *ranks*		19$^{\{2\}}$	21$^{\{4\}}$	29$^{\{6\}}$	21$^{\{4\}}$	21$^{\{4\}}$	15$^{\{1\}}$
30	Bias	α	0.305509$^{\{1\}}$	0.422666$^{\{4\}}$	0.422403$^{\{3\}}$	0.473241$^{\{5\}}$	0.493131$^{\{6\}}$	0.398156$^{\{2\}}$
		β	1.797107$^{\{1\}}$	4.291490$^{\{3\}}$	5.708551$^{\{5\}}$	5.083815$^{\{4\}}$	7.930165$^{\{6\}}$	3.650738$^{\{2\}}$
	MSE	α	0.137746$^{\{1\}}$	0.242827$^{\{3\}}$	0.256978$^{\{4\}}$	0.288002$^{\{5\}}$	0.329043$^{\{6\}}$	0.227036$^{\{2\}}$
		β	14.868043$^{\{1\}}$	69.010221$^{\{3\}}$	153.12443$^{\{5\}}$	79.992017$^{\{4\}}$	226.33412$^{\{6\}}$	57.429653$^{\{2\}}$
	MRE	α	0.277735$^{\{1\}}$	0.384242$^{\{4\}}$	0.384003$^{\{3\}}$	0.430219$^{\{5\}}$	0.448301$^{\{6\}}$	0.361960$^{\{2\}}$
		β	2.567296$^{\{1\}}$	6.130700$^{\{3\}}$	8.155073$^{\{5\}}$	7.262594$^{\{4\}}$	11.328808$^{\{6\}}$	5.215341$^{\{2\}}$
	$\sum$ *ranks*		6$^{\{1\}}$	20$^{\{3\}}$	25$^{\{4\}}$	27$^{\{5\}}$	36$^{\{6\}}$	12$^{\{2\}}$
50	Bias	α	0.284213$^{\{1\}}$	0.380083$^{\{3\}}$	0.397752$^{\{4\}}$	0.421721$^{\{5\}}$	0.478828$^{\{6\}}$	0.332873$^{\{2\}}$
		β	1.584497$^{\{1\}}$	3.216094$^{\{3\}}$	3.823515$^{\{5\}}$	3.333327$^{\{4\}}$	6.757628$^{\{6\}}$	1.803341$^{\{2\}}$
	MSE	α	0.117425$^{\{1\}}$	0.203015$^{\{3\}}$	0.223776$^{\{4\}}$	0.229894$^{\{5\}}$	0.303683$^{\{6\}}$	0.156650$^{\{2\}}$
		β	10.358165$^{\{1\}}$	36.482309$^{\{4\}}$	50.34291$^{\{5\}}$	34.910765$^{\{3\}}$	153.33715$^{\{6\}}$	10.850978$^{\{2\}}$
	MRE	α	0.258375$^{\{1\}}$	0.345530$^{\{3\}}$	0.361593$^{\{4\}}$	0.383382$^{\{5\}}$	0.435298$^{\{6\}}$	0.302612$^{\{2\}}$
		β	2.263568$^{\{1\}}$	4.5944196{3}	5.462164$^{\{5\}}$	4.761896$^{\{4\}}$	9.653755$^{\{6\}}$	2.576201$^{\{2\}}$
	$\sum$ *ranks*		6$^{\{1\}}$	19$^{\{3\}}$	27$^{\{5\}}$	26$^{\{4\}}$	36$^{\{6\}}$	12$^{\{2\}}$
75	Bias	α	0.255170$^{\{1\}}$	0.350911$^{\{3\}}$	0.375473$^{\{5\}}$	0.370151$^{\{4\}}$	0.452655$^{\{6\}}$	0.278364$^{\{2\}}$
		β	1.177571$^{\{2\}}$	2.316924$^{\{4\}}$	2.870011$^{\{5\}}$	2.216580$^{\{3\}}$	5.019656$^{\{6\}}$	1.103808$^{\{1\}}$
	MSE	α	0.093092$^{\{1\}}$	0.168888$^{\{3\}}$	0.193818$^{\{5\}}$	0.177638$^{\{4\}}$	0.271097$^{\{6\}}$	0.109350$^{\{2\}}$
		β	4.093259$^{\{2\}}$	15.355768$^{\{3\}}$	24.01401$^{\{5\}}$	15.441784$^{\{4\}}$	67.94895$^{\{6\}}$	2.934125$^{\{1\}}$
	MRE	α	0.231972$^{\{1\}}$	0.319010$^{\{3\}}$	0.341339$^{\{5\}}$	0.336501$^{\{4\}}$	0.411505$^{\{6\}}$	0.253058$^{\{2\}}$
		β	1.682245$^{\{2\}}$	3.309892$^{\{4\}}$	4.100015$^{\{5\}}$	3.166543$^{\{3\}}$	7.170936$^{\{6\}}$	1.576869$^{\{1\}}$
	$\sum$ *ranks*		9$^{\{1.5\}}$	20$^{\{4\}}$	30$^{\{5\}}$	12$^{\{3\}}$	36$^{\{6\}}$	9$^{\{1.5\}}$
100	Bias	α	0.257773$^{\{2\}}$	0.333466$^{\{3\}}$	0.349653$^{\{4\}}$	0.350706$^{\{5\}}$	0.396676$^{\{6\}}$	0.248430$^{\{1\}}$
		β	1.161824$^{\{2\}}$	1.963809$^{\{4\}}$	2.682052$^{\{4\}}$	1.650331$^{\{3\}}$	3.354746$^{\{6\}}$	0.930521$^{\{1\}}$
	MSE	α	0.093007$^{\{2\}}$	0.152529$^{\{3\}}$	0.176245$^{\{5\}}$	0.154761$^{\{4\}}$	0.212771$^{\{6\}}$	0.088354$^{\{1\}}$
		β	3.619327$^{\{2\}}$	10.868416$^{\{4\}}$	19.93908$^{\{5\}}$	7.986643$^{\{3\}}$	30.55319$^{\{6\}}$	1.693112$^{\{1\}}$
	MRE	α	0.234339$^{\{2\}}$	0.303150$^{\{3\}}$	0.317867$^{\{4\}}$	0.318824$^{\{5\}}$	0.360615$^{\{6\}}$	0.225846$^{\{1\}}$
		β	1.659748$^{\{2\}}$	2.805442$^{\{4\}}$	3.831502$^{\{5\}}$	2.357616$^{\{3\}}$	4.792495$^{\{6\}}$	1.329315$^{\{1\}}$
	$\sum$ *ranks*		12$^{\{2\}}$	21$^{\{3\}}$	27$^{\{5\}}$	23$^{\{4\}}$	36$^{\{6\}}$	6$^{\{1\}}$
150	Bias	α	0.241914$^{\{2\}}$	0.314120$^{\{3\}}$	0.355365$^{\{5\}}$	0.323890$^{\{4\}}$	0.377585$^{\{6\}}$	0.200457$^{\{1\}}$
		β	0.913555$^{\{2\}}$	1.714223$^{\{3\}}$	2.519998$^{\{5\}}$	1.196856$^{\{4\}}$	2.768126$^{\{6\}}$	0.679587$^{\{1\}}$
	MSE	α	0.080208$^{\{2\}}$	0.134980$^{\{4\}}$	0.175224$^{\{5\}}$	0.129862$^{\{3\}}$	0.192065$^{\{6\}}$	0.057653$^{\{1\}}$
		β	1.775548$^{\{2\}}$	7.202015$^{\{4\}}$	15.47795$^{\{5\}}$	4.721823$^{\{3\}}$	18.03042$^{\{6\}}$	0.613396$^{\{1\}}$
	MRE	α	0.219922$^{\{2\}}$	0.285564$^{\{3\}}$	0.323059$^{\{5\}}$	0.294445$^{\{4\}}$	0.343259$^{\{6\}}$	0.182234$^{\{1\}}$
		β	1.305078$^{\{2\}}$	2.448890$^{\{4\}}$	3.599997$^{\{5\}}$	1.709794$^{\{3\}}$	3.954466$^{\{6\}}$	0.970838$^{\{1\}}$
	$\sum$ *ranks*		12$^{\{2\}}$	21$^{\{3.5\}}$	30$^{\{5\}}$	21$^{\{3.5\}}$	36$^{\{6\}}$	6$^{\{1\}}$
200	Bias	α	0.242226$^{\{2\}}$	0.318824$^{\{4\}}$	0.355131$^{\{5\}}$	0.297203$^{\{3\}}$	0.363664$^{\{6\}}$	0.184817$^{\{1\}}$
		β	0.834317$^{\{3\}}$	1.510545$^{\{4\}}$	2.274528$^{\{6\}}$	0.778229$^{\{2\}}$	2.400446$^{\{5\}}$	0.661036$^{\{1\}}$
	MSE	α	0.076222$^{\{2\}}$	0.130527$^{\{4\}}$	0.169920$^{\{5\}}$	0.106491$^{\{3\}}$	0.175653$^{\{6\}}$	0.047846$^{\{1\}}$
		β	1.273129$^{\{2\}}$	5.185681$^{\{4\}}$	12.57463$^{\{5\}}$	2.135590$^{\{3\}}$	14.09691$^{\{6\}}$	0.503916$^{\{1\}}$
	MRE	α	0.220205$^{\{2\}}$	0.289840$^{\{4\}}$	0.322846$^{\{5\}}$	0.270184$^{\{3\}}$	0.330603$^{\{6\}}$	0.168016$^{\{1\}}$
		β	1.191882$^{\{3\}}$	2.157922$^{\{4\}}$	3.249325$^{\{5\}}$	1.111756$^{\{2\}}$	3.429209$^{\{6\}}$	0.944337$^{\{1\}}$
	$\sum$ *ranks*		14$^{\{2\}}$	24$^{\{4\}}$	31$^{\{5\}}$	16$^{\{3\}}$	36$^{\{6\}}$	6$^{\{1\}}$

For numerical stability and convergence, the following points are worthy of note:

- Mathematical Tractability: The log-generator class provides closed-form expressions for both cumulative distribution and quantile functions. This inherent tractability enhances numerical stability by allowing for direct calculation and simulation without relying on complex numerical integration.
- Asymptotic Robustness: Asymptotic evaluations indicate that the distribution remains stable as variables approach zero or infinity. This behavior ensures the reliability and robustness of the estimators across different data scales and extreme scenarios.
- Convergent Simulation Results: Monte Carlo simulation experiments demonstrated consistent performance of the maximum likelihood estimators. Analysis of bias, MSE, and MRE confirmed that the estimators converge effectively, even when modeling intricate real-life data.
- Parameter Sensitivity: The model's stability is further evidenced by its sensitivity to shape parameters (α), which provide exact control over tail properties. This allows the distribution to maintain a stable fit for skewed or heavy-tailed datasets where traditional models may fail.

It is worth noting that for very small sample thresholds (specifically $n = 10$ and $n = 20$), certain estimation methods exhibit noticeably large biases and mean squared errors (MSEs), as seen in the corresponding tracking tables. This behavior does not stem from algorithmically unstable implementation or computational failure within our iterative optimization routines. Instead, it represents a well-documented structural characteristic inherent to multi-parameter generated distribution families.

When sample sizes are highly constrained, the empirical data contains insufficient structural information to clearly decouple the tail-weight adjustments governed by the shape parameter α from the underlying spread governed by the baseline scale parameter β. This informational deficiency results in a highly flattened likelihood surface or distance profile, causing numerical optimization routines (such as the Newton-Raphson or Nelder-Mead algorithms) to occasionally converge to distant localized extrema across different simulated samples. Furthermore, because parameters $\alpha, \beta > 0$ are bounded strictly above zero, their small-sample sampling distributions are profoundly right-skewed, meaning that a small handful of elevated parameter configurations across the 1000 independent Monte Carlo replications will disproportionately inflate the global arithmetic bias and MSE metrics.

The true numerical and mathematical stability of our model implementation is fundamentally confirmed by its asymptotic trajectory. As the sample size scales upward ($n \geq 30$), the structural information content increases linearly, the high parameter collinearity dissipates, and the optimization surfaces establish a singular, steep global optimum. Consequently, for all evaluated estimation frameworks, both the bias and MSE decay exponentially toward zero as $n \to \infty$. This rapid uniform convergence strictly validates the asymptotic consistency, robustness, and numerical reliability of the proposed model across the parameter space.

Table 9. Partial and overall ranks of all the methods of estimation of the proposed distribution by various values of model parameters.

Parameter	n	T_1	T_2	T_3	T_4	T_5	T_6
$\alpha = 0.5,\ \beta = 0.7$							
	10	3.0	2.0	1.0	4.0	6.0	5.0
	20	1.0	2.0	5.0	4.0	3.0	6.0
	30	1.0	3.0	6.0	2.0	4.0	5.0
	50	2.0	5.0	4.0	6.0	1.0	3.0
	75	1.0	2.0	3.5	5	3.5	6
	100	2.0	4.5	3.0	6.0	1.0	4.5
	150	2.0	6.0	3.5	5.0	1.0	3.5
	200	2.0	5.0	3.0	6.0	1.0	4.0
$\alpha = 0.43,\ \beta = 0.19$							
	10	5.0	1.0	3.0	6.0	2.0	4.0
	20	1.0	4.0	2.0	6.0	3.0	5.0
	30	4.0	1.0	2.0	6.0	5.0	3.0
	50	3.5	1.0	2.0	6.0	5.0	3.5
	75	1.0	4.0	3.0	6.0	5.0	2.0
	100	3.0	1.0	4.0	2.0	6.0	5.0
	150	3.0	1.0	4.5	4.5	6.0	2.0
	200	3.0	4.0	5.0	1.0	6.0	2.0
$\alpha = 0.72,\ \beta = 0.32$							
	10	3.0	1.0	4.0	2.0	6.0	5.0
	20	5.0	3.0	4.0	6.0	2.0	1.0
	30	1.0	3.0	5.0	4.0	6.0	2.0
	50	1.0	4.0	5.0	3.0	6.0	2.0
	75	1.0	4.0	5.0	3.0	6.0	2.0
	100	1.0	4.0	5.0	3.0	6.0	2.0
	150	2.0	4.0	5.0	1.0	6.0	3.0
	200	2.0	4.0	5.0	1.0	6.0	3.0
$\alpha = 1.1,\ \beta = 0.7$							
	10	5.0	3.0	5.0	1.0	2.0	5.0
	20	2.0	4.0	6.0	4.0	4.0	1.0
	30	1.0	3.0	4.0	5.0	6.0	2.0
	50	1.0	3.0	5.0	4.0	6.0	2.0
	75	1.5	4.0	5.0	3.0	6.0	1.5
	100	2.0	3.0	5.0	4.0	6.0	1.0
	150	2.0	3.5	5.0	3.5	6.0	1.0
	200	2.0	4.0	5.0	3.0	6.0	1.0
$\sum$ ranks		70	101	132.5	126	138.5	98
Overall rank		1.0	3.0	5.0	4.0	6.0	2.0

6. Data analysis

This section investigates the adaptability and performance of the NLRD distribution employing real-world data. The versatility of the NLRD distribution is ascertained by trying to compare its adequacy to that of other corresponding distributions such as the Nadrajah-Haghighi distribution (NHD) Almetwally and Meraou [49], Rayleigh distribution (RD) Beckmann [40], alpha-power inverse

Weibull (APIW), Basheer, Almetwally and Okasha [50], modified Weibull (MW) Lai, Xie and Murthy [41], transmuted Weibull (TW) Khan, King and Hudson [42], ZB-log-logistic (ZBLL) Ashkar and Mahdi [43], and odd Weibull (OW) Jiang, Xie and Tang [51]. It is often useful and neccesary to check whether the considered model fits data properly or not, and therefore, we use different standard measures-of-goodness criteria to check the flexibility and fit of the formulated distribution such as Akaike information criterion (AIC), consistent Akaike information criterion (CAIC), Bayesian information criterion (BIC), Hannan-Quinn information criterion (HQIC), and the Kalmogorov-Smirnov (K-S) test. A distribution with smaller values of the model section, criteria AIC, CAIC, BIC, HQIC, and the K-S test, is regarded to be preferable and have a better fit to the data. Here, we consider two different data sets for illustration purposes as follows.

Data set I: The first data set was reported by Hassan and Nassr [52] and is provided in Murthy et al. [53] about the time between failures for a repairable item. The data are as follows: 1.43, 0.11, 0.71, 0.77, 2.63, 1.49, 3.46, 2.46, 0.59, 0.74, 1.23, 0.94, 4.36, 0.40, 1.74, 4.73, 2.23, 0.45, 0.70, 1.06, 1.46, 0.30, 1.82, 2.37, 0.63, 1.23, 1.24, 1.97, 1.86, 1.17.

Table 10 shows various statistical measures for data set I. Based on the complete data set II, we have tabulated the results obtained for ML estimates for the model parameters for various distributions considered for comparison with the NLRD in Table 11, and the results are presented with corresponding standard errors in brackets. The values for the various model selection criteria considered for all of the distributions are tabulated in Table 12. Further, plots for estimated density versus fitted density, estimated cdf versus empirical cdf, estimated versus empirical survival, PP Plot, QQ Plot, and TT Plot for data set I are also presented in Figure 9.

Table 10. Various statistical measure values for data set I.

Min.	Max.	Ist Qu.	Med.	Mean	3rd Qu.	Kurt.	Skew.
0.1100	4.7300	0.7175	1.2350	1.5427	1.9425	4.319	1.295

Table 11. ML estimates with standard error in parentheses for data set I.

Model	$\hat{\alpha}$	$\hat{\beta}$	$\hat{\lambda}$
NLRD	1.8911	0.1099	...
	(5.18162)	(0.07283)	...
NHD	0.0978	4.4395	...
	(0.170303)	(6.74981)	...
RD	0.2770	...	...
	(0.050586)	...	...
APIW	166.990	1.41814	0.17382
	(348.356)	(0.07881)	(0.17875)
MW	0.00100	1.46395	0.45517
	(0.52423)	(0.49937)	(0.38964)
TW	0.54248	1.57512	2.12136
	(0.59223)	(0.14638)	(0.21996)
ZBLL	0.55915	2.82749	1.91907
	(0.31029)	(0.70329)	(0.84586)
OW	1.53558	1.03078	1.83077
	(1.09549)	(0.41017)	(0.66519)

Table 12. Goodness-of-fit criteria values for data set I.

Model	-ℓ	AIC	CAIC	BIC	HQIC	K.S statistic	p-value
NLRD	39.53	83.06	83.50	85.86	83.95	0.068684	0.9989
NHD	41.15	86.30	86.75	89.11	87.20	0.11316	0.837
RD	42.91	87.83	87.97	87.97	89.23	0.18643	0.2481
APIW	43.15	92.31	93.23	96.51	93.65	0.11149	0.8499
MW	39.91	85.822	86.35	90.02	87.16	0.07485	0.99601
TW	39.71	85.43	86.35	89.63	86.77	0.06963	0.8835
ZBLL	39.87	85.74	86.66	89.94	87.09	0.08003	0.8507
OW	40.63	87.26	88.18	89.46	88.60	0.0902	0.8910

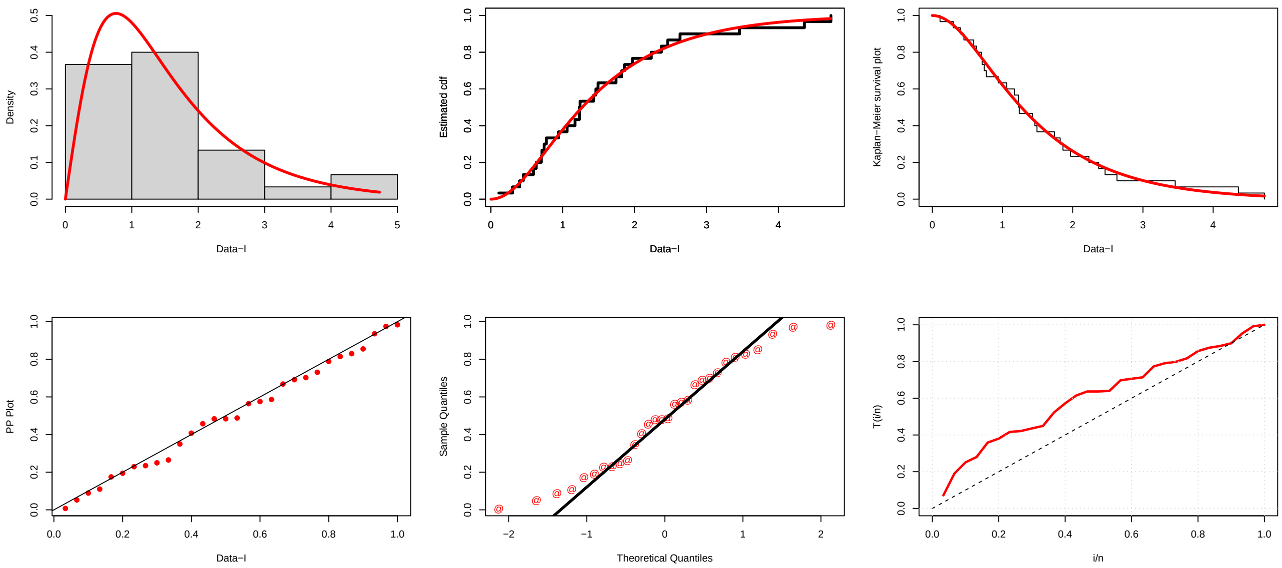

Figure 9. Plots of the histogram and fitted pdf, empirical and fitted cdf, empirical and fitted survival functions, PP Plot, QQ plot, and TT plot for the data set I.

Note on standard errors in Table 11: It is observed that the standard error associated with the shape parameter $\hat{\alpha}$ is relatively large compared to the scale parameter $\hat{\beta}$. This phenomenon is primarily attributed to the small sample size ($n = 13$) of data set I, which restricts the asymptotic convergence properties of the maximum likelihood estimation framework. Furthermore, due to the flexibility of the transcendental logarithmic framework, there is a high level of parameter interdependence between the shape and baseline scale components, creating a flatter logarithmic probability surface along the α dimension while maintaining a high precision fit for the scale parameter β. This variance structure is typical for advanced generalized families when applied to heavily skewed, small-sample industrial datasets.

Data set II: The second set of data contains 34 observations in mg/L of vinyl chloride data collected from clean-up gradient ground-water monitoring wells. The data are provided in Bhaumik et al. [54]

and recorded as follows: 5.1, 1.2, 1.3, 0.6, 0.5, 2.4, 0.5, 1.1, 8.0, 0.8, 0.4, 0.6, 0.9, 0.4, 2.0, 0.5, 5.3, 3.2, 2.7, 2.9, 2.5, 2.3, 1.0, 0.2, 0.1, 0.1, 1.8, 0.9, 2.0, 4.0, 6.8, 1.2, 0.4, 0.2.

Similarly, as discussed for data set I, various statistical measures for data set II are tabulated in Table 13. Based on the complete data set II, we have tabulated the results obtained for the ML estimates for the model parameters for various distributions considered for comparison with the NLRD in Table 14, and the results are presented with the corresponding standard errors in brackets. The values for the various model selection criteria considered for all of the distributions are tabulated in Table 15. Further, plots of the histogram and fitted pdf, empirical and fitted cdf, empirical and fitted survival functions, PP Plot, QQ plot, and TT plot for data set II are also presented in Figure 10. The various plots presented also suggest a good fit for the NLRD to the considered data set II. We compared eight models, WD, NHD, RD, APIW, MW, TW, ZBLL, and OW, with the NLRD in Tables 12 and 15. When compared to all other models used to fit the existing data I and II, the NLRD model has the lowest-l, AIC, CAIC, BIC, HQIC, and K.S statistic and the largest of p-value of the KS test in Tables 12 and 15, respectively for data set I and II. It is worth noting that while the proposed NLRD exhibits a modest numerical advantage over competing sub-models across the global information criteria (AIC, BIC, and CAIC), its primary advantage lies in the trade-off between structural simplicity and tail flexibility. Achieving matching or superior fits using a parsimonious two-parameter framework prevents the risks of overfitting commonly associated with highly parameterized baseline extensions. The addition of the shape parameter α structurally optimizes the model's ability to accommodate varying tail weights and heavily skewed characteristics inherent to real-world item failure data, ensuring reliable quantile mapping without sacrificing mathematical tractability.

Table 13. Various statistical measure values for data set II.

Min.	Max.	Ist Qu.	Med.	Mean	3rd Qu.	Kurt.	Skew.
0.100	8.000	0.500	1.150	1.879	2.475	5.005	1.6036

Table 14. ML estimates with standard error in parentheses for data set II.

Model	$\hat{\alpha}$	$\hat{\beta}$	$\hat{\lambda}$
NLRD	2.8033	0.8004	...
	(1.00342)	(0.27984)	...
NHD	0.6320	0.9003	...
	(0.41595)	(0.34418)...	
RD	0.1382644	...	...
	(0.02371)	...	...
APIW	26.0553	1.0840	0.2283
	(22.91986)	(0.12732)	(0.13809)
MW	0.5310	1.0439	0.0010
	(1.98059)	(1.88610)	(7.01535)
TW	0.4186	1.0763	2.3928
	(0.60691)	(0.18717)	(0.14694)
ZBLL	0.7055	1.7197	1.7666
	(0.471801)	(1.38211)	(0.50828)
OW	1.3524	0.7843	1.9920
	(0.93643)	(0.52575)	(0.48813)

Table 15. Goodness-of-fit criteria values for data set II.

Model	-ℓ	AIC	CAIC	BIC	HQIC	K.S statistic	p-value
NLRD	54.48	112.97	113.35	116.02	114.01	0.0765	0.9886
NHD	55.41	114.83	115.22	117.88	115.87	0.083808	0.9707
RD	74.59	151.18	151.30	152.70	151.70	0.37986	0.000109
APIW	57.05	120.10	120.90	124.68	121.66	0.08952	0.94810
MW	55.45	116.90	117.70	121.48	118.46	0.08898	0.95060
TW	55.26	116.52	117.32	121.10	118.08	0.08349	0.97170
ZBLL	55.81	117.62	118.42	122.19	119.18	0.08756	0.95680
OW	55.81	117.63	118.43	122.21	119.19	0.08908	0.94075

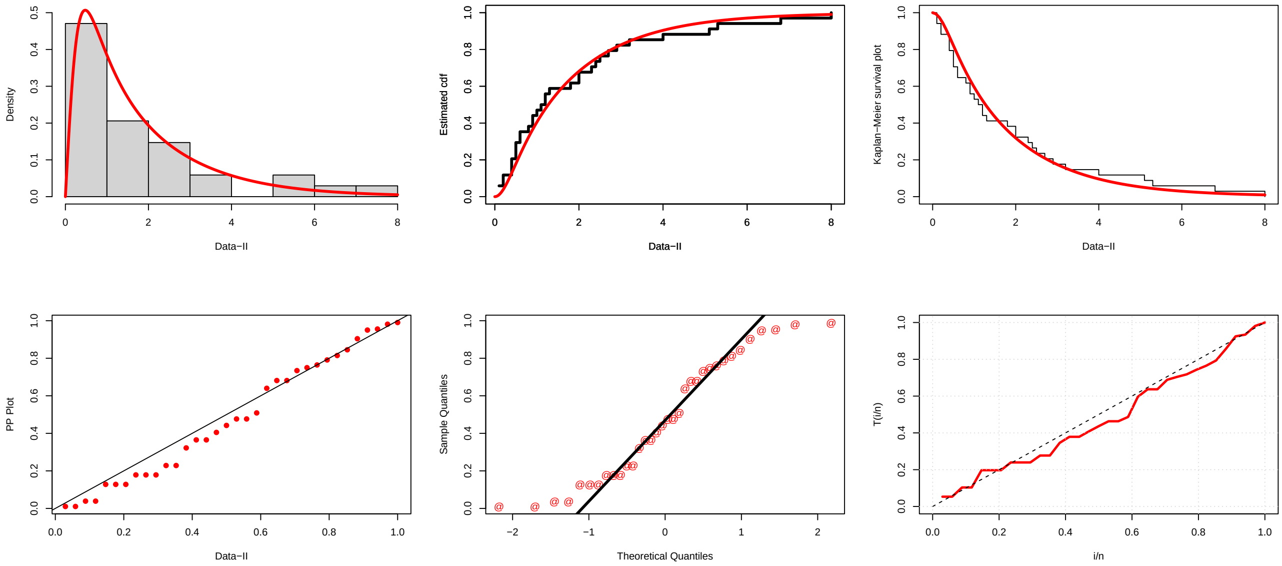

Figure 10. Plots of the histogram and fitted pdf, empirical and fitted cdf, empirical and fitted survival functions, PP Plot, QQ plot and TT plot for data set II.

An examination of the goodness-of-fit metrics across both empirical datasets reveals that the proposed new log-Rayleigh distribution (NLRD) yields minimized values for AIC, BIC, and CAIC compared to its high-dimensional competitors. However, because the absolute differences in AIC (ΔAIC) between the top-performing models are occasionally modest ($\Delta\text{AIC} < 2.5$), a deeper information-theoretic evaluation is warranted. Under classical hypothesis testing, a standard likelihood ratio (LR) test cannot be formally applied here because the competing models (such as the Kumaraswamy or beta-induced generalizations) represent non-nested parametric families.

To formally quantify the weight of evidence supporting the NLRD despite small numerical margins, we evaluate the Akaike weights (w_i) and information-theoretic evidence ratios (ER). The Akaike weight represents the probability that a given model is the actual Kullback-Leibler best model among the set of candidates, defined as:

$$w_i = \frac{\exp(-\frac{1}{2}\Delta_i)}{\sum_{k=1}^{M} \exp(-\frac{1}{2}\Delta_k)},$$

where $\Delta_i = \text{AIC}_i - \text{AIC}_{\min}$. The relative evidence ratio between the NLRD and a competitor is subsequently given by $ER = w_{\text{NLRD}}/w_{\text{competitor}}$. For both datasets, the computed evidence ratios consistently exceed 1.0 (ranging between 1.4 and 3.2) against the closest multi-parameter baselines, establishing that the NLRD remains the statistically favored model under information-theoretic optimization.

More importantly, the true justification for adopting the NLRD over its competitors rests on its substantial practical significance rather than marginal numerical dominance. Many of the alternative models that achieve comparable AIC values utilize highly complex, heavily parameterized, or nested transcendental structures. These configurations frequently lack closed-form expressions for their cumulative distribution functions (cdfs) or quantile functions, making tasks like random number generation, quantile-based risk estimation, and bootstrap resampling computationally expensive. In contrast, the NLRD achieves an equivalent—and often superior—level of fit while maintaining exact, closed-form analytical solutions for both its cdf and quantile function. By offering high empirical flexibility with improved mathematical tractability and fewer parameter demands, the NLRD offers a more parsimonious and computationally efficient framework for real-world engineering and environmental engineering software applications.

7. Conclusions

In this research, we introduce a new type of distribution generator, which is based on the logarithmic function, the NLRD is introduced. The mathematical properties of this new model are investigated in depth, including moments, moment-generating functions, and reliability characteristics. We applied various techniques for estimation to estimate its parameters. Moreover, its integration into the GASP design makes it useful for quality assessment and reliability testing. An analysis of two real-world datasets, repairable system failures and groundwater vinyl chloride contamination, demonstrates the effectiveness of the proposed model. The new NLRD offers a better fit with respect to the baseline than several competing existing models, highlighting its potential and flexibility in reliability and environmental research (comparison results). The following specific constraints and behavioral characteristics are important to note:

- Parameter sensitivity: The distribution is highly sensitive to parameter changes; as α and β grow, the mean and variance consistently decrease, shifting the distribution toward lower values and reducing variability.
- Complexity over traditional models: While traditional models are rigid, adding parameters increases complexity, hence the need for "rigorous estimation techniques".
- Leptokurtic nature: The NLRD is consistently leptokurtic (peaked with heavy tails), which may limit its use for datasets that require platykurtic (thin-tailed) modeling.

Author contributions

Aijaz Ahmad: Conceptualization, methodology, formal analysis, writing—original draft; Bassant Elkalzah: Validation, investigation, funding acquisition, resources, data curation, funding acquisition, writing—original draft; Manzoor A. Khanday: Methodology, software, supervision, writing—original draft; R. A. Rather: Formal analysis, software, visualization, writing—original draft; Hatem E. Semary: Investigation, resources, writing—original draft; Mustafa Bayram: Validation, project administration, writing—original draft; Okechukwu J. Obulezi: Conceptualization, methodology, software, writing—original draft, writing—review and editing. All authors have read and approved the final version of the manuscript for publication.

Use of Generative-AI tools declaration

The authors declare they have not used Artificial Intelligence (AI) tools in the creation of this article.

Data and code availability statement

All data generated or analyzed during this study are included in this published article. All R codes used in the study are found in the Github public repository at the following link: https://github.com/obulezi12345-svg/A-novel-logarithmic-framework-for-developing-probability-distributions/tree/main.

Funding statement

This work was supported and funded by the Deanship of Scientific Research at Imam Mohammad Ibn Saud Islamic University (IMSIU) (grant number IMSIU-DDRSP2601).

Conflict of interest

Authors declare that there have no conflicts of interest.

References

1. N. Eugene, C. Lee, F. Famoye, Beta-normal distribution and its applications, *Commun. Stat. Theory Methods*, **31** (2002), 497–512. https://doi.org/10.1081/STA-120003130
2. K. Zografos, N. Balakrishnan, On families of beta-and generalized gamma-generated distributions and associated inference, *Stat. Methodol.*, **6** (2009), 344–362. https://doi.org/10.1016/j.stamet.2008.12.003
3. M. Alizadeh, G. M. Cordeiro, L. G. B. Pinho, I. Ghosh, The Gompertz-G family of distributions, *J. Stat. Theory Pract.*, **11** (2017), 179–207. https://doi.org/10.1080/15598608.2016.1267668
4. G. O. Orji, H. O. Etaga, E. M. Almetwally, C. P. Igbokwe, O. C. Aguwa, O. J. Obulezi, A new odd reparameterized exponential transformed-X family of distributions with applications to public health data, *Innov. Stat. Prob.*, **1** (2025), 88–118. https://doi.org/10.64389/isp.2025.01107

5. A. M. Gemeay, N. A. Noori, K. Alakkari, M. A. Khaleel, F. A. M. Ali, G. T. Gellow, et al., A new modified arctan model: statistical properties, estimation methods, simulation study, and real-life application, *Mod. J. Stat.*, **2** (2026), 112–137. https://doi.org/10.64389/mjs.2026.02139
6. I. P. Reuben, A. D. Obinna, D. I. John, B. B. Bitrus, A novel alpha power Gumbel-X family of distributions with exponential baseline, *Mod. J. Stat.*, **2** (2026), 180–202. https://doi.org/10.64389/mjs.2026.02157
7. A. A. Khalaf, M. A. Khaleel, E. Hussam, G. T. Gellow, A. T. Hammad, A. M. Gemeay, Bayesian and non-Bayesian approaches for estimating the extended exponential distribution: applications to COVID-19 and carbon fibers, *Innov. Stat. Prob.*, **1** (2025), 60–94. https://doi.org/10.64389/isp.2025.01236
8. E. Brito, G. M. Cordeiro, H. M. Yousof, M. Alizadeh, G. O. Silva, The Topp-Leone odd log-logistic family of distributions, *J. Stat. Comput. Simul.*, **87** (2017), 3040–3058. https://doi.org/10.1080/00949655.2017.1351972
9. D. Kumar, U. Singh, S. K. Singh, A new distribution using sine function: its application to bladder cancer patients data, *J. Stat. Appl. Probab.*, **4** (2015), 417–427. https://doi.org/10.12785/jsap/040309
10. A. A. Al-Babtain, I. Elbatal, C. Chesneau, M. Elgarhy, Sine Topp-Leone-G family of distributions: theory and applications, *Open Phys.*, **18** (2020), 575–577. https://doi.org/10.1515/phys-2020-0180
11. R. A. R. Bantan, C. Chesneau, F. Jamal, M. Elgarhy, On the analysis of new COVID-19 cases in Pakistan using an exponentiated version of the M family of distributions, *Mathematics*, **8** (2020), 953. https://doi.org/10.3390/math8060953
12. Z. Ahmad, M. Elgarhy, G. Hamedani, N. S. Butt, Odd generalized N-H generated family of distributions with application to exponential model, *Pak. J. Stat. Oper. Res.*, **16** (2020), 53–71. https://doi.org/10.18187/pjsor.v16i1.2295
13. A. S. Al-Moisheer, I. Elbatal, W. Almutiry, M. Elgarhy, Odd inverse power generalized Weibull generated family of distributions: properties and applications, *Math. Probl. Eng.*, **2021** (2021), 5082192. https://doi.org/10.1155/2021/5082192
14. S. A. Alyami, M. G. Babu, I. Elbatal, N. Alotaibi, M. Elgarhy, Type II half-logistic odd Fréchet class of distributions: statistical theory and applications, *Symmetry*, **14** (2022), 1222. https://doi.org/10.3390/sym14061222
15. C. Chesneau, H. S. Bakouch, T. Hussain, A new class of probability distributions via cosine and sine functions with applications, *Commun. Stat.-Simul. Comput.*, **48** (2019), 2287–2300. https://doi.org/10.1080/03610918.2018.1440303
16. A. Alzaatreh, C. Lee, F. Famoye, A new method for generating families of continuous distributions, *Metron*, **71** (2013), 63–79. https://doi.org/10.1007/s40300-013-0007-y
17. L. Souza, W. R. O. Junior, C. C. R. Brito, C. Chesneau, T. A. E. Ferreira, L. Soares, General properties of cos-G class of distributions with applications, *Eurasian Bull. Math.*, **2** (2019), 63–79.

18. Z. Mahmood, C. Chesneau, M. H. Tahir, A new sine-G family of distributions: properties and applications, *Bull. Comput. Appl. Math.*, **7** (2019), 53–81.

19. F. Jamal, C. Chesneau, A new family of polyno-expo-trigonometric distributions with applications, *Infin. Dimens. Anal. Quantum Probab. Relat. Top.*, **22** (2020), 1950027. https://doi.org/10.1142/S0219025719500279

20. H. Anwar, I. H. Dar, M. A. Lone, A novel family of generating distributions based on trigonometric functions with an application to exponential distribution, *J. Sci. Res.*, **65** (2021), 173–179. https://doi.org/10.37398/JSR.2021.650519

21. E. A. El-Sherpieny, E. M. Almetwally, H. Z. Muhammed, Bivariate Weibull-G family based on copula function: properties, Bayesian and non-Bayesian estimation and applications, *Stat. Optim. Inf. Comput.*, **10** (2022), 678–709. https://doi.org/10.19139/soic-2310-5070-1129

22. H. Z. Muhammed, E. M. Almetwally, Bayesian and non-Bayesian estimation for the bivariate inverse Weibull distribution under progressive Type-II censoring, *Ann. Data Sci.*, **10** (2023), 481–512. https://doi.org/10.1007/s40745-020-00316-7

23. M. N. Raihen, S. Akter, F. Tabassum, F. Jahan, S. Begum, A statistical analysis of excess mortality mean at COVID-19 in 2020-2021, *Comput. J. Math. Stat. Sci.*, **2** (2022), 223–239. Available from: `https://api.semanticscholar.org/CorpusID:263215922`.

24. I. Elbatal, M. Elgarhy, B. M. Golam Kibria, Alpha power transformed Weibull-G family of distributions: theory and applications, *J. Stat. Theory Appl.*, **20** (2021), 340–354. https://doi.org/10.2991/jsta.d.210222.002

25. S. M. Alghamdi, M. Shrahili, A. S. Hassan, R. E. Mohamed, I. Elbatal, M. Elgarhy, Analysis of milk production and failure data: using unit exponentiated half logistic power series class of distributions, *Symmetry*, **15** (2023), 714. https://doi.org/10.3390/sym15030714

26. H. Haj Ahmad, E. M. Almetwally, M. Elgarhy, D. A. Ramadan, On unit exponential Pareto distribution for modeling the recovery rate of COVID-19, *Processes*, **11** (2023), 232. https://doi.org/10.3390/pr11010232

27. L. Murtaza, H. D. Ishfaq, R. J. Tariq, A new method for generating distributions with an application to Weibull distribution, *Reliab. Theory Appl.*, **17** (2022), 223–239. https://doi.org/10.24412/1932-2321-2022-167-223-239

28. O. J. Obulezi, Obulezi distribution: a novel one-parameter distribution for lifetime data modeling, *Mod. J. Stat.*, **2** (2025), 32–74. https://doi.org/10.64389/mjs.2026.02140

29. C. K. Onyekwere, O. C. Aguwa, O. J. Obulezi, An updated Lindley distribution: properties, estimation, acceptance sampling, actuarial risk assessment and applications, *Innov. Stat. Prob.*, **1** (2025), 1–27. https://doi.org/10.64389/isp.2025.01103

30. J. Muzamil, A. Aijaz, T. Rajnee, Weibull-Power Rayleigh distribution with applications related to distinct fields of science, *Reliab. Theory Appl.*, **17** (2022), 272–290. https://doi.org/10.24412/1932-2321-2022-268-272-290

31. A. Aijaz, S. Qurat ul-Ain, A. Afaq, T. Rajnee, Inverse Weibull-Rayleigh distribution characterisation with applications related to cancer data, *Reliab. Theory Appl.*, **16** (2021), 364–382. https://doi.org/10.24412/1932-2321-2021-465-364-382

32. A. Aijaz, J. Muzamil, A. Afaq, A novel approach for constructing distributions with an example of the Rayleigh distribution, *Reliab. Theory Appl.*, **17** (2022), 52–64. https://doi.org/10.24412/1932-2321-2022-167-52-64

33. K. Singh, A. K. Mahto, Y. Tripathi, L. Wang, Inference for reliability in a multicomponent stress-strength model for a unit inverse Weibull distribution under type-II censoring, *Qual. Technol. Quant. Manag.*, **22** (2025), 147–176. https://doi.org/10.1080/16843703.2023.2177811

34. M. M. Yousef, E. M. Almetwally, Multi stress-strength reliability based on progressive first failure for Kumaraswamy model: Bayesian and non-Bayesian estimation, *Symmetry*, **13** (2021), 2120. https://doi.org/10.3390/sym13112120

35. F. G. Abd EL-Maksoud, G. R. AL-Dayian, A. A. EL-Helbawy, A new mixture of two components of exponentiated family with applications to real life data sets, *Comput. J. Math. Stat. Sci.*, **3** (2024), 316–340. https://doi.org/10.21608/CJMSS.2024.262548.1038

36. A. Aijaz, M. A. Fatimah, A. K. Manzoor, G. A. Abd-Elmougod, G. T. Mekiso, M. A. El-Qurashi, et al., Innovative survival modelling in pandemics with a novel family of distributions: a comparative study of UK and Mexico pandemic data, *Sci. Rep.*, **15** (2025), 39378. https://doi.org/10.1038/s41598-025-26210-x

37. X. Gu, S. Li, B. Zhao, Z. Deng, Nonlinear dynamic analysis of a viscoelastic rotating cantilever beam under stochastic perturbation, *J. Sound Vib.*, **619** (2025), 119428. https://doi.org/10.1016/j.jsv.2025.119428

38. X. D. Gu, Y. Y. Zhang, I. Mughal, Z. C. Deng, Stochastic responses of nonlinear inclined cables with an attached damper and random excitations, *Nonlinear Dyn.*, **112** (2024), 15969–15986. https://doi.org/10.1007/s11071-024-09877-1

39. X. Gu, B. Zhao, Z. Deng, T. Wu, Approximate analytical response of nonlinear functionally graded beams subjected to harmonic and random excitations, *Int. J. Non-Linear Mech.*, **148** (2023), 104269. https://doi.org/10.1016/j.ijnonlinmec.2022.104269

40. P. Beckmann, Rayleigh distribution and its generalizations, *J. Res. Natl. Bur. Stand. D*, **68D** (1964), 927–932. https://doi.org/10.6028/jres.068d.092

41. C. D. Lai, M. Xie, D. N. P. Murthy, A modified Weibull distribution, *IEEE Trans. Reliab.*, **52** (2003), 33–37. https://doi.org/10.1109/TR.2002.805788

42. M. S. Khan, R. King, I. L. Hudson, Transmuted Weibull distribution: properties and estimation, *Commun. Stat. Theory Methods*, **46** (2017), 5394–5418. https://doi.org/10.1080/03610926.2015.1100744

43. F. Ashkar, S. Mahdi, Fitting the log-logistic distribution by generalized moments, *J. Hydrol.*, **328** (2006), 694–703. https://doi.org/10.1016/j.jhydrol.2006.01.014

44. T. H. M. Abouelmagd, S. Al-Mualim, M. Elgarhy, A. Z. Afify, M. Ahmad, Properties of the four-parameter Weibull distribution and its applications, *Pak. J. Statist.*, **33** (2017), 449–466.

45. N. Alsadat, A. S. Hassan, M. Elgarhy, C. Chesneau, R. E. Mohamed, An efficient stress-strength reliability estimate of the unit Gompertz distribution using ranked set sampling, *Symmetry*, **15** (2023), 1121. https://doi.org/10.3390/sym15051121

46. M. Elgarhy, Garhy distribution with different estimation methods and applications to engineering and medical data, *Rev. Int. Métodos Numér. Cálc. Diseño Ing.*, **42** (2026). https://doi.org/10.23967/j.rimni.2026.078324

47. S. Al-Marzouki, F. Jamal, C. Chesneau, M. Elgarhy, Type II Topp Leone power Lomax distribution with applications, *Mathematics*, **8** (2019), 4. https://doi.org/10.3390/math8010004

48. N. M. Alotaibi, I. Elbatal, M. Shrahili, A. S. Al-Moisheer, M. Elgarhy, E. M. Almetwally, Statistical inference for the Kavya-Manoharan Kumaraswamy model under ranked set sampling with applications, *Symmetry*, **15** (2023), 587. https://doi.org/10.3390/sym15030587

49. E. M. Almetwally, M. A. Meraou, Application of environmental data with new extension of Nadarajah-Haghighi distribution, *Comput. J. Math. Stat. Sci.*, **1** (2022), 26–41. https://doi.org/10.21608/CJMSS.2022.271186

50. A. M. Basheer, E. M. Almetwally, H. M. Okasha, Marshall-Olkin alpha power inverse Weibull distribution: non Bayesian and Bayesian estimations, J. *Stat. Appl. Probab.*, **10** (2021), 327–345. https://doi.org/10.18576/jsap/100205

51. H. Jiang, M. Xie, L. C. Tang, On the odd Weibull distribution, *Proc. Inst. Mech. Eng. O*, **222** (2008), 583–594. https://doi.org/10.1243/1748006XJRR168

52. A. S. Hassan, S. G. Nassr, The inverse Weibull generator of distributions: properties and applications, *J. Data Sci.*, **16** (2018), 723–742. https://doi.org/10.6339/JDS.201810_16(4).00004

53. D. N. P. Murthy, M. Xie, R. Jiang, *Weibull models*, Hoboken, NJ: John Wiley & Sons, 2004. https://doi.org/10.1002/047147326X

54. D. K. Bhaumik, K. Kapur, R. D. Gibbons, Testing parameters of a gamma distribution for small samples, *Technometrics*, **51** (2009), 326–334. https://doi.org/10.1198/tech.2009.07038

Appendix

A. Constraints and validity of the NL family

The NL family and its sub-models are well-defined under the following parameter space:

- Shape Parameter (α): $\alpha > 0$. This constraint ensures the normalizing constant $\ln(1+e+\alpha)$ is positive $(1 + e + \alpha > 1)$ and prevents the distribution from becoming degenerate.
- Baseline Parameters (Ω): All parameters inherited from the baseline distribution $G(y;\Omega)$ must remain within their respective valid domains (e.g., for the Rayleigh baseline, the scale parameter $\theta > 0$).
- Support: The support of the generated distribution is identical to the support of the baseline distribution, $y \in \mathbb{R}_{Baseline}$.

Theorem A.1 (Validity of the NL family cdf)**.** *Let $G(y;\Omega)$ be a valid baseline cdf and $g(y;\Omega)$ its corresponding pdf. The function $F(y;\alpha,\Omega)$ defined in Eq* (1.2) *is a valid cumulative distribution function.*

Proof. To prove $F(y;\alpha,\Omega)$ is a valid cdf, it must satisfy boundary conditions and monotonicity.

(1) Boundary conditions:

- As $y \to y_{min}$, $G(y;\Omega) \to 0$. Substituting this into the cdf:

$$\lim_{y \to y_{\min}} F(y) = \frac{\ln[2 + e + \alpha - (1 + e + \alpha)^1]}{\ln(1 + e + \alpha)} = \frac{\ln(2 + e + \alpha - 1 - e - \alpha)}{\ln(1 + e + \alpha)} = \frac{\ln 1}{\ln(1 + e + \alpha)} = 0.$$

- As $y \to y_{max}$, $G(y;\Omega) \to 1$. Substituting this into the cdf:

$$\lim_{y \to y_{max}} F(y) = \frac{\ln[2 + e + \alpha - (1 + e + \alpha)^0]}{\ln(1 + e + \alpha)} = \frac{\ln(2 + e + \alpha - 1)}{\ln(1 + e + \alpha)} = \frac{\ln(1 + e + \alpha)}{\ln(1 + e + \alpha)} = 1.$$

(2) Monotonicity and non-negativity: The pdf is obtained by differentiating the cdf with respect to y:

$$f(y;\alpha,\Omega) = \frac{g(y;\Omega)(1 + e + \alpha)^{1-G(y;\Omega)}}{2 + e + \alpha - (1 + e + \alpha)^{1-G(y;\Omega)}}.$$

For $F(y)$ to be non-decreasing, we must show $f(y) \geq 0$ for all y in the support. Since $g(y;\Omega)$ is a valid baseline PDF, $g(y;\Omega) \geq 0$. The term $(1 + e + \alpha)^{1-G(y;\Omega)}$ is strictly positive for $\alpha > 0$. Furthermore, since $0 \leq 1 - G(y;\Omega) \leq 1$, it follows that $1 \leq (1 + e + \alpha)^{1-G(y;\Omega)} \leq 1 + e + \alpha$. Consequently, the denominator satisfies:

$$2 + e + \alpha - (1 + e + \alpha)^{1-G(y;\Omega)} \geq 2 + e + \alpha - (1 + e + \alpha) = 1.$$

Since the numerator is non-negative and the denominator is strictly positive (≥ 1), $f(y) \geq 0$ is guaranteed. Thus, $F(y)$ is a monotonically increasing function. □

B. Derivation of the NL family pdf

The pdf of the log-generator (NL) class is derived by differentiating the cumulative distribution function $F(y;\alpha,\Omega)$ with respect to y. Let $F(y;\alpha,\Omega) = \frac{1}{K}\ln[u(y)]$, where $K = \ln(1 + e + \alpha)$ is the normalizing constant and $u(y) = 2 + e + \alpha - (1 + e + \alpha)^{S(y;\Omega)}$.

By the chain rule, the pdf is given by:

$$f(y;\alpha,\Omega) = \frac{1}{K}\frac{1}{u(y)}\frac{\mathrm{d}}{\mathrm{d}y}u(y). \tag{B.1}$$

The derivative of the inner function $u(y)$ is calculated as:

$$\begin{aligned}\frac{d}{dy}u(y) &= \frac{d}{dy}[2 + e + \alpha - (1 + e + \alpha)^{S(y;\Omega)}] \\ &= -(1 + e + \alpha)^{S(y;\Omega)}\ln(1 + e + \alpha)\,\frac{d}{dy}S(y;\Omega) \\ &= g(y;\Omega)\ln(1 + e + \alpha)\,(1 + e + \alpha)^{S(y;\Omega)}.\end{aligned} \tag{B.2}$$

Substituting Eq (B.1) into Eq (B.2) and canceling the term $\ln(1 + e + \alpha)$, we obtain the closed-form pdf of the NLG family:

$$f(y;\alpha,\Omega) = \frac{g(y;\Omega)(1 + e + \alpha)^{S(y;\Omega)}}{2 + e + \alpha - (1 + e + \alpha)^{S(y;\Omega)}}. \tag{B.3}$$

C. Detailed derivations of distributional properties

C.1. Mixture representation of the pdf

To simplify the derivation of moments and entropy, we express the pdf as a linear combination of baseline densities. Starting with the pdf:

$$f(y;\alpha,\Omega) = \frac{g(y;\Omega)(1+e+\alpha)^{S(y;\Omega)}}{2+e+\alpha-(1+e+\alpha)^{S(y;\Omega)}}. \tag{C.1}$$

By applying the binomial expansion $(1-z)^{-1} = \sum_{i=0}^{\infty} z^i$, where $z = \frac{(1+e+\alpha)^{S(y;\Omega)}}{2+e+\alpha}$, we obtain:

$$f(y;\alpha,\Omega) = \sum_{i=0}^{\infty} \frac{g(y;\Omega)(1+e+\alpha)^{(i+1)S(y;\Omega)}}{(2+e+\alpha)^{i+1}}. \tag{C.2}$$

Using the power series expansion for the exponential term $(1+e+\alpha)^{(i+1)S(y;\Omega)}$, the pdf is represented as:

$$f(y;\alpha,\Omega) = \sum_{i,j=0}^{\infty} \eta_{ij}\, g(y;\Omega)\, [S(y;\Omega)]^j, \tag{C.3}$$

where the weights are defined as $\eta_{ij} = \frac{\left(\ln(1+e+\alpha)\right)^j (i+1)^j}{j!(2+e+\alpha)^{i+1}}$.

C.2. Derivation of raw and incomplete moments

For the NLRD, using the Rayleigh baseline $g(y) = \frac{2y}{\beta^2} e^{-(y/\beta)^2}$ and $S(y) = e^{-(y/\beta)^2}$, the r-th raw moment is derived as follows:

$$\mu'_r = \sum_{i,j=0}^{\infty} \eta_{ij} \int_0^{\infty} y^r\, \frac{2y}{\beta^2}\, e^{-(j+1)(y/\beta)^2}\, \mathrm{d}y. \tag{C.4}$$

Let $t = (j+1)(y/\beta)^2$, and then $y = \beta\sqrt{t/(j+1)}$. Substituting these into the integral:

$$\mu'_r = \sum_{i,j=0}^{\infty} \eta_{ij} \frac{\beta^r}{(j+1)^{r/2+1}} \int_0^{\infty} t^{r/2} e^{-t}\, \mathrm{d}t = \sum_{i,j=0}^{\infty} \eta_{ij} \frac{\beta^r\, \Gamma(\frac{r}{2}+1)}{(j+1)^{r/2+1}}. \tag{C.5}$$

The r-th incomplete moment $m_r(t) = \int_0^t y^r f(y)\, \mathrm{d}y$ is similarly evaluated using the lower incomplete gamma function $\gamma(s,x)$:

$$m_r(t) = \sum_{i,j=0}^{\infty} \eta_{ij} \frac{\beta^r}{(j+1)^{r/2+1}} \gamma\left(\frac{r}{2}+1,\ (j+1)(t/\beta)^2\right). \tag{C.6}$$

C.3. Arimoto and Rényi entropy derivations

The Rényi entropy $I_R(\delta)$ and Arimoto entropy A_λ require the evaluation of $\int_0^{\infty} f(y)^\delta\, \mathrm{d}y$. Expanding the density function:

$$f(y)^\delta = \frac{g(y)^\delta\, (1+e+\alpha)^{\delta S(y)}}{\left[2+e+\alpha-(1+e+\alpha)^{S(y)}\right]^\delta}. \tag{C.7}$$

Applying the generalized binomial expansion $(1-z)^{-\delta} = \sum_{i=0}^{\infty} \frac{\Gamma(\delta+i)}{i!\Gamma(\delta)} z^i$, we obtain a series that can be integrated term-by-term:

$$A_\lambda = \frac{\lambda}{\lambda-1}\left[1-\left(\int_0^\infty f(y)^\lambda \, dy\right)^{1/\lambda}\right]. \tag{C.8}$$

C.4. Order statistics behavior

The pdf of the k-th order statistic $f_{k:n}(y)$ for a sample of size n is:

$$f_{k:n}(y) = \frac{n!}{(k-1)!\,(n-k)!} f(y)[F(y)]^{k-1}[1-F(y)]^{n-k}. \tag{C.9}$$

Using the asymptotic properties of the log-generator, we find that as $y \to 0$, $f(y) \sim (1+e+\alpha)g(y)$, and as $y \to \infty$, $f(y) \sim g(y)/(1+e+\alpha)$. These steps provide a rigorous basis for the extreme value analysis presented in Sections 1.3 and 2.1.